# AN ANALYSIS OF PERTURBED CONFOCAL RESONATORS

Thesis by

John Fredrich Asmus

In Partial Fulfillment of the Requirements

For the Degree of

Doctor of Philosophy

California Institute of Technology

Pasadena, California

1965

(Submitted December 3, 1964)

# ACKNOWLEDGMENTS

The author wishes to express his indebtedness to his advisor, Professor Nicholas George, for his guidance and encouragement throughout the course of this research.

The author further acknowledges helpful discussions with Dr. Wilbur P. Brown and Dr. Kenneth M. Mitzner. Mrs. Olive List who typed the manuscript and Mrs. Paula Samazan of the library are also thanked.

Financial support from the California Institute of Technology, Tektronix Foundation, Schlumberger Foundation and U. S. Naval Ordinance Laboratory is gratefully acknowledged.

# ABSTRACT

An analytical technique is developed for computing mode functions and associated diffraction losses of perturbed multimode optical resonators. It is based upon a consistent field formulation of resonance in an open two-mirror system.

To illustrate the method the theory of confocal resonators is extended to include configurations differing from the confocal case by small geometrical perturbations. This involves computing and expanding a perturbed Green's function for such near confocal resonators. Diffraction losses for certain statistical and deterministic perturbations are computed and related to disturbances arising from an imperfect figure, polish or alignment of the mirrors.

The design and construction of a stable laser spectrometer consisting of a single mode tuneable gas laser and a swept interferometer are described. Measurements of the diffraction losses of perturbed confocal resonators are found to be in agreement with the above analysis.

TABLE OF CONTENTS

# CHAPTER I

# INTRODUCTION

## 1.1 Optical Maser Multimode Resonators

The recent advent of the optical maser has stimulated considerable interest in multimode resonators. Due to its simplicity and high resolving power this interest has centered around the Fabry-Perot interferometer. In their classic paper Schawlow and Townes (1) suggested the plane-parallel Fabry-Perot resonator as did Prokhorov (2) and Dicke (3). Fox and Li (4) carried out extensive machine computations on the mode patterns and associated diffraction losses of this type of resonator.

Upon the realization that the confocal or spherical Fabry-Perot could be conveniently employed as a maser multimode resonator with its associated higher resolving power Boyd and Gordon (5), Boyd and Kogelnik (6), Soohoo (7) and Fox and Li (4) analyzed its properties with reference to this application. From an electromagnetic theory point of view these papers develop a basic mathematical approach and work out the diffraction losses for a variety of resonators of the spherical Fabry-Perot family. The usual analytical approach employed in these treatments is based upon the following general argument. A scalar field distribution is assumed on one of the mirrors. By means of the Green's function for the scalar Helmholtz equation the resulting field at the opposite mirror may be computed. With a small angle approximation and confocal geometry the integral reduces very conveniently to the finite Fourier transform of the initial field distribution

function. Then requiring the field to reproduce itself in form at each mirror implies that the eigenfunction fields are those which are invariant under a finite Fourier transformation. One is thus led to the angular and radial prolate spheroidal wave functions, respectively, for the eigenfunctions and eigenvalues of the confocal resonator.

Many papers have dealt with various aspects of multimode resonators and quite a number have extended, modified and broadened the works cited above. Among these are (8 - 18).

In addition the consistent field approach outlined above served to inspire an optics oriented discussion by G. Toraldo di Francia (19) which employs the plane wave representation of a radiation field. Discussions of the decomposition of an arbitrary field into an angular spectrum of plane waves may be found in Courant-Hilbert (20), Stratton (21) or Born and Wolf (22). Following this method an initial scalar field function $a(x,y)$ on one of the mirrors generates an angular spectrum of plane waves with an amplitude distribution given by

$$A(\alpha,\beta) = \frac{1}{\lambda^2} \int_S a(x,y) \exp\left[-ik(\alpha x + \beta y)\right] dxdy,$$

where $\lambda$ signifies the radiation wavelength and $k = 2\pi/\lambda$. The integral is over the surface of the mirror and $\alpha$ and $\beta$ are the direction cosines of the propagation vector. As the resonator is confocal each plane wave $A(\alpha,\beta)$ will be brought to a focus at the coordinates $x' = \alpha b$, $y' = \beta b$ on the surface of the second mirror. $b$ is the mirror separation. In (19) it is stated that as a consequence the amplitude distribution on the second mirror will be the Fourier

transform of that on the first. However, we must realize that the total intensity in the focal plane is a superposition of a distribution of Fraunhofer diffraction patterns. For rectangular mirror apertures the Fraunhofer field distribution about each focal point will be of the form

$$\left( \frac{\sin \frac{2\pi\alpha a_1}{\lambda}}{\frac{2\pi\alpha a_1}{\lambda}} \right) \qquad \left( \frac{\sin \frac{2\pi\beta a_2}{\lambda}}{\frac{2\pi\beta a_2}{\lambda}} \right) ,$$

where the dimensions of each mirror are $2a_1$ and $2a_2$. Dropping the constants multiplying the integral for simplicity of notation we find the total intensity at the plane of the second mirror will be

$$a'(x',y') = \int_{-\infty}^{\infty}\int A\left(\frac{x'-\bar{x}'}{b}, \frac{y'-\bar{y}'}{b}\right) \frac{\sin \frac{2\pi a_1 \bar{x}'}{\lambda b}}{\frac{2\pi a_1 \bar{x}'}{\lambda b}} \cdot \frac{\sin \frac{2\pi a_2 \bar{y}'}{\lambda b}}{\frac{2\pi a_2 \bar{y}'}{\lambda b}} \, d\bar{x}' d\bar{y}'$$

$$= \int_{-\infty}^{\infty} d\bar{x}' \int_{-\infty}^{\infty} d\bar{y}' \int_{-a_1}^{a_1} dx \int_{-a_2}^{a_2} dy \; a(x,y) \exp\left[-ik\left(\frac{x'-\bar{x}'}{b}x + \frac{y'-\bar{y}'}{b}y\right)\right]$$

$$\frac{\sin \frac{2\pi a_1 \bar{x}'}{\lambda b}}{\frac{2\pi a_1 \bar{x}'}{\lambda b}} \cdot \frac{\sin \frac{2\pi a_2 \bar{y}'}{\lambda b}}{\frac{2\pi a_2 \bar{y}'}{\lambda b}} ,$$

where it has been assumed that the radiation remains close to the optical axis so that small angle approximations may be employed. Carrying

out the integration over $\bar{x}'$ and $\bar{y}'$ we find

$$a'(x',y') = \iint_S a(x,y)\, \exp\left[-ik(xx' + yy')\right] dxdy \ .$$

The above equation demonstrates that focal plane intensity is just that deduced from geometrical optics. Consequently, a finite Fourier transform does indeed relate the amplitude distributions on the two mirrors.

## 1.2 Perturbed Fabry-Perot Resonators

With any physical multimode resonator will be associated geometrical defects as well as inhomogeneities in the media between the mirrors. It is the purpose of this investigation to study the detailed manner in which mirror perturbations arising from an imperfect figure, polish or alignment degrade the characteristics of such resonators.

In particular we are concerned with the effect of such considerations on optical maser performance. For example, let us consider the threshold condition for oscillation in a maser. Requiring the gain through stimulated emission to equal or exceed the resonator losses it can be shown (1) that for oscillation

$$n_1 - n_2 \geq h\nu\, \Delta\nu / 4\pi\mu^2 Q_s \ , \qquad (1.1)$$

where $n_1$ and $n_2$ are the numbers of systems in the upper and lower states, respectively, $v$ is the cavity volume, $\Delta\nu$ is the half-width of the atomic resonance, $\mu$ is the transition matrix element and $Q_s$

is quality factor for a particular resonator mode s. In 1.1 the threshold population inversion is inversely proportional to mode quality factor. Therefore, as cavity perturbations degrade $Q_s$ it will require correspondingly greater population inversions to achieve oscillation. Before proceeding with the role cavity perturbations play in the computation of $Q_s$ let us review the concept of the quality factor.

The quality factor $Q_s$ of the normal mode s with a resonant angular frequency $\omega_s$ may be defined (23)

$$Q_s = \omega_s \frac{\text{total time-average energy stored}}{\text{time-average power dissipated}} . \tag{1.2}$$

Signifying the average energy by $W_s$ we have equivalently,

$$\frac{dW_s}{dt} = - \frac{\omega_s}{Q_s} W_s . \tag{1.3}$$

Assuming an initial energy $W_{so}$ in a passive cavity and solving 1.3 we find

$$W_s(t) = W_{so} e^{- \frac{\omega_s}{Q_s} t} , \tag{1.4}$$

illustrating that the quality factor may be considered as a normalized decay time constant for the mode. The harmonic electric field magnitude corresponding to 1.4 is

$$E_s(t) = E_o e^{-i\omega_s t} e^{- \frac{\omega_s}{2Q_s} t} , \tag{1.5}$$

with a Fourier transform

$$S_s(\omega) = \frac{E_o}{2\pi} \frac{1}{i(\omega_s - \omega) + \frac{\omega_s}{2Q_s}} \quad . \tag{1.6}$$

The half-power frequencies are at $\omega = \omega_s \pm \omega_s/2Q_s$ and thus the resonance width $\Delta\omega$ is

$$\Delta\omega = \frac{\omega_s}{Q_s} \quad . \tag{1.7}$$

Having assembled the basic formulas relating to the concept of mode Q let us now consider the characteristics of a multimode confocal resonator. The field in such a resonator can be thought of as a superposition of waves traversing the space between the mirrors in opposite directions. Call the energy crossing a plane perpendicular to the optical axis in one direction per unit time P. For a resonator of length b the total stored energy is $\frac{2bP}{c}$ where c is the velocity of light. Assume each mirror has a small fractional power loss $\alpha_s$ so that the stored energy changes little during one transit time. The time average power dissipated will be $2\alpha_s P$. From 1.2 we find

$$Q_s = \omega_s \left(\frac{2bP}{c}\right) \left(\frac{1}{2\alpha_s P}\right) = \frac{2\pi b}{\alpha_s \lambda_s} \quad . \tag{1.8}$$

In optics one of the important performance figures of a Fabry-Perot resonator is the finesse F. It is defined (22) as the ratio of fringe separation and half-width. From Appendix IV we find an axial mode separation of c/2d in the frequency domain. From 1.7

$$F = \left(\frac{c}{2b}\right) \left(\frac{\lambda_s}{c} Q_s\right) = \frac{\lambda_s}{2b} Q_s = \frac{\pi}{\alpha_s} \quad . \tag{1.9}$$

The commonly employed expression for the finesse of a Fabry-Perot resonator (22) is

$$F = \frac{\pi\sqrt{R}}{1-R} = \frac{\pi\sqrt{R}}{\alpha_s} , \tag{1.10}$$

where $R$ is the reflectance of each mirror. Comparing 1.9 and 1.10 we see that the two expressions are equivalent in the limit of high mirror reflectance or in what we shall term the high $Q$ approximation.

Now let us consider a resonator with perfectly reflecting mirrors which are slightly irregular. We may characterize the optical length of such a cavity by a distribution function $D(b) = dS/db$, $dS$ being the mirror surface area where the corresponding resonator length lies between $b$ and $b + db$. Referring to Appendix IV we see that a variation in resonator length is related to a variation in resonant frequency by the relation

$$\frac{\Delta f}{f_s} = \frac{\Delta b}{b} . \tag{1.11}$$

Thus, we deduce that the Dirac resonance peaks of the ideal cavity are replaced by peaks of the form $D(f - f_s)$ for the perturbed resonator. Signifying the variance of the mirror surface as $\sigma$ and recalling 1.7 we find a perturbed resonator $Q$ of

$$Q_s = \frac{b}{\sigma} . \tag{1.12}$$

Returning to the threshold equation for an optical maser 1.1 we see that the population inversion necessary for oscillation is directly proportional to mirror surface roughness when other loss

mechanisms are neglected.

$$n_1 - n_2 \geq h\nu\,(\Delta\nu)\,\sigma/4\pi\mu^2 b \qquad (1.13)$$

Clearly, mirror roughness can be of importance in an optical maser. Of course the Q approximation given by 1.12 is quite crude and in subsequent chapters we shall look at it much more closely.

In addition imperfect mirrors will distort the cavity mode patterns. This in turn means that waves emerging from an optical maser will be distorted, and hence such a beam will not have ideal collimation and focusing properties. As these factors are quite important to many optical maser applications they are also treated.

Finally, it should be emphasized that the scope of this paper is limited to the confocal Fabry-Perot resonator. The convenience with which the confocal geometry may be handled analytically is the primary motivation for this restriction. One would thus expect this study to be applicable to gas laser theory where the confocal geometry has been widely employed. However, Evtuhov (17) has presented evidence that the confocal theory is more appropriate than plane-parallel resonator theory for ruby lasers with plane ends. This results from a characteristic spatial variation in the refractive index of ruby crystals giving them the appearance of having curved ends when the ends are physically flat. This suggests that confocal theory may correctly describe the field characteristics of most optical maser resonators currently in use.

## 1.3 Scattering from Irregular Surfaces

Central to the problem of determining the resonance characteristics of a perturbed cavity is the theory of electromagnetic scattering from a rough surface. A large number of papers have been published treating this field from various points of view and for a range of geometries. Much of this work was initiated through a need to gain a fuller understanding of radar sea clutter; therefore, its validity is restricted to cases where the radiation wavelength is negligible relative to the heights of the surface irregularities. These studies then are not applicable to scattering in an optical resonator where the roughness must be very slight by necessity. Mitzner (29) has recently presented a theory of scattering from irregular surfaces which contains a comprehensive bibliography and review of such sea clutter oriented papers. In this paper that aspect of the general scattering problem will not be commented upon further.

Some recent work has been reported concerning scattering from surfaces with small scale roughness (25-28). These studies are based, either implicitly or explicitly, on a perturbation treatment. They postulate a scalar electromagnetic wave incident upon a perfectly conducting surface of infinite extent. The surface deviates only slightly from a perfect plane. The random process describing the irregularities is assumed to be single-valued and bounded such that no areas are shadowed from the radiation. Thus, the maximum deviation must be small relative to the radiation wavelength and the surface slope must be small. Bass and Bocharov (25) work out the rigorous

perturbation series in generality. Davies (27) assumes that surface currents are set up of the same magnitude as those in the smooth surface but with phases varying according to the local height of the irregularities. His method is equivalent to taking the first perturbation term of Bass and Bocharov.

Davies' results give the specular reflectance at normal incidence of a slightly rough, perfectly conducting plane surface;

$$R_s = \exp\left[-(4\pi\sigma)^2/\lambda^2\right] \quad , \tag{1.14}$$

where $\sigma$ is the root mean square roughness. If it is assumed that the irregularities have a very short correlation distance we may take the radiation field in a resonator as being statistically independent of the roughness and then approximate the diffraction loss by 1.14. The $Q$ of a resonator with one such rough mirror becomes

$$Q \cong \frac{b\lambda}{4\pi\sigma^2} \quad . \tag{1.15}$$

We see that 1.14 is quite different from the approximation of 1.12. Curiously, they yield the same value for $Q$ when $\sigma = \frac{\lambda}{4\pi}$, which is not far from the roughness one might encounter in practice.

By employing two common techniques for estimating the $Q$ of an optical resonator we have obtained quite different results. It is clear from both, however, that the $Q$ is a very sensitive function of mirror roughness.

The above considerations suggest performing a more exact analysis of the relationship between roughness and $Q$ not only as a practical matter in laser technology but to provide an improved means

of studying surface irregularities. Surfaces with small scale imperfections are frequently studied via their reflectivity. Unfortunately, for slight roughness the specular reflectance as given by 1.14 is a rather insensitive function of $\sigma$. When the scattering is measured in some other manner it generally depends on several aspects of the surface such as the root mean square slope, root mean square deviation and correlation distance. However, we would expect the $Q$ to depend on the characteristics of the roughness in much the same fashion as the specular reflectance. Thus employing an optical resonator for roughness measurements appears attractive and should be less amenable to experimental error than previous methods.

# CHAPTER II

## CONVENTIONAL CONFOCAL RESONATOR THEORY

### 2.1 The Symmetric Spherical Fabry-Perot Resonator

In this section the Boyd and Gordon (5) treatment of the confocal resonator with identical spherical reflectors separated by their common radius of curvature is reviewed. Such a resonator is illustrated schematically in Figure 2.1.

The radiation wavelength is assumed negligible in comparison to the resonator dimensions. In addition we require $b \gg a$. Postulating a linearly polarized electric field distribution on the primed reflector $E_o f_m(x')g_n(y')$, the field on the other mirror, $E_y$, may be computed with the aid of the Kirchhoff formulation of Huygen's principle. Then

$$E_y = \iint_{-a}^{+a} \frac{ik}{2\pi\rho} e^{-ik\rho} E_o f_m(x')g_n(y')dx'dy' \quad . \tag{2.1}$$

The quantity $K = \frac{2\pi}{\lambda}$, where $\lambda$ is the radiation wavelength. $\rho$ is the distance between two arbitrary points on the two mirrors. We require $E_y$ to be proportional to the initial field in order to obtain the normal modes. We set $E_y = \sigma_m \sigma_n E_o f_m(x)g_n(y)$ in 2.1 and obtain

$$\sigma_m \sigma_n f_m(x)g_n(y) = \frac{ik}{2\pi} \iint_{-a}^{+a} \frac{e^{-ik\rho}}{\rho} f_m(x')g_n(y')dx'dy' \quad , \tag{2.2}$$

where $\sigma_m \sigma_n$ is the transfer factor expressing the phase shift and diffraction loss in making one transit of the resonator. As the

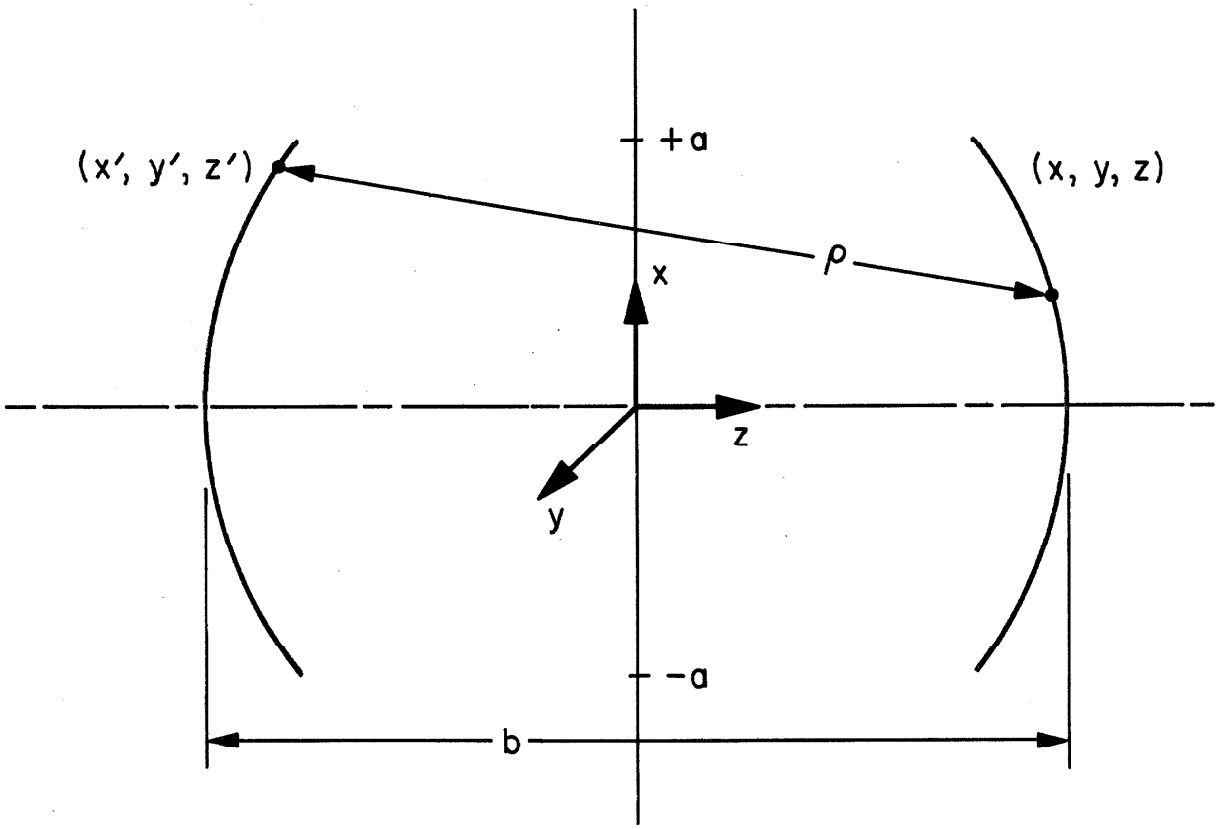


Fig. 2.1 Confocal resonator with square mirrors and spherical curvature.

aperture 2a is small relative to the separation b and the geometry is confocal the distance $\rho$ may be approximated;

$$\rho \cong b - \frac{xx' + yy'}{b} \quad . \tag{2.3}$$

2.3 is employed in the exponent and little error is incurred by taking only the first term of 2.3 where $\rho$ appears in the denominator of the integrand. With these substitutions equation 2.2 becomes

$$\sigma_m \sigma_n f_m(x) g_n(y) = \frac{ike^{-ikb}}{2\pi b} \int_{-a}^{+a}\int e^{i\frac{k}{b}(xx'+yy')} f_m(x') g_n(y') dx'dy' \quad . \tag{2.4}$$

Consequently, the transverse eigenfunctions satisfy integral equations of exactly the same form. They are

$$\sigma_m f_m(x) = \frac{c^{i(\frac{\pi}{4} - \frac{kb}{2})}}{\sqrt{\lambda b}} \int_{-a}^{+a} e^{i\frac{k}{b}xx'} f_m(x')dx' \quad , \tag{2.5}$$

$$\sigma_n g_n(y) = \frac{e^{i(\frac{\pi}{4} - \frac{kb}{2})}}{\sqrt{\lambda b}} \int_{-a}^{+a} e^{i\frac{k}{b}yy'} g_n(y')dy' \quad . \tag{2.6}$$

Considering only 2.5 for the moment and defining the normalized variables $\eta \equiv \frac{x}{a}$, $\eta' \equiv \frac{x'}{a}$ and the quantity $c \equiv \frac{ka^2}{b}$ we have

$$\sigma_m f_m(\eta) = \sqrt{\frac{c}{2\pi}}\, e^{i(\frac{\pi}{4} - \frac{kb}{2})} \int_{-1}^{+1} e^{ic\eta\eta'} f_m(\eta')d\eta' \quad . \tag{2.7}$$

It is clear that the eigenfunctions of this integral equation are self reciprocal under a finite Fourier transformation. From Flammer (24) it

is clear that the angular prolate spheroidal wave functions $S_{om}(c,\eta)$ have just this property and satisfy the equation

$$2i^m R_{om}^{(1)}(c,1)\, S_{om}(c,t) = \int_{-1}^{+1} e^{icts}\, S_{om}(c,s)ds \ , \tag{2.8}$$

where $R_{om}^{(1)}(c,1)$ is the radial prolate spheroidal wave function. By identification between 2.7 and 2.8 we find the eigenfunctions and eigenvalues of the confocal resonator.

$$f_m(\eta) = S_{om}(c,\eta) \tag{2.9}$$

$$\sigma_m = \sqrt{\frac{2c}{\pi}}\, i^m\, R_{om}^{(1)}(c,1)\, e^{i(\frac{\pi}{4} - \frac{kb}{2})} \tag{2.10}$$

Thus, the electric field at an aperture is

$$E_y = \sigma_m \sigma_n E_o S_{om}(c,\tfrac{x}{a})\, S_{on}(c,\tfrac{y}{a}) \ , \tag{2.11}$$

and the corresponding transfer factor becomes

$$\sigma_m \sigma_n = \frac{2c}{\pi}\, R_{om}^{(1)}(c,1)\, R_{on}^{(1)}(c,1)\, e^{i\left[\frac{\pi}{2}(m+n+1) - kb\right]} \ . \tag{2.12}$$

The resonance condition is obtained by setting the round trip phase shift equal to an integer $q$ times $2\pi$. Then

$$2\pi q = 2\left|\tfrac{\pi}{2}(m+n+1) - kb\right| \ , \tag{2.13}$$

or

$$\frac{4b}{\lambda} = 2q + (m+n+1) \ . \tag{2.14}$$

The fractional power loss per transit, $\alpha_D$, due to diffraction follows from 2.12 and the fact that the power is proportional to the electric

field squared.

$$\alpha_D = 1 - |\sigma_m \sigma_n|^2$$

$$= 1 - \left(\frac{2c}{\pi}\right)^2 \left[R_{om}^{(1)}(c,1)\, R_{on}^{(1)}(c,1)\right]^2 . \qquad (2.15)$$

The various modes are designated as $TEM_{mnq}$ where $m$ and $n$ refer to the transverse order and $q$ refers to the longitudinal order.

This completes the formal summary of the Boyd-Gordon approach to confocal resonator theory. Before proceeding into an analysis of perturbed resonators some extensions of this treatment, needed later, will be presented now.

## 2.2 Asymptotic Solutions for the Confocal Resonator

In subsequent sections of this paper it will be necessary to evaluate certain integrals involving spheroidal wave functions. This is most readily accomplished through the use of the asymptotic expressions for the resonator eigenfunctions in the limit of large $c$. This is the same as taking the limit as the wavelength approaches zero, which is consistent with the analytical treatment presented so far. Referring to equation 2.5 the eigenfunctions must satisfy

$$\sigma_m f_m(t) = \frac{e^{i\left(\frac{\pi}{4} - \frac{kb}{2}\right)}}{\sqrt{2\pi}} \int_{-\sqrt{c}}^{+\sqrt{c}} e^{itt'} f_m(t')dt' , \qquad (2.16)$$

where $t \equiv \frac{k}{b} x$ , $t' = \frac{k}{b} x'$ . In the zero wavelength limit the eigenfunctions are self reciprocal under a common Fourier transformation.

$$\sigma_m f_m(t) = \frac{c^{i(\frac{\pi}{4} - \frac{kb}{2})}}{\sqrt{2\pi}} \int_{-\infty}^{\infty} e^{itt'} f_m(t')dt' \tag{2.17}$$

It is well known that the functions having this property are the Hermite polynomials with a gaussian density function. In other words the functions satisfying the equation

$$\phi_n(u) = \frac{i^{-n}}{\sqrt{2\pi}} \int_{-\infty}^{\infty} e^{iuv} \phi_n(v)dv \tag{2.18}$$

are given by the relation

$$\phi_n(u) = e^{-\frac{1}{2}u^2} H_n(u) \ . \tag{2.19}$$

It follows that the limiting form of the resonator eigenfunction is

$$f_m(\sqrt{c}\eta) = e^{-\frac{1}{2}c\eta^2} H_m(\sqrt{c}\eta) \ . \tag{2.20}$$

In this case the transfer factor is imaginary indicating zero diffraction loss.

$$\sigma_m = i^m e^{i(\frac{\pi}{4} - \frac{kb}{2})} \tag{2.21}$$

## 2.3 The Planar-Spherical Resonator

Let us consider now the configuration illustrated in Figure 2.2. This hybrid cavity which we shall term the planar-spherical resonator is of practical importance and may be visualized as derivable from the confocal system by locating a flat reflector at the common focal plane of the spherical mirrors. Thus, it is a folded over confocal resonator. Its resonance properties may be deduced readily from

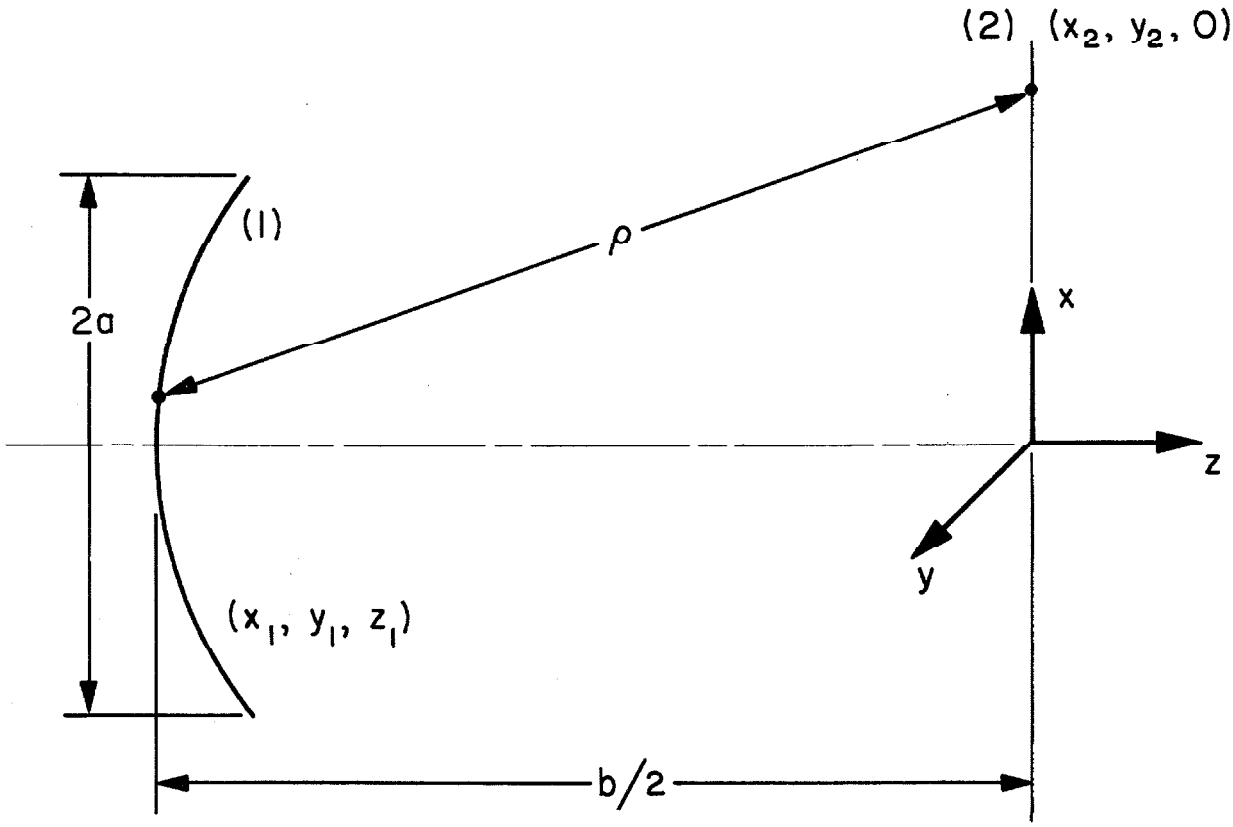


Fig. 2.2 Half confocal resonator with infinite plane mirror.

those of the spherical Fabry-Perot. In addition inspection of 2.5 and 2.6 leads one to the conclusion that it is unnecessary to consider the problem in three dimensions. The separated equations for the x and y dependence will be identical within a phase factor to the equation for a two-dimensional strip resonator.

Rather than accepting the above statements from deduction it will be instructive to prove them directly. In addition the working out of the analytical details will be useful later when considering perturbed resonators.

Referring to Figure 2.2 we define a spherical surface (1) with a radius of curvature b and square sides of width 2a. It is located at a distance $\frac{b}{2}$ to the left of an infinite plane mirror (2). We want to show that this half resonator has the same eigenfunction field distributions on mirror (1) as the equivalent full resonator. Our approach will be to postulate an initial field distribution on mirror (1) and compute the resultant field on mirror (2). Then by a similar computation work back to (1). Considering the image of mirror (1) in (2) we would expect this (1)-(2)-(1) propagation to be equivalent to a single transit of the full confocal system of Section 2.1.

By means of Kirchhoff's formulation of Huygen's principle the field distribution on mirror (2), $E_2(x_2,y_2)$, is computed from that on mirror (1).

$$E_2(x_2,y_2) = \frac{ik}{2\pi} \int_{-a}^{a}\int \frac{e^{-ik\rho_1}}{\rho_1} E_1(x_1,y_1)dx_1dy_1 \ , \qquad (2.22)$$

where $\rho_1$ is the distance from $(x_1,y_1)$ to $(x_2,y_2)$ and is given by

$$\rho_1 = b\left[\left(1 - \frac{x_1^2 + y_1^2}{b^2}\right)^{\frac{1}{2}} - \frac{1}{2}\right]\left[1 + 4\,\frac{(x_2 - x_1)^2 + (y_2 - y_1)^2}{b^2}\right]^{\frac{1}{2}}$$

$$\cong \frac{b}{2}\left[1 + \frac{2}{b^2}\left(x_2^2 - 2x_1x_2 + \frac{x_1^2}{2} + y_2^2 - 2y_1y_2 - \frac{y_1^2}{2}\right)\right]$$

Similarly, the field $\bar{E}_1(\bar{x}_1,\bar{y}_1)$ reradiated back to (1) from (2) is

$$\bar{E}_1(\bar{x}_1,\bar{y}_1) = -\frac{ik}{2\pi}\iint_{-\infty}^{\infty}\frac{e^{-ik\rho_2}}{\rho_2}\,E_2(x_2,y_2)\,dx_2dy_2\ , \qquad (2.23)$$

where the distance $\rho_2$ between the locations $(x_2,y_2)$ and $(\bar{x}_1,\bar{y}_1)$ is

$$\rho_2 = b\left[\left(1 - \frac{\bar{x}_1^2 + \bar{y}_1^2}{b^2}\right)^{\frac{1}{2}} - \frac{1}{2}\right]\left[1 + 4\,\frac{(x_2 - \bar{x}_1)^2 + (y_2 - \bar{y}_1)^2}{b^2}\right]^{\frac{1}{2}}$$

$$\cong \frac{b}{2}\left[1 + \frac{2}{b^2}\left(x_2^2 - 2\bar{x}_1x_2 + \frac{\bar{x}_1^2}{2} + y_2^2 - 2\bar{y}_1y_2 - \frac{\bar{y}_1^2}{2}\right)\right]\ .$$

Combining 2.22 and 2.23 we find an approximate expression for $\bar{E}_1(\bar{x}_1,\bar{y}_1)$ in terms of the initial field $E_1(x_1,y_1)$.

$$\bar{E}_1(\bar{x}_1,\bar{y}_1) = \frac{k^2}{\pi^2 b^2}\int_{-\infty}^{\infty}dx_2dy_2\int_{-a}^{a}dx_1dy_1\,E_1(x_1,y_1)\,e^{-ik(\rho_1+\rho_2)} \qquad (2.24)$$

In arriving at 2.24 we set $\rho_1$ and $\rho_2$ equal to $\frac{b}{2}$ in the denominator of the integrand. The exponential term involves the sum of $\rho_1$ and $\rho_2$ and referring to their approximate expressions we see that this involves no cross terms between $x$ and $y$ coordinates.

Consequently, 2.24 may be separated into integrals over x and y. Now, separating the field functions $\bar{E}_1(\bar{x}_1,\bar{y}_1)$ and $E_1(x_1,y_1)$ into orthogonal amplitude factors as follows;

$$E_1(x_1,y_1) = E_1(x_1)\, E_1(y_1) ,$$

$$\bar{E}_1(\bar{x}_1,\bar{y}_1) = \bar{E}_1(\bar{x}_1)\, \bar{E}_1(\bar{y}_1) ,$$

we have for 2.24

$$\bar{E}_1(\bar{x}_1)\, \bar{E}_1(\bar{y}_1) \cong \frac{i^2 e^{-ikb}}{\pi^2 b^2} \int_{-\infty}^{\infty} dx_2 \int_{-a}^{a} dx_1\, E_1(x_1)$$

$$e^{-\frac{ik}{b}\left[2x_2^2 - 2x_2(x_1+\bar{x}_1)+\frac{x_1^2+\bar{x}_1^2}{2}\right]} \int_{-\infty}^{\infty} dy_2 \int_{-a}^{a} dy_1\, E_1(y_1)$$

$$e^{-\frac{ik}{b}\left[2y_2^2 - 2y_2(y_1+\bar{y}_1)+\frac{y_1^2+\bar{y}_1^2}{2}\right]} .$$

Performing the $x_2$ and $y_2$ integrations;

$$\bar{E}_1(\bar{x}_1)\, \bar{E}_1(\bar{y}_1) \cong \frac{k}{2\pi b}\, e^{-i\left(kb-\frac{\pi}{2}\right)} \int_{-a}^{a} dx_1\, E_1(x_1)\, e^{-ikx_1\bar{x}_1}$$

$$\int_{-a}^{a} dy_1\, E_1(y_1)\, e^{-iky_1\bar{y}_1} , \qquad (2.25)$$

which is identical to the full confocal resonator integral equation as was to be shown.

Having demonstrated that the same mathematics describes both

the full and half resonators let us now go one step further and show that when treating such cavities we do not need to treat the three-dimensional case. Let us consider a two-dimensional infinite strip half resonator. Let such a resonator consist of a circular trough of width 2a and radius of curvature b at a distance $\frac{b}{2}$ from an infinite plane. We may refer again to Figure 2.2 but now there is no y dependence.

By means of Kirchhoff's two-dimensional formulation of Huygen's principle the one-dimensional field distribution on mirror (2), $E_2(x_2)$, is computed in terms of that on the curved strip mirror (1).

$$E_2(x_2) = \frac{e^{i\frac{\pi}{4}}}{\sqrt{\lambda}} \int_{-a}^{a} \frac{e^{-ik\rho_1}}{\sqrt{\rho_1}} E_1(x_1)dx_1$$

Similarly, for the radiation returning to (1);

$$\bar{E}_1(\bar{x}_1) = -\frac{e^{-i\frac{\pi}{4}}}{\sqrt{\lambda}} \int_{-\infty}^{\infty} \frac{e^{-ik\rho_2}}{\sqrt{\rho_2}} E_2(x_2)dx_2 ,$$

where

$$\rho_1 \cong \frac{b}{2}\left[1+\frac{2}{b^2}\left(\frac{x_1^2}{2} - 2x_1x_2 + x_2^2\right)\right] ,$$

$$\rho_2 \cong \frac{b}{2}\left[1+\frac{2}{b^2}\left(\frac{\bar{x}_1^2}{2} - 2\bar{x}_1x_2 + x_2^2\right)\right] .$$

Combining these expressions as before,

$$\bar{E}_1(\bar{x}_1) = \frac{e^{-i(kb-\frac{\pi}{4})}}{\sqrt{\lambda b}} \int_{-a}^{a} dx_1\, e^{i\frac{k}{b}x_1\bar{x}_1} E_1(x_1) . \qquad (2.26)$$

Comparing 2.26 for the strip resonator and 2.25 for the three-dimensional half-confocal resonator we see that with the exception of the multiplying constant the orthogonal field distribution functions obey exactly the same equations in the two cases. Bearing this in mind we shall limit the analysis to two-dimensional resonators henceforth, remembering that it is a simple matter to generalize the results to three-dimensional cases.

To complete the analysis of the half resonator we now let the width of the trough become infinite and reduce the plane mirror to width 2a. Now an initial field distribution is assumed on the plane mirror (2) and we follow it in propagating to mirror (1) and back to its starting point, mirror (2). In this way the field distribution on the flat mirror may be computed through the self consistent field analysis. The reason for interchanging the finite and infinite widths of the two mirrors is to facilitate the intermediate integration which can be performed readily over infinite limits. Then the total diffraction loss of such a resonator may be found approximately by adding the loss for a finite width curved mirror resonator and finite width plane mirror resonator.

Now we may start with a field distribution on a flat mirror of width 2a and require that it reproduce itself after being reflected by a concave mirror of infinite extent and at a distance of one half its radius of curvature. With the same notation as before we find a one-dimensional equation analogous to 2.24, but for the field distribution on the flat mirror instead.

$$\bar{E}_2(\bar{x}_2) = -\frac{2ie^{-ikb}}{\lambda b}\int_{-a}^{a} dx_2\, e^{-i\frac{k}{b}(x_2^2+\bar{x}_2^2)}\, I_2(x_2,\bar{x}_2)\, E_2(x_2)\,, \tag{2.27}$$

where

$$I_2(x_2,\bar{x}_2) = \int_{-\infty}^{\infty} e^{-\frac{ik}{b}\left[x_1^2 - 2x_1(x_2+\bar{x}_2)\right]}\, dx_1 \tag{2.28}$$

$$= e^{-i\frac{\pi}{4}}\sqrt{\frac{\pi b}{\lambda}}\, e^{i\frac{k}{b}(x_2+\bar{x}_2)^2}\,.$$

Inserting 2.28 into 2.27 we have

$$\bar{E}_2(\bar{x}_2) = -\sqrt{\frac{2}{\lambda b}}\, e^{i(\frac{\pi}{4}-kb)}\int_{-a}^{+a} e^{i\frac{2k}{b}x_2\bar{x}_2}\, E_2(x_2)dx_2\,. \tag{2.29}$$

Equation 2.29 shows just what could have been deduced from general confocal resonator theory. It indicates that the field distribution functions are the angular spheroidal wave functions and that the spot size on the flat mirror is $2^{-\frac{1}{2}}$ times that on the curved surface. However, by such a treatment as in this section we are able to predict the diffraction loss of such a resonator when both mirrors are finite. It will be simply the sum of the losses of the two configurations treated here.

Inspection of 2.26 yields a transfer factor for the infinite plane mirror case of

$$\sigma_{n1} = \sqrt{\frac{2c_1}{\pi}}\, i^n\, e^{i(\frac{\pi}{4}-kb)}\, R_{on}^{(1)}(c,1)\,, \tag{2.30}$$

where $c_1 = \frac{ka_1^2}{b}$, and $a_1$ is the half aperture of the curved mirror. From 2.29 we find

$$\sigma_{n2} = 2\sqrt{\frac{c_2}{\pi}}\, i^n\, e^{i(\frac{\pi}{4} - kb)}\, R_{on}^{(1)}(2c_2, 1) \ . \qquad (2.31)$$

Here $c_2 = \frac{ka_2^2}{b}$, $a_2$ being the flat mirror half aperture.

The diffraction losses associated with the above transfer factors will be

$$\alpha_{n1} = 1 - \frac{2c_1}{\pi}\left[R_{on}^{(1)}(c,1)\right]^2 ,$$

$$\alpha_{n2} = 1 - \frac{4c_2}{\pi}\left[R_{on}^{(1)}(2c_2,1)\right]^2 .$$

It follows that the diffraction loss to first order of a half resonator with finite apertures at both mirrors will be

$$\alpha_n = \alpha_{n1} + \alpha_{n2}$$

$$= 2 - \frac{2c_1}{\pi}\left[R_{on}^{(1)}(c_1,1)\right]^2 - \frac{4c_2}{\pi}\left[R_{on}(2c_2,1)\right]^2 .$$

If the apertures are equal, then $a_1 = a_2$ and

$$\alpha_n = 2\left\{1 - \frac{c}{\pi}\left[R_{on}^{(1)}(c,1)\right]^2 + 2\left[R_{on}^{(1)}(2c,1)\right]^2\right\} . \qquad (2.32)$$

For the case of the ratio of spot size to aperture size being the same at both mirrors we have $a_1 = 2\,a_2$. Then

$$\alpha_r = 2\left\{1 - \frac{2c}{\pi}\left[R_{on}^{(1)}(c,1)\right]^2\right\} . \qquad (2.33)$$

Equation 2.33 indicates that a half resonator with finite apertures of ratio $\sqrt{2}$ will have twice the diffraction loss of the equivalent full resonator.

In this section the relations necessary to a perturbation treatment of such a resonator have been developed.

## 2.4 The Mathematical Technique for Unsymmetrical Confocal Resonators

When considering a confocal resonator as illustrated in Figure 2.1 the characteristic integral equation is formulated by requiring the field to reproduce itself in form after one transit of the resonator. This procedure is legitimate for a symmetrical resonator. As the final topic in this preparatory chapter we consider the manner in which such a resonator may be treated when it is not quite symmetrical, say, due to random irregularities on the reflectors. At this point we will not explicitly introduce the perturbation, but will treat the ideal resonator as if it were unsymmetrical.

This being the case the field distribution must reproduce itself in form after a round trip through the resonator. With this requirement the equations can then be formulated in exactly the same manner as those for the half resonator of the preceding section. Doing this the equation corresponding to equation 2.29 is

$$\sigma^2 E_1(\bar{x}_1) = \frac{ie^{-2ikb}}{\lambda b} \int_{-a}^{+a} dx_1 \; k(x_1, \bar{x}_1) \; E_1(x_1) \; , \qquad (2.34)$$

where

$$k(x_1,\bar{x}_1) = \int_{-a}^{+a} dx_2 \; e^{\frac{ik}{b}(x_1+\bar{x}_1)x_2}$$

$$= \frac{2b}{k} \frac{\sin \frac{ka}{b}(x_1+\bar{x}_1)}{(x_1+\bar{x}_1)} \quad . \tag{2.35}$$

$E_1(x_1)$ is the field distribution on one of the mirrors and $\sigma^2$ is the round trip transfer factor. Introducing normalized variables as in Section 2.1 we have

$$\sigma^2 E_1(\bar{\eta}_1) = \frac{ice^{-2ikb}}{\pi} \int_{-1}^{+1} d\eta_1 \frac{\sin c(\eta_1+\bar{\eta}_1)}{c(\eta_1+\bar{\eta}_1)} E_1(\eta_1) \; . \tag{2.36}$$

Referring to Flammer (24) we find that the spheroidal wave functions satisfy this integral equation. Fortunately, we find exactly the same solutions as when considering a single transit.

# CHAPTER III

# ELECTROMAGNETIC SCATTERING FROM AN IRREGULAR SURFACE

## 3.1 Perturbation Treatment of the Boundary Conditions

Let us consider a plane wave incident on a perfectly conducting surface which deviates slightly from the plane $z = 0$. This deviation is represented by $z = g(x,y)$, where the function $g(x,y)$ is assumed to be continuous, single-valued and bounded such that its maxima are small compared to the radiation wavelength. This will insure that no parts of the surface are shielded from near normal radiation.

In calculating the radiation scattered by such a surface the perturbation approach of Bass and Bocharov (25) is employed. For the perfectly conducting surface introduced above the boundary conditions may be expressed as follows:

$$\begin{aligned} E_x + E_z \frac{\partial g}{\partial x} &= 0 \,, \\ E_y + E_z \frac{\partial g}{\partial y} &= 0 \,. \end{aligned} \tag{3.1}$$

Next the total field $E$ on the surface is expressed as a power series in $g$.

$$E(x,y,g(x)) = E(x,y,0) + \left|\frac{\partial E}{\partial z}\right|_{z=0} g + \frac{1}{2}\left|\frac{\partial^2 E}{\partial z^2}\right|_{z=0} g^2 + \ldots \tag{3.2}$$

We seek a series solution for the radiation field of the form

$$E(x,y,z) = E^{(0)}(x,y,z) + E^{(1)}(x,y,z) + E^{(2)}(x,y,z) + \ldots \tag{3.3}$$

In 3.3 $E^{(o)}$ represents the unperturbed total field above a perfectly smooth surface. The terms $E^{(n)}$ are the various orders of perturbation fields excited by the surface roughness. Introducing 3.3 and 3.2 into 3.1 we effectively satisfy the boundary conditions at the plane $z = 0$ and determine the magnitudes of the $E^{(n)}$ there. The first two perturbation fields fall out easily and are

$$E^{(1)}_{x,y} = - \frac{\partial E^{(o)}_{x,y}}{\partial z} g \ ,$$

$$E^{(2)}_{x,y} = - \frac{\partial E^{(1)}_{x,y}}{\partial z} g \ . \qquad (3.4)$$

In obtaining 3.4 the $E^{(n)}_z$ were set equal to zero in light of the transverse field solutions of Chapter II. Also it was noted that $\partial^2 E^{(o)}_{x,y}/\partial z^2$ vanishes at the plane $z = 0$. By means of 3.4 and the Kirchhoff formula the field at any point in space may now be computed in terms of an integral over the surface $z = 0$.

## 3.2 Derivation of the Perturbed Green's Function

The confocal resonator field solution presented earlier is based on Kirchhoff's formulation of the scalar Huygens-Fresnel principle. For the geometry of interest the Kirchhoff formula for a transverse field component may be expressed in the form

$$E_y = \frac{ik}{2\pi} \int_s E_o G(\rho) ds \ , \qquad (3.5)$$

where

$$G(\rho) = \frac{e^{-ik\rho}}{\rho} \ .$$

By means of the method of Bass and Bocharov the perturbation terms for the field on the regular surface were computed in the preceding section. The results are

$$E_y^{(1)} = -\frac{\partial E^{(o)}}{\partial z} g \,,$$
$$E_y^{(2)} = -\frac{\partial E^{(1)}}{\partial z} g \,. \tag{3.6}$$

In the confocal problem $E_z = 0$ and in the neighborhood of the surface the total unperturbed field may be written,

$$E^{(o)} = E_o(e^{-ikz} - e^{ikz})\, e^{i\omega t} \,.$$

Now the perturbation terms are easily evaluated. Dropping the time dependence they are

$$\left.\begin{aligned} E^{(1)} &= 2ikg\, E_o \\ E^{(2)} &= -2k^2g^2\, E_o \end{aligned}\right\} \quad z = 0 \tag{3.7}$$

Employing these values in 3.5 we find the expression for the perturbed diffracted field.

$$E_y' = \frac{ik}{2\pi} \int_s E_o(1 + 2ikg - 2k^2g^2)\, \frac{e^{-ik\rho}}{\rho}\, ds \,. \tag{3.8}$$

Thus the perturbed Green's function may be written,

$$G'(\rho) = (1 + 2ikg - 2k^2g^2)\, \frac{e^{-ik\rho}}{\rho} \,. \tag{3.9}$$

For the sake of comparison we may derive an alternate perturbed Green's function as follows. Assume that each localized region

of the confocal surface scatters as an unperturbed plane surface. Then introduce the effect of the surface displacement $g$ as a variation in the distance $\rho$. The phase shift in a reflected wave will be $-2ikg$ so we have alternately

$$G'(\rho) = \frac{e^{-ik\rho + 2ikg}}{\rho}$$
$$= (1 + 2ikg - 2k^2g^2 - \frac{4}{3} ik^3g^3 + \ldots) \frac{e^{-ik\rho}}{\rho} . \qquad (3.10)$$

Comparing 3.9 and 3.10 it is evident that the first three terms in their respective expansions are identical. We see that the two approaches are essentially equivalent when dealing solely with transverse field components. At the same time we have demonstrated the equivalence of the two types of treatments to be found in the literature.

In deriving these perturbed kernels it was assumed that in the neighborhood of the surface the field behaves as if it were a plane wave. Now in a spherical Fabry-Perot resonator each mirror is at the effective focus of the spherical wave converging upon it from the other mirror. Thus, each mirror is at the localized Fraunhoffer region of the focal plane. Therefore, let us look at the detailed nature of a three-dimensional field near the focus.

Consider first the wave intensity. According to Born and Wolf (22) we have in the focal region

$$I(u,v) = \left(\frac{2}{u}\right)^2 \left[ U_1^2(u,v) + U_2^2(u,v) \right] I_o , \qquad (3.11)$$

where the $U_n$ are Lommel functions given by

$$U_n(u,v) = \sum_{s=0}^{\infty} (-1)^s \left(\frac{u}{v}\right)^{h+2s} J_{n+2s}(v) \ . \qquad (3.12)$$

The quantity $u$ is a normalized longitudinal distance and $v$ is a normalized transverse coordinate. $I_o$ is the intensity at the geometrical focus $u,v = 0$. We are interested in the behavior of $I(u,v)$ for very small values of $u$. Then,

$$U_1(u,v) \cong \left(\frac{u}{v}\right) \left[J_1(v) - \left(\frac{u}{v}\right)^2 J_3(v)\right] \ ,$$

$$U_2(u,v) \cong \left(\frac{u}{v}\right)^2 J_2(v) \ .$$

Using these approximate expressions in 3.11 we find,

$$I(u,v) \cong \left(\frac{2}{u}\right)^2 \left\{\left(\frac{u}{v}\right)^2 \left[J_1(v) - \left(\frac{u}{v}\right)^2 J_3(v)\right]^2 + \left(\frac{u}{v}\right)^4 J_2^2(v)\right\} I_o \ . \qquad (3.13)$$

$$\cong \left(\frac{2}{v}\right)^2 I_o \, J_1^2(v) \ .$$

From 3.13 it is clear that the field strength is constant for small deviations from the focal plane.

Next we consider the phase behavior near the focal plane. This is given by

$$\phi(u,v) = \left(\frac{f}{a}\right)^2 u - \chi(u,v) - \frac{\pi}{2} \ ,$$

where

$$\sin \chi = \frac{s}{\sqrt{c^2 + s^2}} ,$$

$$c(u,v) = \frac{\cos \frac{1}{2}u}{\frac{1}{2}u} U_1(u,v) + \frac{\sin \frac{1}{2}u}{\frac{1}{2}u} U_2(u,v) ,$$

$$s(u,v) = \frac{\sin \frac{1}{2}u}{\frac{1}{2}u} U_1(u,v) - \frac{\cos \frac{1}{2}u}{\frac{1}{2}u} U_2(u,v) .$$

For small u we have

$$c(u,v) \cong \frac{2}{v} J_1(v) - \left(\frac{u}{v}\right)^2 \left[\frac{J_1(v)}{\frac{1}{2}v} - J_2(v)\right] ,$$

$$s(u,v) \cong \frac{u}{v} \left[J_1(v) - \frac{2}{v} J_2(v)\right] .$$

Then

$$\sin \chi \cong \frac{u}{2} \left[1 - \frac{2}{v} \frac{J_2(v)}{J_1(v)}\right] ,$$

and the expression for the relative phase reduces to

$$\phi(u,v) \cong u \left[\left(\frac{f}{a}\right)^2 - \frac{1}{2} + \frac{1}{v} \frac{J_2(v)}{J_1(v)}\right] - \frac{\pi}{2} .$$

This expression shows that we may assume a linear phase shift when looking at sufficiently small deviations of a surface from the exact focal plane.

In this section the perturbed Green's function was derived assuming that in the immediate vicinity of the irregular surface the incident wave may be represented by a plane wave. By studying the behavior of a converging spherical wave near its geometrical focus we

found that such an assumption is justified.

## 3.3 The Scattered Field: Statistical Considerations and Orthogonal Expansion

Before proceeding to evaluate the eigenfunctions and eigenvalues of the perturbed confocal resonator let us take a look at some characteristics of the field scattered by a general irregular surface. As a starting point consider the two-dimensional formulation of 3.8.

$$E'_y = \frac{e^{i\frac{\pi}{4}}}{\sqrt{\lambda}} \int_s E_o(1 + 2ikg(x) - 2k^2g^2(x)) \frac{e^{-ik\rho}}{\sqrt{\rho}} dx \qquad (3.14)$$

The function $g(x)$ is assumed to be a stationary gaussian random process with zero mean, variance $\sigma_s^2$ and a correlation function $R(x - x') = \langle g(x)\, g(x') \rangle$ . Taking the expectation of 3.14 the mean value of the scattered field becomes

$$\langle E'_y \rangle = \frac{e^{i\frac{\pi}{4}}}{\sqrt{\lambda}} (1 - 2k^2\sigma_s^2) \int_s E_o \frac{e^{-ik\rho}}{\sqrt{\rho}} dx \ . \qquad (3.15)$$

Thus, the mean of the scattered field changes only to second order. Similarly the variance of the total scattered field may be determined.

$$\langle E'_y\, E'^{*}_y \rangle = \frac{1}{\lambda} \iint_{ss} E_o(x)\, E_o^*(x') \left[1 - 4k^2\sigma_s^2 + 4k^2R(x - x')\right] \qquad (3.16)$$

$$\frac{e^{-ik(\rho - \rho')}}{\sqrt{\rho\rho'}} dxdx'$$

Finally, the variance of the perturbation field is

$$\left\langle (E_y' - E^{(o)})\ (E_y' - E^{(o)})^* \right\rangle = \frac{1}{\lambda} \iint_{S S'} E_o(x)\ E_o(x')^* \left[ 4k^2 R(x - x') \right] \frac{e^{-ik(\rho - \rho')}}{\sqrt{\rho\rho'}}\, dx dx' \qquad (3.17)$$

$$= \left\langle E^{(1)} E^{(1)*} \right\rangle \quad .$$

The preceding manipulations have illustrated the manner in which the characteristics of a scattered field may be handled. They have also brought into the open the fundamental difficulty that must be faced when attacking the problem of a perturbed resonator. We are dealing with a statistical quantity $g(x)$ which cannot be represented explicitly in the integral equation. It would be desirable to take the expectation of the entire integral equation and then solve for the statistical eigenfunctions and the statistical eigenvalues. If we were to attempt to proceed in this manner, expressions of the form $\langle g(x)\ E_o(x) \rangle$ would arise. In general we must first be able to solve the eigenvalue problem before such terms can be evaluated. In the following chapter we will approach the problem from this point of view by assuming the unperturbed confocal solutions in the integrand of the characteristic integral equation.

Before proceeding in that manner let us consider an alternate approach. The random process $g(x)$ may be expanded in an orthogonal series. If the terms are properly chosen the coefficients in the

expansion will be statistically independent random variables. The expansion may be represented as follows:

$$g(x) = \sum_s c_s \phi_s(x) \ , \tag{3.18}$$

where

$$\langle c_s \rangle = 0 \ ,$$

$$\langle c_s c_t \rangle = \begin{cases} 0 & \text{if} \quad s \neq t \\ 1 & \text{if} \quad s = t \ . \end{cases}$$

The functions $\phi_s(x)$ are orthogonal over the aperture. Now the first order surface perturbation term may be written as

$$E^{(1)} = 2ik \, E_o \sum_s c_s \phi_s(x) \ . \tag{3.19}$$

With this substitution in 3.14 we have

$$E'_y = \frac{e^{i\frac{\pi}{4}}}{\sqrt{\lambda}} \int_{-a}^{+a} E_o(x) \left[ 1 + 2ik \sum_s c_s \phi_s(x) \right] \frac{e^{-ik\rho}}{\sqrt{\rho}} \, dx \ . \tag{3.20}$$

Requiring the field to reproduce itself we arrive at the characteristic integral equation

$$\sigma \, E_o(x') = \frac{e^{i\frac{\pi}{4}}}{\sqrt{\lambda}} \int_{-a}^{+a} E_o(x) \left[ 1 + 2ik \sum_s c_s \phi_s(x) \right] \frac{e^{-ik\rho}}{\sqrt{\rho}} \, dx \ . \tag{3.21}$$

which can be solved in principle. The variance of the eigenvalue field can be obtained by simply squaring the solution $E_o(x)$ and making use of the statistical properties of the $c_s$'s.

In this chapter we have introduced two possible approaches to the boundary value problem of a perturbed confocal resonator. In

the next two chapters both of these techniques will be developed more fully. The first leads directly to a closed form approximation of the field distributions. In the second the determination of the eigenvalues for the resonator is easily carried out.

# CHAPTER IV

## SCATTERING FROM AN IMPERFECT CONFOCAL SURFACE

### 4.1 Formulation of the Scattering Integral for a Perturbed Confocal Resonator.

Let us begin by recapitulating our analytical development to this point. We found that when considering a confocal geometry in three dimensions the characteristic equation separates and the transverse solutions are independently solutions of the two-dimensional problem. We may thus neglect the three-dimensional character of the problem at this point. Then treating an infinite strip resonator with confocal mirrors the equation relating the field on a surface with normalized primed coordinates to that on the surface with unprimed coordinates is

$$E(\eta) = \sqrt{\frac{c}{2\pi}}\, e^{i(\frac{\pi}{4} - kb)} \int_{-1}^{+1} e^{ic\eta\eta'} E_o(\eta')d\eta' \ . \qquad (4.1)$$

Introducing an irregularity on the primed reflector by the normalized random function $h(\eta')$ the integral becomes

$$E(\eta) = \sqrt{\frac{c}{2\pi}}\, e^{i(\frac{\pi}{4} - kb)} \int_{-1}^{+1} e^{ic\eta\eta' + ikh(\eta')} E_o(\eta')d\eta' \ . \qquad (4.2)$$

Our procedure in this chapter will be to seek to integrate equations of the form of 4.2 for the statistical properties of the scattered field. The scattered field $E(\eta)$ will not be required to match the incident field $E_o(\eta')$. The incident field will be

represented by the unperturbed solutions of Chapter II. The approximate resonator eigenfunctions computed in this manner will not be as rigorous as those of the next chapter because correlation between the irregularities and eigenfunctions is neglected. However, the solutions obtained here can be represented in a simple functional form rather than as the sum of an infinite series of functions.

The important quantity which we wish to compute is the covariance of the scattered field. From 4.2 we find

$$\langle E(\eta_1)\, E^*(\eta_2)\rangle = \frac{c}{2\pi} \int_{-1}^{+1}\int e^{ic(\eta_1\eta_1' - \eta_2\eta_2')} \left\langle e^{ik\left[h(\eta_1') - h(\eta_2')\right]}\right\rangle E_o(\eta_1')E_o(\eta_2')d\eta_1'd\eta_2' \quad . \tag{4.3}$$

Assuming a gaussian correlation function for $h(\eta')$ and a correlation length $\ell$, 4.3 becomes

$$\langle E(\eta_1)\, E^*(\eta_2)\rangle = \frac{c}{2\pi} \int_{-1}^{+1}\int e^{ic(\eta_1\eta_1' - \eta_2\eta_2')}\, e^{-k^2\sigma_h^2\left[1 - R(\eta_1',\eta_2')\right]} E_o(\eta_1')E_o(\eta_2')d\eta_1'd\eta_2' \quad , \tag{4.4}$$

where

$$R(\eta_1',\eta_2') = e^{-(\eta_1' - \eta_2')^2/\ell^2} \quad ,$$

and $\sigma_h^2$ is the variance of the normalized roughness $h(\eta')$. Recalling that $k^2\sigma_h^2 \ll 1$ and requiring the surface correlation distance to be large compared to the mode spot size we find

$$\langle E(\eta_1)\, E^*(\eta_2)\rangle = \frac{c}{2\pi} \iint_{-1}^{+1} e^{ic(\eta_1\eta_1' - \eta_2\eta_2')} \left[1 - \frac{k^2\sigma_h^2}{\ell^2}(\eta_1' - \eta_2')^2\right] E_o(\eta_1')E_o(\eta_2')d\eta_1'd\eta_2' \,. \tag{4.5}$$

Setting $E_o(\eta')$ equal to the unperturbed confocal solutions $S_n(c,\eta')$ the covariance becomes

$$\langle E(\eta_1)\, E^*(\eta_2)\rangle = \frac{2c}{\pi}\left[R_{on}^{(1)}(c,1)\right]^2 S_{on}(c,\eta_1)\, S_{on}(c,\eta_2) - \frac{ck^2\sigma_n^2}{2\pi\ell^2} I(\eta_1,\eta_2) \,, \tag{4.6}$$

where

$$I(\eta_1,\eta_2) = \iint_{-1}^{+1} (\eta_1' - \eta_2')^2\, e^{ic(\eta_1\eta_1' - \eta_2\eta_2')} S_{on}(c,\eta_1')\, S_{on}(c,\eta_2')d\eta_1'd\eta_2' \,. \tag{4.7}$$

Now to find the covariance we must determine solutions of 4.7.

## 4.2 Evaluation of the Scattering Integral by the Method of Steepest Descents.

In the preceding section the following integral was encountered:

$$I(\eta_1,\eta_2) = \iint_{-1}^{+1} (\eta_1' - \eta_2')^2\, e^{ic(\eta_1\eta_1' - \eta_2\eta_2')} S_{on}(c,\eta_1')\, S_{on}(c,\eta_2')d\eta_1'd\eta_2' \,. \tag{4.8}$$

For large values of the parameter $c$ the field distribution functions may be approximated by appropriate Hermite functions. Thus,

$$S_{on}(c,\eta) \cong H_n(\sqrt{c}\,\eta)\; e^{-\frac{1}{2}c\eta^2}\,, \tag{4.9}$$

and 4.8 becomes

$$I(\eta_1,\eta_2) = \iint_{-1}^{+1} (\eta_1' - \eta_2')^2\, H_n(\sqrt{c}\,\eta_1')\, H_n(\sqrt{c}\,\eta_2') \; e^{ic(\eta_1\eta_1' - \eta_2\eta_2') - \frac{c}{2}(\eta_1'^2 + \eta_2'^2)}\, d\eta_1' d\eta_2' \,. \tag{4.10}$$

This may be rewritten as

$$I(\eta_1,\eta_2) = \int_{-1}^{+1} d\eta_2'\, H_n(\sqrt{c}\,\eta_2')\; e^{-c(i\eta_2\eta_2' + \frac{\eta_2'^2}{2})} \int_{-1}^{+1} d\eta_1'\, H_n(\sqrt{c}\,\eta_1')\, (\eta_1' - \eta_2')^2\; e^{c(i\eta_1\eta_1' - \frac{\eta_1'^2}{2})} \,. \tag{4.11}$$

The Hermite polynomials are represented by the series

$$H_n(x) = n! \sum_{\nu=0}^{[n/2]} \frac{(-1)^\nu}{\nu!}\, \frac{(2x)^{n-2\nu}}{(n-2\nu)!} \,. \tag{4.12}$$

With the aid of 4.12 the integrand of $I(\eta_1,\eta_2)$ may be expressed in terms of a polynomial in $\eta$ and solved in generality for any value of $n$. However, to avoid the rather involved expressions resulting from a solution of 4.11 for an arbitrary $n$ we will pick a specific Hermite polynomial, $n = 2$, to illustrate the method of solution.

For the particular mode $n = 2$ 4.11 is

$$I(\eta_1,\eta_2) = \int_{-1}^{+1} d\eta_2' \,(2c\eta_2'^2 - 1)\, e^{-c(i\eta_2\eta_2' + \frac{\eta_2'^2}{2})} \int_{-1}^{+1} d\eta_1'(2c\eta_1' - 1)\,(\eta_1' - \eta_2')^2\, e^{c(i\eta_1\eta_1' - \frac{\eta_1'^2}{2})} . \tag{4.13}$$

We concern ourselves initially with the first integration:

$$I_1 = \int_{-1}^{+1} (2c\eta_1'^2 - 1)\,(\eta_1' - \eta_2')^2\, e^{c\phi_1}\, d\eta_1' , \tag{4.14}$$

where $\phi_1$ is defined

$$\phi_1 = i\eta_1\eta_1' - \frac{\eta_1'^2}{2} .$$

As the parameter $c$ is very large the behavior of $I_1$ will depend strongly on the function $\phi_1$. To evaluate this integral we replace the limits of integration by $\pm\infty$ and then deform the contour so that it passes through the saddle point along the path of steepest descent. In the complex $\eta_1'$ plane the saddle point is located by setting $d\phi_1/d\eta_1' = 0$. We find

$$\frac{d\phi_1}{d\eta_1'} = i\eta_1 - \eta_1' ,$$

or

$$\eta_{1s}' = i\eta_1 .$$

In addition

$$\phi_{1s} = \frac{\eta_1^2}{2}$$

$$\frac{d^2\phi_{1s}}{d\eta_1'^2} \equiv \phi_{1s}'' = -1 \ ,$$

where a subscript s refers to the magnitude of a quantity at the saddle point. The original and deformed paths of integration are shown in Figure 4.1.

We next define a new variable $u_1$ which is real on the path of steepest descent.

$$-u_1 \equiv \phi_1 - \phi_{1s}$$

Now,

$$I_1 = e^{c\phi_{1s}} \int_{\text{contour}} \left[2c\eta_1'^2(u_1) - 1\right] \left[\eta_1'(u_1) - \eta_2'\right]^2 e^{-cu_1} \frac{d\eta_1'(u_1)}{du_1} du_1 \ . \quad (4.15)$$

To find $\eta_1'(u_1)$ we expand $u_1$ in a Taylor series about $\eta_1' = \eta_{1s}'$ .

$$-u_1(\eta_1') = (\phi_{1s} - \phi_{1s}) + \frac{\phi_{1s}'}{1!}(\eta_1' - \eta_{1s}') + \frac{\phi_{1s}''}{2!}(\eta_1' - \eta_{1s}')^2 + \ldots .$$

$$= -\frac{1}{2}(\eta_1' - \eta_{1s}')^2 \ .$$

So

$$(\eta_1' - \eta_{1s}')^2 = 2u_1 \ ,$$

$$\eta_1'(u_1) = \pm\sqrt{2u_1} + \eta_{1s}' \ ,$$

and

$$\frac{d\eta_1'}{du_1} = \pm \frac{1}{\sqrt{2u_1}} \ .$$

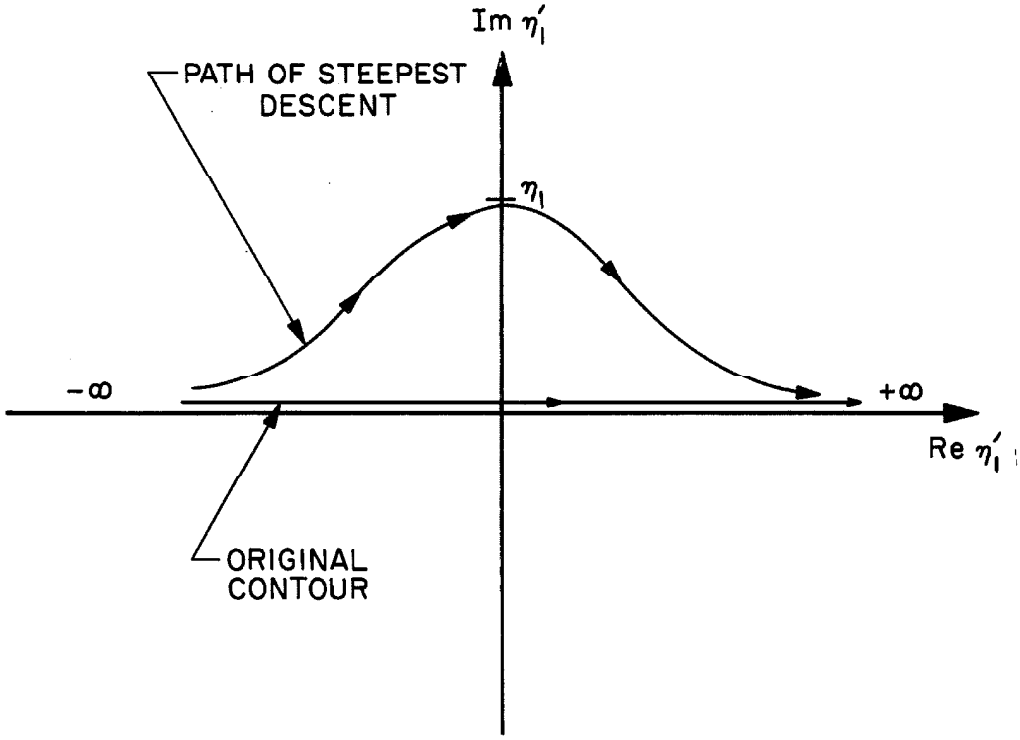


Fig. 4.1 Contours of integration in the complex $\eta_1'$ - plane.

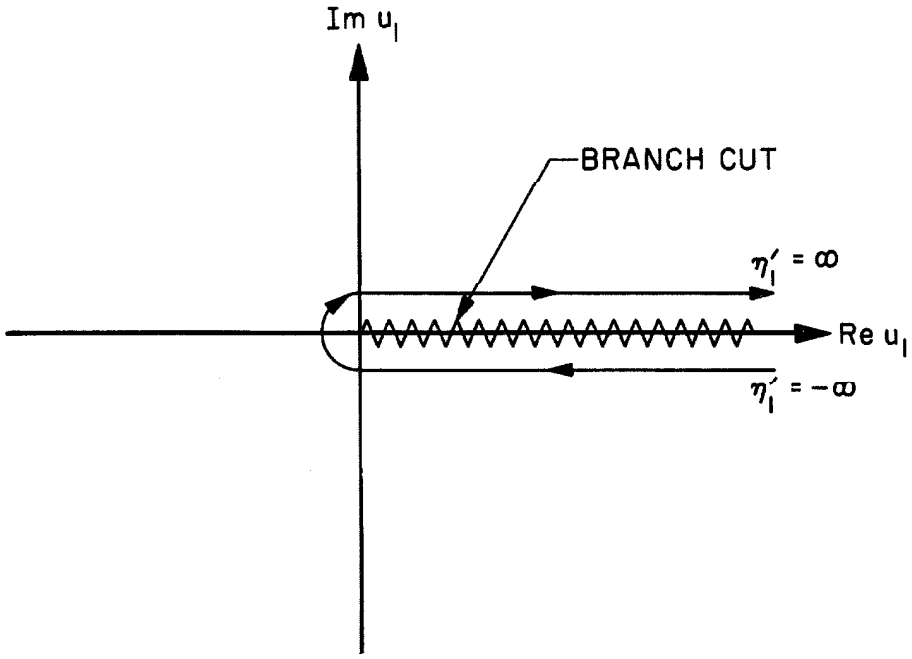


Fig. 4.2 Contour of integration in the $u_1$ - plane.

The integration path in the $u_1$-plane is shown in Figure 4.2.

Additional terms needed in the integration are

$$\eta_1'^2 = 2u_1 \pm 2\sqrt{2u_1}\,\eta_{1s}' + \eta_{1s}'^2$$

$$\eta_1'^3 = 2^{3/2} u_1^{3/2} + 6u_1\eta_{1s}' \pm 3\sqrt{2u_1}\,\eta_{1s}'^2 + \eta_{1s}'^3$$

$$\eta_1'^4 = 4u_1^2 \pm 8u_1\sqrt{2u_1} + 12u_1\eta_{1s}'^2 \pm 4\sqrt{2u_1}\,\eta_{1s}'^3 + \eta_{1s}'^4 .$$

Using these relations 4.15 becomes

$$I_1 = 2e^{c\phi_{1s}} \int_0^\infty d\eta_1 \, e^{-cu_1} \left[ 2c\left(2u_1\sqrt{2u_1} + 6\sqrt{2u_1}\,\eta_{1s}'^2 + \frac{\eta_{1s}'^4}{2u_1}\right) \right.$$

$$-4c\eta_2'\left(3\sqrt{2u_1}\,\eta_{1s}' + \frac{\eta_{1s}'^3}{\sqrt{2u_1}}\right) + (2c\eta_2'^2 - 1)\left(\sqrt{2u_1} + \frac{\eta_{1s}'^2}{\sqrt{2u_1}}\right) \qquad (4.16)$$

$$\left. +2\eta_2'\frac{\eta_{1s}'}{\sqrt{2u_1}} - \frac{\eta_2'^2}{\sqrt{2u_1}} \right],$$

where we have taken note of the fact that the plus and minus signs arrived at by taking the square root of $u_1$ refer to the contour on opposite sides of the branch cut. From the elementary integral relations

$$\int_0^\infty u^{3/2} e^{-cu}\, du = \frac{3}{4c^2}\sqrt{\frac{\pi}{c}} ,$$

$$\int_0^\infty u^{1/2} e^{-cu}\, du = \frac{1}{2c}\sqrt{\frac{\pi}{c}}$$

$$\int_0^\infty u^{-1/2}\, e^{-cu}\, du = \sqrt{\frac{\pi}{c}}\ ,$$

$I_1$ is evaluated and reduces to

$$I_1 = 2\sqrt{\frac{\pi}{c}}\, e^{c\phi_{1s}} \left[\left(\frac{5}{\sqrt{2}c} + \frac{11}{\sqrt{2}}\,\eta'^{2}_{1s} + \sqrt{2}c\,\eta'^{4}_{1s}\right)\right. \tag{4.17}$$

$$\left. - \left(5\sqrt{2}\,\eta'_{1s} + 2\sqrt{2}c\,\eta'^{3}_{1s}\right)\,\eta'_2 + \left(\frac{1}{\sqrt{2}} + \sqrt{2}\,c\,\eta'^{2}_{1s}\right)\,\eta'^{2}_2\right]\ .$$

We can now proceed to perform the second integration of $I(\eta_1, \eta_2)$ in precisely the same fashion. Using the result of the $I_1$ integration,

$$I(\eta_1, \eta_2) = 2\sqrt{\frac{\pi}{c}}\, e^{c\phi_{1s}} \int_{-1}^{+1} d\eta'_2\, e^{-c\left(i\eta_2\eta'_2 + \frac{\eta'^{2}_2}{2}\right)}$$

$$\left[2c\,\eta'^{2}_2 - 1\right]\left[\left(\frac{5}{\sqrt{2}c} + \frac{11}{\sqrt{2}}\,\eta'^{2}_{1s} + \sqrt{2}c\,\eta'^{4}_{1s}\right)\right. \tag{4.18}$$

$$\left. - \left(5\sqrt{2}\eta'_{1s} + 2\sqrt{2}c\eta'^{3}_{1s}\right)\,\eta'_2 + \left(\frac{1}{\sqrt{2}} + \sqrt{2}c\,\eta'^{2}_{1s}\right)\eta'^{2}_2\right]\ .$$

Performing the indicated multiplication,

$$I(\eta_1,\eta_2) = 2\sqrt{\frac{\pi}{c}}\, e^{i\phi_{1s}} \int_{-1}^{+1} d\eta_2'\, e^{-c\left(i\eta_2\eta_2' + \frac{\eta_2'^2}{2}\right)}$$

$$\left[-\left(\frac{5}{\sqrt{2}c} + \frac{11}{\sqrt{2}}\eta_{1s}'^2 + \sqrt{2}c\eta_{1s}'^4\right) + \left(5\sqrt{2}\eta_{1s}' + 2\sqrt{2}c\eta_{1s}'^3\right)\eta_2'\right.$$

$$+ \left(\frac{9}{\sqrt{2}} + \sqrt{2}\,10c\eta_{1s}'^2 + 2\sqrt{2}c^2\eta_{1s}'^4\right)\eta_2'^2$$

$$\left. - \left(10\sqrt{2}c\eta_{1s}' + 4\sqrt{2}c^2\eta_{1s}'^3\right)\eta_2'^3 + \left(\sqrt{2}c + \sqrt{2}\,2c^2\eta_{1s}'^2\right)\eta_2'^4\right] .$$

Again we define a quantity $\phi$ such that

$$\phi_2 \equiv -i\eta_2\eta_2' - \frac{\eta_2'^2}{2} .$$

Then

$$\phi_2' = -i\eta_2 - \eta_2'$$

$$\phi_2'' = -1 ,$$

and the saddle point is located at

$$\eta_{2s}' = -i\eta_2 .$$

The value of $\phi_2$ at the saddle point is

$$\phi_{2s} = -\frac{\eta_2^2}{2} .$$

A before we define a new variable $u_2$ which is real along the contour.

$$-\eta_2 \equiv \phi_2 - \phi_{2s}$$

Now $u_2$ is expanded in a Taylor series about the saddle point and we find $\eta_2'$ and $d\eta_2'/du_2$ in terms of $u_2$. The transformation again maps the path of integration around a branch cut from zero to infinity as shown in Figures 4.3 and 4.4.

We now have the straightforward integral

$$I(\eta_1, \eta_2) = 4\sqrt{\frac{\pi}{c}}\, e^{c(\phi_{1s} + \phi_{2s})} \int_0^\infty du_2\, e^{-cu_2}$$

$$\left[ -\left( \frac{5}{2c} + \frac{11}{2}\eta_{1s}'^2 + c\eta_{1s}'^4 \right) \frac{1}{\sqrt{u_2}} + \left( 5\eta_{1s}' + 2c\eta_{1s}'^3 \right) \frac{\eta_{2s}'}{\sqrt{u_2}} \right.$$

$$+ \left( \frac{9}{\sqrt{2}} + 10\sqrt{2}c\eta_{1s}'^2 + 2\sqrt{2}c^2\eta_{1s}'^4 \right) \left( 2u_2 + \frac{\eta_{2s}'^2}{\sqrt{2u_2}} \right)$$

$$- \left( 10\sqrt{2}c\eta_{1s}' + 4\sqrt{2}c^2\eta_{1s}'^3 \right) \left( 3\sqrt{2u_2}\eta_{2s}' + \frac{\eta_{2s}'^3}{2u_2} \right)$$

$$\left. + \left( \sqrt{2}c + 2\sqrt{2}c^2\eta_{1s}'^2 \right) \left( 2u_2\sqrt{2u_2} + 6\sqrt{2u_2}\eta_{2s}'^2 + \frac{\eta_{2s}'^4}{\sqrt{2u_2}} \right) \right] .$$

Performing the integration,

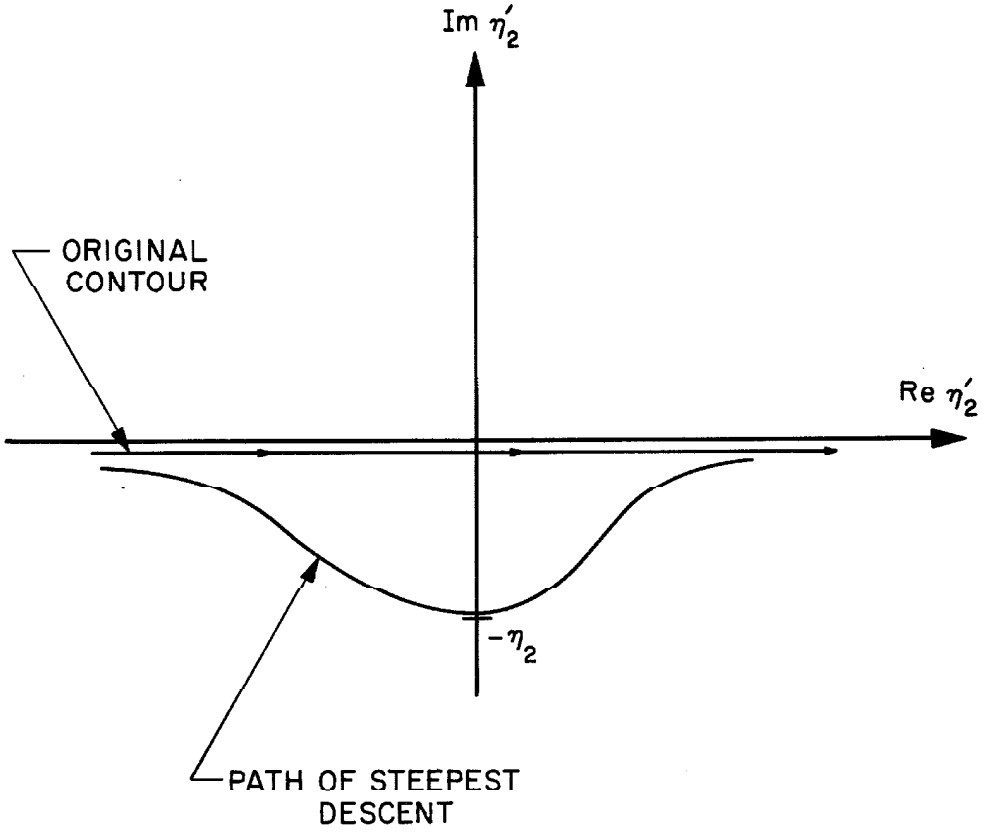


Fig. 4.3 Contours of integration in the complex $\eta_2'$ - plane.

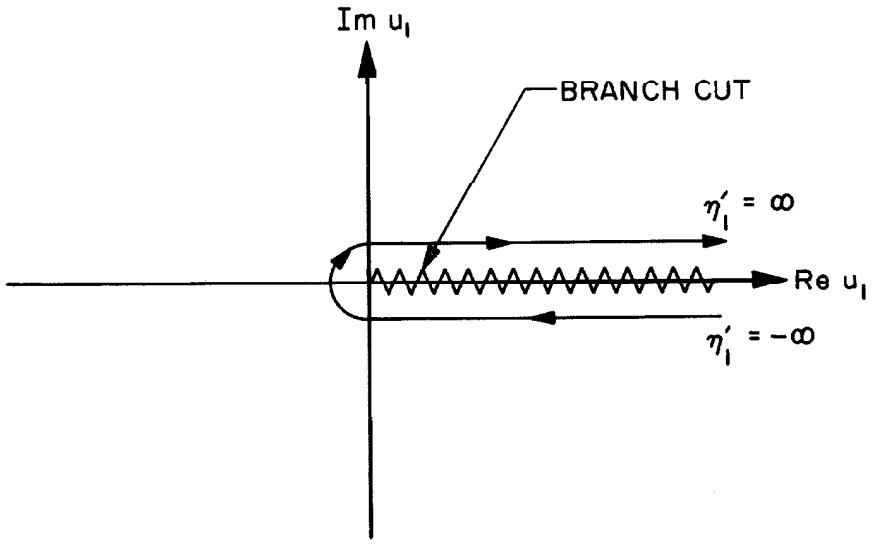


Fig. 4.4 Contour of integration in the complex $u_2$ - plane.

$$I(\eta_1,\eta_2) = \frac{4\pi}{2} e^{c(\phi_{1s} + \phi_{2s})} \left[\frac{5}{c} + \frac{21}{c}\eta_{1s}'^{2} + c\eta_{1s}'^{4}\right.$$

$$-25\eta_{1s}'\eta_{2s}' - 10c\eta_{1s}'^{3}\eta_{2s}' + \frac{21}{2}\eta_{2s}'^{2} + 22c\eta_{2s}'^{2}\eta_{1s}'^{2} \qquad (4.19)$$

$$\left.+2c^2\eta_{1s}'^{4}\eta_{2s}'^{2} - 10c\eta_{1s}'\eta_{2s}'^{3} - 4c^2\eta_{1s}'^{3}\eta_{2s}'^{3} + c\eta_{2s}'^{4} + 2c^2\eta_{1s}'^{2}\eta_{2s}'^{4}\right] .$$

Now recalling the relations

$$\eta_{1s}' = i\eta_1 \ , \qquad \eta_{2s}' = -i\eta_2 \ ,$$

$$\phi_{1s} = -\frac{\eta_1^2}{2} \ , \qquad \phi_{2s} = -\frac{\eta_2^2}{2} \ ,$$

therefore, 4.19 reduces to

$$I(\eta_1,\eta_2) = \frac{4\pi}{c} e^{-\frac{c}{2}(\eta_1^2 + \eta_2^2)} \left[\frac{5}{c} - \frac{21}{2}\eta_1^2 + c\eta_1^4\right.$$

$$-25\eta_1\eta_2 + 10c\eta_1^3\eta_2 - \frac{21}{2}\eta_2^2 + 22c\eta_2^2\eta_1^2 \qquad (4.20)$$

$$\left.-2c^2\eta_1^4\eta_2^2 + 10c\eta_1\eta_2^3 - 4c^2\eta_1^3\eta_2^3 + c\eta_2^4 - 2c^2\eta_1^2\eta_2^4\right] .$$

To find the perturbation intensity we set

$$\eta = \eta_1 = \eta_2 \ .$$

Then the perturbation intensity is simply

$$I(\eta) = \frac{4\pi}{c^2} e^{-c\eta^2} \left[5 - 46\, c\eta^2 + 44c^2\eta^4 - 8c^3\eta^6\right] . \qquad (4.21)$$

Rather than directly looking into the implications of this result, at this point we will proceed with the analysis of the second approach suggested in Chapter III. Then with the mathematics of both techniques worked out their implications and validity will be delved into.

# CHAPTER V

# PERTURBATION TREATMENT OF THE CHARACTERISTIC EQUATION FOR A CONFOCAL RESONATOR WITH AN IRREGULAR MIRROR

## 5.1 Formal Development of the Series Solution

In Section 3.3 the following integral equation was derived for a perturbed confocal resonator;

$$\sigma E_o(x') = \frac{e^{i\frac{\pi}{4}}}{\sqrt{\lambda}} \int_{-a}^{+a} E_o(x) \left[1 + 2ik \sum_s c_s \phi_s(x)\right] \frac{e^{-ik\rho}}{\sqrt{\rho}}\, dx \ . \quad (5.1)$$

Introducing the geometrical approximations and the normalized notation of earlier chapters this becomes

$$\sigma E_o(\eta') = \sqrt{\frac{c}{2\pi}}\, e^{i(\frac{\pi}{4} - kb)} \int_{-1}^{+1} e^{ic\eta\eta'} \left[1 + 2ik \sum_s c_s \phi_s(\eta)\right] E_o(\eta) d\eta \ . \quad (5.2)$$

To solve this equation for its eigenfunctions and eigenvalues, we expand the unperturbed kernel in an orthogonal series of spheroidal functions.

$$G(\eta,\eta') = e^{ic\eta\eta'} = \sum_m A_m S_{om}(c,\eta) \quad (5.3)$$

In order to find the $A_m$, we multiply both sides of the equation by $S_{on}(c,\eta)d\eta$ and integrate over the range -1 to +1.

$$\int_{-1}^{+1} e^{ic\eta\eta'} S_{on}(c,\eta)d\eta = \int_{-1}^{+1} \sum_m A_m S_{om}(c,\eta) S_{on}(c,\eta) d\eta \quad (5.4)$$

Then

$$2i^n R_{on}^{(1)}(c,1)\, S_{on}(c,\eta') = A_n \int_{-1}^{+1} \left[S_{on}(c,u)\right]^2 du \,. \qquad (5.5)$$

And for the expansion coefficients, we have

$$A_n = \frac{2i^n R_{on}^{(1)}(c,1)}{\int_{-1}^{+1} \left[S_{on}(c,u)\right]^2 du}\; S_{on}(c,\eta') \,. \qquad (5.6)$$

There are some limited tables available from which the integral in the denominator may be calculated; however, for large values of the parameter c the spheroidal function may be approximated by a Hermite function and the integral can be evaluated approximately through such a substitution. First, the Hermite function must be normalized in the same manner as the spheroidal function. Following the normalization of Flammer (17), we have

$$S_{on}(c,o) = P_n(o) = \frac{(-1)^{\frac{n}{2}}\, n!}{2^n (\frac{n}{2})!\; (\frac{n}{2})!} \quad , \; n \text{ even} \,.$$

When its argument is zero, the Hermite function reduces to a Hermite polynomial and becomes

$$H_n(o) = \frac{(-1)^{\frac{n}{2}}\, n!}{(\frac{n}{2})!} \quad , \; n \text{ even} \,.$$

With proper normalization, it follows that

$$S_{on}(c,\eta) \cong \frac{H_n(\sqrt{c}\eta)}{2^n\,\Gamma(\frac{r}{2}+1)}\,(1-\eta^2)^{\frac{1}{2}}\,e^{-\frac{1}{2}c\eta^2}\quad . \tag{5.7}$$

Now, going back to the integral in the limit $c \to \infty$,

$$\int_{-1}^{+1}\left[S_{on}(c,u)\right]^2\,du \equiv N_{on}$$

$$\cong \frac{\int_{-\infty}^{\infty}\left[H_n(u)\right]^2\,e^{-u^2}\,du}{2^{2h}\,\sqrt{c}\left[\Gamma\left(\frac{n}{2}+1\right)\right]^2} \tag{5.8}$$

$$= \frac{n!}{2^h\left[\Gamma(\frac{n}{2}+1)\right]^2}\,\sqrt{\frac{\pi}{c}}$$

Finally, the expansion for the kernel may be written as

$$G(\eta,\eta') = \sum_m \frac{2i^m R_{om}^{(1)}(c,1)}{N_{om}}\,S_{om}(c,\eta)\,S_{om}(c,\eta') \tag{5.9}$$

$$= \sum_m \frac{2^{m+1}}{m!}\,i^m\left[\Gamma(\frac{m}{2}+1)\right]^2 R_{om}^{(1)}(c,1)\sqrt{\frac{c}{\pi}}\,S_{om}(c,\eta)\,S_{om}(c,\eta')\quad .$$

We may now proceed to write the perturbed integral equation with the expanded Kernel as

$$\sigma E_o(\eta') = \sqrt{\frac{2c}{\pi}}\, e^{i(\frac{\pi}{4} - kb)} \sum_m \frac{i^m R_{om}^{(1)}(c,1)}{N_{om}} S_{om}(c,\eta')$$

$$\int_{-1}^{+1} S_{om}(c,\eta) \left[1 + \sum_s 2ikc_s \phi_s(\eta)\right] E_o(\eta) d\eta \ . \tag{5.10}$$

The zeroth approximation of the perturbed field distribution results from setting $E_o(\eta)$ in the integrand equal to the unperturbed mode of interest, or

$$E_o(\eta) = S_{on}(c,\eta) \ .$$

Then

$$\sigma_n E_{on}(\eta') \cong \sqrt{\frac{2c}{\pi}}\, e^{i(\frac{\pi}{4} - kb)} \sum_m \frac{i^m R_{om}^{(1)}(c,1)}{N_{om}} S_{om}(c,\eta')$$

$$\int_{-1}^{+1} S_{om}(c,\eta) \left[1 + \sum_s 2ikc_s \phi_s(\eta)\right] S_{on}(c,\eta) d\eta \ . \tag{5.11}$$

When the perturbation coefficient $c_s$ goes to zero, the series reduces to one term with the result

$$\sigma_n E_{on}(\eta') = \sqrt{\frac{2c}{\pi}}\, e^{i(\frac{\pi}{4} - kb)}\, i^n R_{on}^{(1)}(c,1)\, S_{on}(c,\eta') \ , \tag{5.12}$$

yielding the unperturbed solutions obtained previously.

The first integration of 5.11 is readily evaluated and we arrive at the final form of the series solution for the perturbed resonator.

$$\sigma_n E_{on}(\eta') = \sqrt{\frac{2c}{\pi}}\, i^n R^{(1)}_{on}(c,1)\, e^{i(\frac{\pi}{4} - kb)}\, S_{on}(c,\eta')$$

$$+ 2ik\sqrt{\frac{2c}{\pi}}\, e^{i(\frac{\pi}{4} - kb)} \sum_m \frac{i^m R^{(-)}_{om}(c,1)}{N_{om}}\, \alpha_{mn}\, S_{om}(c,\eta') \,, \tag{5.13}$$

where

$$\alpha_{mn} = \sum_s C_s \int_{-1}^{+1} S_{om}(c,\eta)\, \phi_s(\eta)\, S_{on}(c,\eta)d\eta \,. \tag{5.14}$$

To obtain explicit solutions we must now evaluate integrals of the form

$$\alpha^s_{mn} = C_s \int_{-1}^{+1} S_{om}(c,\eta)\, \phi_s(\eta)\, S_{on}(c,\eta)d\eta \,. \tag{5.15}$$

In the next section we shall work out an example for a particular orthogonal function $\phi_s(\eta)$ .

## 5.2 Evaluation of the Perturbation Integral for Surfaces with Trigonometric Expansions

In Appendix I it is shown that a random function $g(\eta)$ may be expanded in a discrete series of trigonometric functions when the correlation function has an exponential form. By choosing the series properly it can be assured that the coefficients $c_s$ of the expansion are uncorrelated random variables. With such an expansion 5.15 assumes the form

$$\alpha^s_{mn} = c_s d_s n_s \int_{-1}^{+1} S_{om}(c,\eta) \begin{Bmatrix} \sin P_s\eta \\ \cos \hat{P}_s\eta \end{Bmatrix} S_{on}(c,\eta)d\eta \,. \tag{5.16}$$

Since the cosine and sine are expressible, respectively, as the sum and difference of a positive and a negative exponential, we need only evaluate the integral

$$I^{s}_{mn}(\pm) = \int_{-1}^{+1} S_{om}(c,\eta)\ e^{\pm ip_s\eta}\ S_{on}(c,\eta)d\eta\ . \qquad (5.17)$$

Again, we approach an integral involving spheroidal functions by substituting the approximate Hermite functions and evaluating the integral in the limit $c \to \infty$. Defining a new variable $u \equiv \sqrt{c}\eta$ and letting $\sqrt{c}$ approach infinity in the limits of integration, we have

$$I^{s}_{mn}(\pm) = \frac{\int_{-\infty}^{\infty} e^{\pm iq_s u}\ H_m(u)\ H_n(u)\ e^{-u^2}\ du}{\sqrt{c}\,2^{m+n}\sqrt{c}\ \Gamma(\frac{m}{2}+1)\ \Gamma(\frac{n}{2}+1)}\ ,$$

where $q_s \equiv P_s/\sqrt{c}$. Except for a trivial constant, this is simply the Fourier transform of the product

$$\left[e^{-u^2/2}\ H_m(u)\right]\left[e^{-u^2/2}\ H_n(u)\right]\ .$$

By means of the convolution theorem, the integral may be written as

$$I^{s}_{mn}(,) = \frac{i^{m+n}\int_{-\infty}^{\infty} e^{-v^2/2}\ H_m(v)\ e^{-(q_s - v)^2/2}\ H_n(q_s - v)dv}{\sqrt{c}\,2^{m+n}\ \Gamma(\frac{m}{2}+1)\ \Gamma(\frac{n}{2}+1)}\ ,$$

where, for the present, we have taken only the positive $q_s$. Now we set

$$A = \frac{i^{m+n}}{2^{m+n}\sqrt{c}\,\Gamma(\frac{m}{2}+1)\,\Gamma(\frac{n}{2}+1)} \quad .$$

Then

$$I^s_{mn}(+) = (-1)^n A \int_{-\infty}^{\infty} e^{-v^2/2} H_m(v)\, e^{-(v-q_s)^2/2} H_n(v-q_s)dv \ .$$

Changing to a new variable

$$\omega = v - q_s/2 \ ,$$

$$I^s_{mn}(+) = (-1)\, A \int_{-\infty}^{\infty} e^{-(\omega+q_s/2)^2/2} H_m(\omega+q_s/2)$$

$$e^{-(\omega-q_s/2)^2/2} H_n(\omega - q_s/2)d\omega$$

$$= (-1)^n A\, e^{-q_s^2/4} \int_{-\infty}^{\infty} e^{-\omega^2} H_m(\omega+q_s/2)\, H_n(\omega - q_s/2)d\omega \ .$$

Now, defining a new variable of integration $u = \sqrt{2}\omega$ ,

$$I^s_{mn}(+) = \frac{(-1)^n A}{2} e^{-q_s^2/4} \int_{-\infty}^{\infty} e^{-u^2/2} H_m\left(\frac{u+q_s/\sqrt{2}}{2}\right) H_n\left(\frac{u-q_s/\sqrt{2}}{2}\right)du \qquad (5.18)$$

$$= \frac{(-1)\, A\, e^{-q_s^2/4}}{2^{-\frac{1}{2}(m+n-1)}} \int_{-\infty}^{\infty} e^{-u^2/2} He_m(u+\frac{q_s}{\sqrt{2}})\, He_n(u-\frac{q_s}{\sqrt{2}})du \ ,$$

where the polynomials $He_n(x)$ are defined by the equations:

$$He_n(x) = 2^{n/2}\, H_n(2^{-\frac{1}{2}}x) = e^{x^2/2}\,(-\tfrac{d}{dx})^n\, e^{-x^2/2} \ .$$

The integral of 5.18 can be found tabulated in the literature (30). We arrive at the expression

$$I^s_{mn}(+) = \frac{i^{n-m}\sqrt{\pi}\ m!}{2^n\sqrt{c}\ \Gamma(\frac{m}{2}+1)\ \Gamma(\frac{n}{2}+1)}\ e^{-q_s^2/4}\ q_s^{n-m}\ L_m^{n-m}(q_s^2/2)\ , \qquad (5.19)$$

$$m \le n \ ,$$

where the functions $L_m^{n-m}(x)$ are Laguerre polynomials. It follows immediately that

$$I^s_{mn}(-) = \frac{i^{m-n}\sqrt{\pi}\ m!}{2^n\sqrt{c}\ \Gamma(\frac{m}{2}+1)\ \Gamma(\frac{n}{2}+1)}\ e^{-q_s^2/4}\ q_s^{n-m} L_m^{n-m}(q_s^2/2)\ , \qquad (5.20)$$

$$m \le n \ .$$

Recalling 5.16, we have for the terms in the perturbation expansion

$$\alpha^s_{mn}(\sin) = \frac{c_s d_s n_s}{2i}\left[I^s_{mn}(+) - I^s_{mn}(-)\right] ,$$

$$\alpha^s_{mn}(\cos) = \frac{\hat{c}_s \hat{d}_s \hat{n}_s}{2}\left[I^s_{mn}(+) + I^s_{mn}(-)\right] .$$

Defining the quantity

$$B^s_{mn} = \sqrt{\frac{\pi}{c}} \frac{m!\, q_s^{n-m} e^{-q_s^2/4}}{2^n\, \Gamma(\frac{m}{2}+1)\, \Gamma(\frac{n}{2}+1)} \; L_m^{n-m}(q_s^2/2)$$

$$= \sqrt{\frac{\pi}{c}} \frac{m!\, P_s^{n-m} e^{-P_s^2/4c}}{2^n\, c^{(n-m)/2}\, \Gamma(\frac{m}{2}+1)\, \Gamma(\frac{n}{2}+1)} \; L_m^{n-m}(P_s^2/2c) \,, \qquad (5.21)$$

$$m \le n \,,$$

the perturbation terms may be written simply as

$$\alpha^s_{mn}\ (\sin) = c_s d_s n_s\ B^s_{mn},\ n - m = 1, 5, 9, \ldots$$

$$\alpha^s_{mn}\ (\sin) = -c_s d_s n_s\ B^s_{mn},\ n - m = 3, 7, 11, \ldots$$

$$\alpha^s_{mn}\ (\sin) = 0,\ n - m = 0, 2, 4, \ldots$$

$$\alpha^s_{mn}\ (\cos) = \hat{c}_s \hat{d}_s \hat{n}_s\ B^s_{mn},\ n - m = 0, 4, 8, \ldots$$

$$\alpha^s_{mn}\ (\cos) = -\hat{c}_s \hat{d}_s \hat{n}_s\ B^s_{mn},\ n - m = 2, 6, 10, \ldots$$

$$\alpha^s_{mn}\ (\cos) = 0,\ n - m = 1, 3, 5, \ldots$$

These are tabulated below for m, $n \le 3$ .

$$B^s_{00} = \sqrt{\frac{\pi}{c}}\, L_0^0(\frac{P_s^2}{2c})\, e^{-P_s^2/4c} = \sqrt{\frac{\pi}{c}}\, e^{-P_s^2/4c}$$

$$B^s_{01} = \frac{P_s}{c}\, L_0^1(\frac{P_s^2}{2c})\, e^{-P_s^2/4c} = \frac{P_s}{c}\, e^{-P_s^2/4c}$$

$$B_{10}^{s} = \frac{P_s}{c} L_0^1\left(\frac{P_s^2}{2c}\right) e^{-P_s^2/4c} = \frac{P_s}{c} e^{-P_s^2/4c}$$

$$B_{11}^{s} = \frac{2}{\sqrt{\pi c}} L_1^0\left(\frac{P_s^2}{2c}\right) e^{-P_s^2/4c} = \frac{2}{\sqrt{\pi c}} \left(1 - \frac{P_s^2}{2c}\right) e^{-P_s^2/4c}$$

$$B_{02}^{s} = \sqrt{\frac{\pi}{c}} \frac{P_s^2}{4c} L_0^2\left(\frac{P_s^2}{2c}\right) e^{-P_s^2/4c} = \sqrt{\frac{\pi}{c}} \frac{P_s^2}{4c} e^{-P_s^2/4c}$$

$$B_{20}^{s} = \sqrt{\frac{\pi}{c}}\left(\frac{P_s^2}{4c}\right) L_0^2 \frac{P_s^2}{2c} e^{-P_s^2/4c} = \sqrt{\frac{\pi}{c}} \frac{P_s^2}{4c} e^{-P_s^2/4c}$$

$$B_{12}^{s} = \frac{P_s}{2c} L_1^1\left(\frac{P_s^2}{2c}\right) e^{-P_s^2/4c} = \frac{P_s}{2c} \left(2 - \frac{P_s^2}{2c}\right) e^{-P_s^2/4c}$$

$$B_{21}^{s} = \frac{P_s}{2c} L_1^1\left(\frac{P_s^2}{2c}\right) e^{-P_s^2/4c} = \frac{P_s}{2c} \left(2 - \frac{P_s^2}{2c}\right) e^{-P_s^2/4c}$$

$$B_{22}^{s} = \frac{1}{2}\sqrt{\frac{\pi}{c}} L_2^0\left(\frac{P_s^2}{2c}\right) e^{-P_s^2/4c} = \frac{1}{2}\sqrt{\frac{\pi}{c}} \left(1 - \frac{P_s^2}{c} + \frac{P_s^4}{8c^2}\right) e^{-P_s^2/4c}$$

$$B_{03}^{s} = \frac{P_s^3}{6c^2} L_0^3\left(\frac{P_s^2}{2c}\right) e^{-P_s^2/4c} = \frac{P_s^3}{6c^2} e^{-P_s^2/4c}$$

$$B_{30}^{s} = \frac{P_s^3}{6c^2} L_0^3\left(\frac{P_s^2}{2c}\right) e^{-P_s^2/4c} = \frac{P_s^3}{6c^2} e^{-P_s^2/4c}$$

$$B_{13}^{s} = \frac{P_s^2}{3c\sqrt{\pi c}} L_1^2\left(\frac{P_s^2}{2c}\right) e^{-P_s^2/4c} = \frac{P_s^2}{3c\sqrt{\pi c}} \left(3 - \frac{P_s^2}{2c}\right) e^{-P_s^2/4c}$$

$$B_{31}^{s} = \frac{P_s^2}{3c\sqrt{\pi c}} L_1^2\left(\frac{P_s^2}{2c}\right) e^{-P_s^2/4c} = \frac{P_s^2}{3c\sqrt{\pi c}} \left(3 - \frac{P_s^2}{2c}\right) e^{-P_s^2/4c}$$

$$B_{23}^{s} = \frac{P_s}{3c} L_2^1\left(\frac{P_s^2}{2c}\right) e^{-P_s^2/4c} = \frac{P_s}{3c}\left(3 - \frac{3P_s^2}{2c} + \frac{P_s^4}{8c^2}\right) e^{-P_s^2/4c}$$

$$B_{32}^{s} = \frac{P_s}{3c} L_2^1\left(\frac{P_s^2}{2c}\right) e^{-P_s^2/4c} = \frac{P_s}{3c}\left(3 - \frac{3P_s^2}{2c} + \frac{P_s^4}{8c^2}\right) e^{-P_s^2/4c}$$

$$B_{33}^{s} = \frac{4}{2\sqrt{\pi c}} L_3^0\left(\frac{P_s^2}{2c}\right) e^{-P_s^2/4c} = \frac{4}{3\sqrt{\pi c}}\left(1 - \frac{3P_s^2}{2c} + \frac{3P_s^4}{8c^2} - \frac{P_s^6}{48c^3}\right) e^{-P_s^2/4c}$$

## 5.3 Calculation of Perturbed Eigenvalues

In 5.1 we developed a series expansion for the field distribution of a perturbed resonator. Now we want to determine the eigenvalues for the perturbed system in order to find the effect of surface roughness on $Q$ and resonant frequency. The modes of the cavity were represented by the solutions of an integral equation of the form

$$E_o(\eta') = \chi \int_{-1}^{+1} G(\eta',\eta)\, u(\eta)\, E_o(\eta)\, d\eta \,, \tag{5.22}$$

where $u(\eta)$ represents the effect of the surface roughness. The Kernel was expanded in an orthogonal series,

$$G(\eta',\eta) = \sum_m C_m\, S_{om}(c,\eta')\, S_{om}(c,\eta) \,.$$

With this substitution the integral becomes

$$E_o(\eta') = \chi \sum_m C_m\, S_{om}(c,\eta') \int_{-1}^{+1} S_{om}(c,\eta)\, u(\eta)\, E_o(\eta)\, d\eta \,. \tag{5.23}$$

The series representation of the perturbed eigenfunction is

$$E_o(\eta') = \sum_m D_m \, S_{om}(c,\eta') \ . \tag{5.24}$$

Introducing 5.24 on the left hand side of 5.23 yields for each value of $m$

$$D_m = \chi \, C_m \int_{-1}^{+1} S_{om}(c,\eta) \, u(\eta) \, E_o(\eta) d\eta \ . \tag{5.25}$$

Expressing the eigenfunction in the integrand by a similar series representation we find,

$$\begin{aligned} D_m &= \chi \, C_m \int_{-1}^{+1} S_{om}(c,\eta) \, u(\eta) \sum_n D_n \, S_{on}(c,\eta) d\eta \\ &= \chi \, C_m \sum_n D_n \, \mu_{mn} \ , \end{aligned} \tag{5.26}$$

where

$$\mu_{mn} = \int_{-1}^{+1} S_{om}(c,\eta) \, u(\eta) \, S_{on}(c,\eta) d\eta \ .$$

Equation 5.26 may be written in the more compact form,

$$\sum_n (\chi \, C_m \, \mu_{mn} - S_{mn}) \, D_n = 0 \ .$$

Thus, for nonzero solutions for $D_n$ to exist the determinant of the coefficients must vanish. Consequently, the eigenvalues $\chi$ may be found from the determinantal equation

$$\left| \chi \, C_m \, \mu_{mn} - \delta_{mn} \right| = 0 \ , \tag{5.27}$$

where

$$C_m = \frac{2i^m R_{om}^{(1)}(c,1)}{N_{om}}$$

$$= \frac{2^{m+1} i^m}{m!} \frac{c}{\pi} \left[\Gamma(\tfrac{m}{2} + 1)\right]^2 R_{om}^{(1)}(c,1) ,$$

and

$$\mu_{mn} = \int_{-1}^{+1} S_{om}(c,\eta) \left[1 + 2ikg(\eta)\right] S_{on}(c,\eta) d\eta ,$$

or

$$\mu_{mn} = N_{om} \delta_{mn} + 2ik\alpha_{mn} ,$$

where

$$\alpha_{mn} = \sum_s C_s \int_{-1}^{+1} S_{om}(c,\eta) \phi_s(\eta) S_{on}(c,\eta) d\eta .$$

## 5.4 The Perturbed Eigenvalues: Numerical Examples

First, let us look at the determinantal equation 5.27 in our often employed limit of $c$ approaching infinity. Inspection of 5.21 indicates that we may neglect the off-diagonal terms in this case. Then 5.27 reduces to the simple product

$$\prod_{m=0}^{\infty} (\chi C_m \mu_{mm} - 1) = 0 . \qquad (5.28)$$

The individual eigenvalues may be determined independently and they are given by

$$\chi_m = \left\{ 2i^m R_{om}^{(1)}(c,1) \left(1 + \frac{2^{m+1} ik}{m!} \sqrt{\frac{c}{\pi}} \left[\Gamma(\tfrac{m}{2} + 1)\right]^2 \alpha_{mm}\right) \right\}^{-1} ,$$

where

$$\alpha_{mm} = \sum \hat{c}_s \hat{d}_s \hat{n}_s \sqrt{\frac{\pi}{c}} \; \frac{m!\; e^{-P_s^2/4c}}{2^m \left[\Gamma(\frac{m}{2} + 1)\right]^2} \; L_m^o(P_s^2/2c) \; .$$

Therefore,

$$\chi_m = \left\{ 2i^m \, R_{om}^{(1)}(c,1) \left( 1 + \sum_s c_s d_s n_s (2ik) \; e^{-P_s^2/4c} \; L_m^o(P_s^2/2c) \right) \right\}^{-1} .$$

As $c$ is very large we set the exponential and the Laguerre polynomial equal to unity.

$$\chi_m = \left\{ 2i^m \, R_{om}^{(1)}(c,1) \left[ 1 + 2ik \sum_s \hat{c}_s \hat{d}_s \hat{n}_s \right] \right\}^{-1} \qquad (5.29)$$

The eigenvalues and the transfer factors are related by the following expression.

$$\chi_m = \sqrt{\frac{c}{2\pi}} \; \frac{e^{i(\frac{\pi}{4} - \frac{kb}{2})}}{\sigma_m} \; .$$

It follows that the perturbed transfer factor is

$$\sigma_m = \sqrt{\frac{2c}{\pi}} \; i^m \; e^{i(\frac{\pi}{4} - \frac{kb}{2})} \; R_{om}^{(1)}(c,1) \left[ 1 + 2ik \sum_s \hat{c}_s \hat{d}_s \hat{n}_s \right] , \qquad (5.30)$$

and for its square we have

$$\sigma_m^2 = \frac{2c}{\pi} \; i^{2m} \; e^{i(\frac{\pi}{2} - kb)} \left[ R_{om}^{(1)}(c,1) \right]^2 \left[ 1 - 4k^2 \sum_s \hat{d}_s^2 \hat{n}_s^2 \right] . \qquad (5.31)$$

Now let us consider specific numerical examples as worked out in Appendix II. For $\ell = 1.0$ the series of expansion coefficients may be summed approximately.

Thus,

$$\sigma_m^2 \cong \frac{2c}{\pi} i^{2m+1} e^{-ikb} \left[R_{om}^{(1)}(c,1)\right]^2 \left[1 - 4k^2 (0.97) g_o^2\right] .$$

For $\ell = 0.1$

$$\sum_s \hat{d}_s^2 \hat{n}_s^2 \cong 0.09 \, g_o^2 .$$

Then,

$$\sigma_m^2 \cong \frac{2c}{\pi} i^{2m+1} e^{-ikb} \left[R_{om}^{(1)}(c,1)\right]^2 \left[1 - 4k^2 (0.09) g_o^2\right] .$$

For $\ell = 0.01$

$$\sigma_m \cong \frac{2c}{\pi} i^{2m+1} e^{-ikb} \left[R_{om}^{(1)}(c,1)\right]^2 \left[1 - 4k^2 (0.006) g_o^2\right] ,$$

as

$$\sum_s \hat{d}_s^2 \hat{n}_s^2 \cong 0.006 \, g_o^2 .$$

The above results lead us to a number of conclusions. First, shorter correlation distances imply lower diffraction losses for the same surface variance. This is consistent with a general result of scattering theory which states that for sufficiently fine scale roughness the incoherent scattering may be neglected. Secondly, for the correlation distances considered the diffraction losses are significantly less than those predicted by the simple theories presented in the introduction. This is a consequence of the highly corrected nature of the confocal system as discussed in reference (1). Finally, we

note that in this large $c$ approximation the relative decrease in the transfer factor is the same for all modes.

For a resonator with square mirrors the diffraction loss is

$$\alpha_D = 1 - \frac{4c^2}{\pi^2}\left[R_{om}^{(1)}(c,1)\right]^2\left[R_{on}^{(1)}(c,1)\right]^2 (1 - 4k^2 F\sigma^2) ,$$

where $\sigma^2$ is the total variance of a surface with two orthogonal random processes $g_1(x)$ and $g_2(y)$ which are assumed to have identical statistical properties. $F$ is the sum of the squares of their expansion coefficients:

$$F = \frac{1}{g_o^2}\sum_s \hat{d}_s^2 \hat{n}_s^2 .$$

For low order modes with high $c$

$$\frac{2c}{\pi} R_{om}^{(1)}(c,1) \cong 1 ,$$

and the perturbed diffraction loss may be approximated

$$\alpha_D \cong 4k^2 F \sigma^2 . \qquad (5.32)$$

Now considering a half confocal resonator with mirror separation $b$ we find

$$Q \cong \frac{b\lambda}{4\pi F \sigma^2} . \qquad (5.33)$$

Comparing 5.33 with 1.5 it is clear that the perturbed $Q$ may be from ten to one hundred times greater than that predicted by the simple theory for the range of correlation lengths considered.

As a further example suppose a mirror roughness has a

standard deviation of one hundredth of an optical wavelength and $\ell = 0.01$. Then

$$\alpha_D \cong 4(2\pi)^2 \, (0.006) \times 10^{-4}$$

$$\cong 0.01\% \, ,$$

which is negligible compared to typical transmission and absorption losses. Thus, the diffraction losses introduced by imperfections in the figuring of high quality optical surfaces can probably be neglected.

# CHAPTER VI

## EXTENSIONS AND IMPLICATIONS OF THE PERTURBATION TREATMENT

### 6.1 Analysis of a Full Confocal Resonator with Rough Mirrors

In preceding sections we considered a confocal resonator with a rough mirror and treated this problem by requiring that the field distribution on the second mirror be of the same form as that on the first. As a confocal resonator with rough mirrors is no longer symmetrical we should require the field distribution on a mirror one to generate the same distribution again on the first mirror after being reflected by a second mirror. This procedure would then be correct for a full confocal system, whereas the solution of the previous chapter is rigorous only for the half confocal system; i.e. a resonator with a plane mirror at the focus of a rough spherical mirror (treated in 6.2).

We will now compute the round trip field for a perturbed confocal system. As the roughnesses on the two mirrors will be statistically independent functions, we need to consider a resonator with only one rough mirror when treating the statistics of the field distribution. The geometry of such a situation is depicted in Figure 6.1.

The normalized harmonic perturbation $c_s \phi_s(x_1)$ may as usual represent one of the statistically independent terms in the orthogonal expansion of a random surface.

In terms of the field $E_1(x_1)$ on the confocal surface at mirror 1 the field on the second mirror is

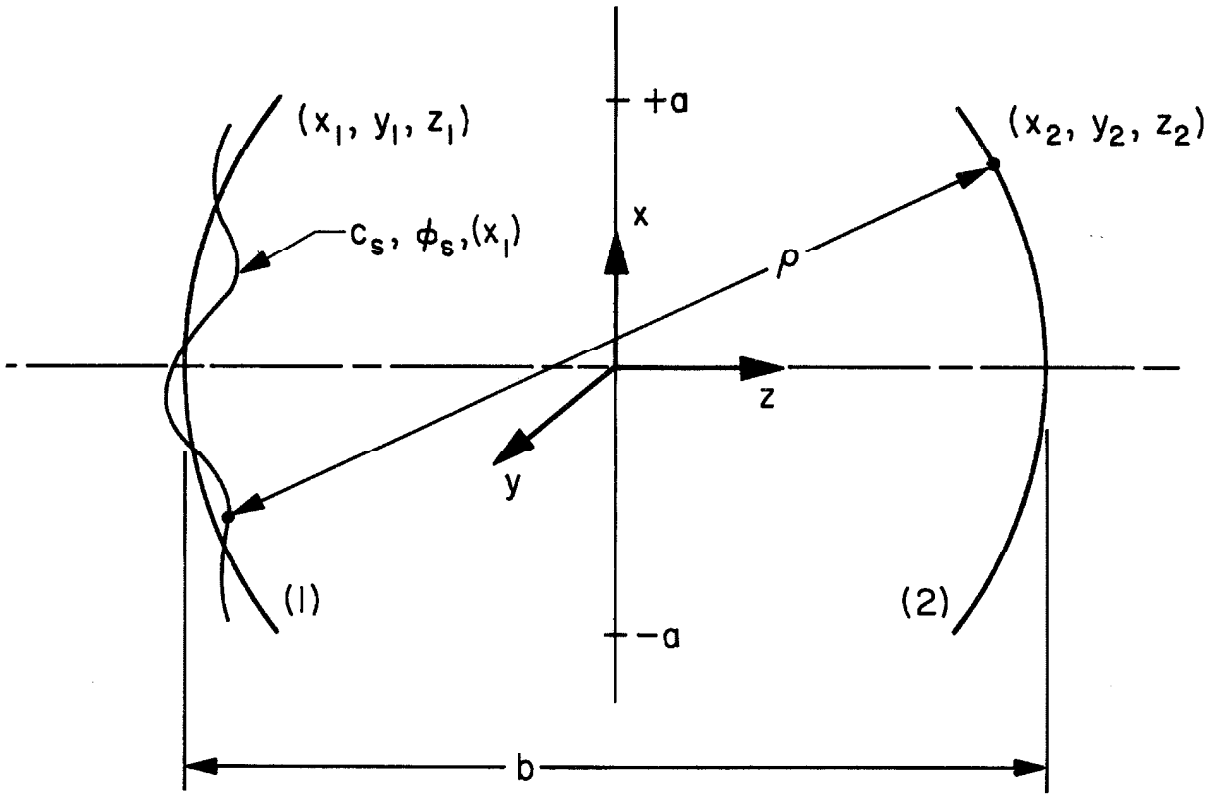


Fig. 6.1 Confocal resonator with an harmonic perturbation on mirror (1).

$$E_2(x_2) = \frac{e^{i\frac{\pi}{4}}}{\sqrt{\lambda}} \int_{-a}^{+a} \frac{e^{-ik\rho_1}}{\sqrt{\rho_1}} E_1(x_1)dx \ . \qquad (6.1)$$

Similarly, in terms of $E_2(x_2)$ we have for the field at 1,

$$\bar{E}_1(\bar{x}_1) = \frac{e^{i\frac{\pi}{4}}}{\sqrt{\lambda}} \int_{-a}^{+a} \frac{e^{-ik\rho_2}}{\sqrt{\rho_2}} E_2(x_2)dx_2 \ . \qquad (6.2)$$

With the usual approximation $\rho_1$ and $\rho_2$ are

$$\rho_1 \cong b - \frac{1}{b} x_1 x_2 + c_s \phi_s(x_1) \ ,$$

$$\rho_2 \cong b - \frac{1}{b} x_2 \bar{x}_1 \ .$$

Introducing 6.1 into 6.2 and employing the approximations for $\rho_1$ and $\rho_2$ we find $E_1(x_1)$ must satisfy the following integral equation:

$$\sigma_m^2 E_1(\bar{x}_1) = \frac{ie^{-2ikb}}{b\lambda} \int_{-a}^{+a} dx_2 \, e^{\frac{ik}{b} x_2 \bar{x}_1} \int_{-a}^{+a} dx_1 \, e^{\frac{ik}{b} x_1 x_2} \, e^{-ik\, c_s \phi_s(x_1)} \ , \qquad (6.3)$$

where the transfer factor $\sigma$ has been defined as in previous sections. Interchanging the order of integration this becomes,

$$\sigma_m^2 E_1(\bar{x}_1) = \frac{ie^{-2ikb}}{\lambda b} \int_{-a}^{+a} dx_1 \, e^{-ik c_s \phi_s(x_1)} E_1(x_1) \, k(x_1, \bar{x}_1) \ , \qquad (6.4)$$

where

$$k(x_1,\bar{x}_1) = \int_{-a}^{+a} dx_2\, e^{\frac{ik}{b} x_2(x_1 + \bar{x}_1)} = \frac{2b}{k} \frac{\sin \frac{ka}{b}(x_1 + \bar{x}_1)}{(x_1 + \bar{x}_1)} . \qquad (6.5)$$

In order to solve the above perturbed integral equation we expand the unperturbed kernel $k(x_1,\bar{x}_1)$ in an orthogonal series of spheroidal wave functions and then evaluate the resulting series of integrals using as a trial function the unperturbed solution for $E_1(x_1)$. For convenience we first define the dimensionless variables $\eta_1 = x_1/a$ and $\bar{\eta}_1 = \bar{x}_1/a$ and the quantity $c = ka^2/b$. With these definitions we rewrite 6.4 and 6.5 as

$$\sigma_m^2 E_1(\bar{\eta}_1) = \frac{ic\, e^{-2ikb}}{\pi} \int_{-1}^{+1} d\eta_1\, e^{-ikc_s\phi_s(\eta_1)} E_1(\eta_1) \frac{\sin c(\eta_1 + \bar{\eta}_1)}{c(\eta_1 + \bar{\eta}_1)} . \qquad (6.6)$$

The expansion of the kernel will be of the form

$$\frac{\sin c(\eta_1 + \bar{\eta}_1)}{c(\eta_1 + \bar{\eta}_1)} = \sum_n A_n S_{on}(c,\eta_1) . \qquad (6.7)$$

To find $A_n$ both sides of the equation are multiplied by $S_{om}(c,\eta_1)$ and integrated over the range of $\eta_1$.

$$\int_{-1}^{+1} d\eta_1 \frac{\sin c(\eta_1 + \bar{\eta}_1)}{c(\eta_1 + \bar{\eta}_1)} S_{om}(c,\eta_1) = \sum_n A_n \int_{-1}^{+1} S_{on}(c,\eta_1)\, S_{om}(c,\eta_1) d\eta_1$$

$$2(-1)^m \left[R_{om}^{(1)}(c,1)\right]^2 S_{om}(c,\bar{\eta}_1) = A_m \int_{-1}^{+1} \left[S_{om}(c,\eta_1)\right]^2 d\eta_1$$

Therefore,

$$A_m = \frac{2(-1)^m \left[R_{om}^{(1)}(c,1)\right]^2 S_{om}(c,\bar{\eta}_1)}{N_{om}} , \tag{6.8}$$

where

$$N_{om} = \int_{-1}^{+1} \left[S_{om}(c,\eta_1)\right]^2 d\eta_1 . \tag{6.9}$$

The expansion of 6.6 becomes

$$\sigma_m^2 E_1(\bar{\eta}_1) = \frac{ice^{-2ikb}}{\pi} \int_{-1}^{+1} d\eta_1 \, e^{-ikc_s\phi_s(\eta_1)} E_1(\eta_1)$$

$$\sum_n \frac{2(-1)^n \left[R_{on}^{(1)}(c,1)\right]^2}{N_{on}} S_{on}(c,\bar{\eta}_1) S_{on}(c,\eta_1) . \tag{6.10}$$

The perturbation exponential is expanded to yield

$$\sigma_m^2 E_1(\bar{\eta}_1) = \frac{2ic}{\pi} (-1)^m e^{-2ikb} \left[R_{om}^{(1)}(c,1)\right]^2 S_{om}(c,\bar{\eta}_1)$$

$$-ikc_s \frac{2ic}{\pi} e^{-2ikb} \sum_n (-1)^n \frac{\left[R_{on}^{(1)}(c,1)\right]^2}{N_{on}} S_{on}(c,\bar{\eta}_1) \tag{6.11}$$

$$\int_{-1}^{+1} S_{om}(c,\eta_1) \phi_s(\eta_1) S_{on}(c,\eta_1) d\eta_1 ,$$

where we have utilized the property of the orthogonality of the spheroidal functions and the definition of $N_{on}$ . Using the notation of Chapter V the series may be written

$$\sigma_m^2 E_1(\bar{\eta}_1) = \frac{2ic}{\pi} (-1)^m e^{-2ikb} \left[R_{om}^{(1)}(c,1)\right]^2 S_{om}(c,\bar{\eta}_1)$$

$$-ikc_s \frac{2ic}{\pi} e^{-2ikb} \sum_n (-1)^n \frac{\left[R_{on}^{(1)}(c,1)\right]^2}{N_{on}} \alpha_{mn}^s S_{on}(c,\bar{\eta}_1) \ . \tag{6.12}$$

The perturbation coefficient is defined,

$$\alpha_{mn}^s = \int_{-1}^{+1} S_{om}(c,\eta_1) \phi_s(\eta_1) S_{on}(c,\eta_1) d\eta_1 \ . \tag{6.13}$$

Clearly, the mathematics pertinent to this resonator was worked out in the preceding chapter. Comparing 6.12 and 5.13 we see that the solution for a full resonator with one rough mirror is identical to that obtained by successive application of the perturbed and unperturbed solutions of Chapter V and Chapter II, respectively.

## 6.2 The Half Confocal Resonator with a Rough Mirror

Having developed the equations characterizing the half resonator in Section 2.3 we now consider the effect of mirror roughness on such a cavity. For practical experimental reasons we are primarily interested in the case of roughness on the flat mirror; however, for the sake of comparison we shall consider in turn roughness on each mirror.

With roughness on the curved reflector 1 of Section 2.3 the integral equation satisfied by its field distribution function is

$$\bar{E}_1(\bar{x}_1) = \frac{i}{\lambda b}\int_{-\infty}^{\infty} dx_2\, e^{-ik\rho_2}\int_{-a_1}^{+a_1} dx_1\, E_1(x_1)\, e^{-ik\rho_1} . \qquad (6.14)$$

In 6.14

$$\rho_2 \cong \frac{b}{2}\left[1 + \frac{2}{b^2}\left(\frac{\bar{x}_1^2}{2} - 2\bar{x}_1 x_2 + x_2^2\right)\right] ,$$

$$\rho_1 \cong \frac{b}{2}\left[1 + \frac{2}{b^2}\left(\frac{x_1^2}{2} - 2x_1 x_2 + x_2^2\right)\right] + c_s\phi_s(x_1) ,$$

where $c_s\phi_s(x_1)$ represents a normalized harmonic perturbation. Now 6.14 becomes

$$\bar{E}_1(\bar{x}_1) = \frac{ic^{-ikb}}{\lambda b}\int_{-\infty}^{\infty} dx_2\, e^{-\frac{ik}{b}\left(\frac{x_1^2}{2} - 2\bar{x}_1 x_2 + x_2^2\right)}$$

$$\int_{-a_1}^{+a_1} dx_1\, E_1(x_1)\, e^{-ikc_s\phi_s(x_1)}\, e^{-\frac{ik}{b}\left(\frac{x_1^2}{2} - 2x_1 x_2 + x_2^2\right)} . \qquad (6.15)$$

As before the order of integration may be reversed, and the integration over $x_2$ is performed directly. The perturbation does not affect this and the resulting equation is

$$\sigma E_1(\bar{x}_1) = \frac{e^{i\left(\frac{\pi}{4} - kb\right)}}{\sqrt{\lambda b}}\int_{-a_1}^{+a_1} dx_1\, E_1(x_1)\, e^{i\frac{k}{b}x_1\bar{x}_1}\, e^{-ikc_s\phi_s(x_1)} . \qquad (6.16)$$

In terms of the dimensionless variable $\eta_1 = x_1/a_1$ 6.16 becomes,

$$\sigma E_1(\bar{\eta}_1) = \sqrt{\frac{c_1}{2\pi}}\, e^{i\left(\frac{\pi}{4} - kb\right)}\int_{-1}^{+1} e^{ic_1\eta_1\bar{\eta}_1}\, e^{-ikc_s\phi_s(\eta_1)}\, E_1(\eta_1)d\eta_1 , \qquad (6.17)$$

where

$$c_1 \equiv \frac{ka_1^2}{b} .$$

This equation is identical to that developed for a single pass in a full resonator; therefore, our assumption that we could treat a half resonator with a rough curved mirror in such a manner was justified. Hence we may apply the results of Chapter V to the half resonator configuration.

To complete this treatment of such a resonator we must look into the case of roughness on the flat reflector. The perturbed integral equation for the field distribution on the flat mirror is

$$\bar{E}_2(\bar{x}_2) = \sqrt{\frac{2}{\lambda b}}\, e^{i(\frac{\pi}{4} - kb)} \int_{-a_2}^{+a_2} e^{i\frac{2k}{b} x_2 \bar{x}_2}\, e^{-ikc_s \phi_s(x_2)}\, E_2(x_2)dx_2 . \quad (6.18)$$

In terms of dimensionless variables

$$\sigma E_2(\bar{\eta}_2) = \sqrt{\frac{c_2}{\pi}}\, e^{i(\frac{\pi}{4} - kb)} \int_{-1}^{+1} e^{2ic_2 \eta_2 \bar{\eta}_2}\, e^{-ikc_s \phi_s(\eta_2)}\, E_2(\eta_2)d\eta_2 , \quad (6.19)$$

where

$$c_2 \equiv \frac{ka_2^2}{b} .$$

For the sake of comparison let us relate the characteristics of such a resonator to one of the previous type with an unperturbed diffraction loss of the same magnitude. This requires that $c_1 = 2c_2$; i.e., the ratio of the spot size to aperture size is the same at the finite aperture of each resonator. Thus, 6.19 may be written as

$$\sigma E_2(\bar{\eta}_2) = \sqrt{\frac{c_1}{2\pi}}\, e^{i(\frac{\pi}{4} - kb)} \int_{-1}^{+1} e^{ic_1\eta_2\bar{\eta}_2}\, e^{-ikc_s\phi_s(\eta_2)}\, E_2(\eta_2)d\eta_2 \ . \qquad (6.20)$$

This is identical to 6.18. Consequently, the perturbation induced loss of such a resonator has the same geometrical dependence as the normal diffraction loss. We see that in an unsymmetrical system such as the half confocal resonator it makes no difference which mirror is perturbed as long as the spot size to aperture size ratio remains constant.

## 6.3 Diffraction Losses for Slightly Nonconfocal Resonators

Previously, we found the eigenvalue determinant for a perturbed spherical Fabry-Perot resonator of the form .

$$| \chi C_m \mu_{mn} - \delta_{mn} | = 0 \ . \qquad (6.21)$$

Rather than considering the perturbation as a random irregularity and obtaining an expected value for the eigenvalue, we may take one of the random harmonics on the mirror as a definite distortion of the confocal geometry and determine the characteristics of such a resonator. For instance a resonator with nonconfocal spacing may be approximated by adding an even harmonic to the mirror contour. One with imperfect alignment would be represented by adding an odd harmonic.

As an example of such a procedure let us look at the eigenvalue determinant for $m,n = 0,1$ .

$$\begin{vmatrix} \chi\,(N_{oo} + 2ik\,\alpha^{s}_{oo})\,C_o - 1 & \chi\,(2ik\,\alpha^{s}_{o1})\,C_1 \\ \chi\,(2ik\,\alpha^{s}_{o1})\,C_o & \chi\,(N_{o1} + 2ik\,\alpha^{s}_{11})\,C_1 - 1 \end{vmatrix} = 0 \tag{6.22}$$

Using the notation of Chapter V this may be rewritten as

$$\begin{vmatrix} \chi\,(1 + 2ik\sqrt{\frac{c}{\pi}}\,\alpha^{s}_{oo}) - \frac{1}{2R^{(1)}_{oo}(c,1)} & \chi\,(ik\sqrt{\pi c}\,\alpha^{s}_{o1}) \\ \chi\,(2ik\sqrt{\frac{c}{\pi}}\,\alpha^{s}_{o1}) & \chi\,(1 + ik\sqrt{\pi c}\,\alpha^{s}_{11}) - \frac{1}{2iR^{(1)}_{o1}(c,1)} \end{vmatrix} = 0 \tag{6.23}$$

Consulting table of perturbation terms in Chapter V it is clear that the off-diagonal terms are negligible when $c \cong 100$ and the perturbation period is comparable to the aperture size. Consequently, within the region of validity of the solutions misalignment losses may be neglected.

Now expanding 6.23 we have approximately

$$\left[\chi\,(1 + 2ik\sqrt{\frac{c}{\pi}}\,\alpha^{s}_{oo}) - \frac{1}{2R^{(1)}_{oo}(c,1)}\right]\left[\chi\,(1 + ik\sqrt{\pi c}\,\alpha^{s}_{11}) - \frac{1}{2iR^{(1)}_{o1}(c,1)}\right] = 0 \tag{6.24}$$

The eigenvalues are

$$\chi_o = \left[2R_{oo}^{(1)}(c,1)\ (1 + 2ik\sqrt{\frac{c}{\pi}}\,\alpha_{oo}^{s})\right]^{-1} ,$$

$$\chi_1 = \left[2iR_{o1}^{(1)}(c,1)\ (1 + ik\sqrt{\pi c}\,\alpha_{11}^{s})\right]^{-1} .$$

It follows that the corresponding transfer factors are

$$\sigma_o = \sqrt{\frac{2c}{\pi}}\,R_{oo}^{(1)}(c,1)\ e^{i(\frac{\pi}{4} - \frac{kb}{2})}\left[1 + 2ikc_s\, e^{-P_s^2/4c}\right] ,$$

$$\sigma_1 = \sqrt{\frac{2c}{\pi}}\,iR_{o1}^{(1)}(c,1)\ e^{i(\frac{\pi}{4} - \frac{kb}{2})}\left[1 + 2ikc_s\left(1 - \frac{P_s^2}{2c}\right) e^{-P_s^2/4c}\right] .$$

Setting $P_s = \frac{\pi}{2}$ these become

$$\sigma_o \cong \sqrt{\frac{2c}{\pi}}\,R_{oo}^{(1)}(c,1)\ e^{i(\frac{\pi}{4} - \frac{kb}{2})}\ (1 + 2ikc_s) , \qquad (6.25)$$

$$\sigma_1 \cong \sqrt{\frac{2c}{\pi}}\,iR_{o1}^{(1)}(c,1)\ e^{i(\frac{\pi}{4} - \frac{kb}{2})}\ (1 + 2ikc_s) , \qquad (6.26)$$

for large $c$. We have taken $c_s$ as the amplitude of the perturbation harmonic. However, it cannot have quite such a simple interpretation. In deriving the perturbed Green's function it was required that the surface irregularity be a random process with zero mean. Obviously the even perturbation chosen above is not of zero mean. We may compensate for this by going back to the original characteristic integral and dividing the perturbed Green's function by its mean magnitude. For convenience we take the mean as its value at the spot size radius or, typically, at $\eta \cong 0.1$. Now 6.25 becomes

$$\sigma_o \cong \sqrt{\frac{2c}{\pi}}\, R_{oo}^{(1)}(c,1)\, e^{i\left(\frac{\pi}{4} - \frac{kb}{2}\right)} \left(\frac{1 + 2ik c_s}{1 + 2\,(0.98)\, k^2 c_s^2}\right) .$$

This implies that just as in the misalignment case the imperfect spacing loss will be negligible within the region of validity of this expansion.

Let us now see just what the foregoing implies. An odd perturbation harmonic with an amplitude of one twentieth the radiation wavelength corresponds to a mirror rotation of approximately $10^{-4}$ radian or 20 seconds. For rotations of this magnitude the change in diffraction loss should be small relative to 1%. An even perturbation harmonic with a comparable amplitude corresponds to a variation of about 1 cm. in a basic 1 m. mirror separation and this should introduce a similarly small increase in the diffraction loss.

## 6.4 Characteristics of the Perturbed Field at the Aperture

In Chapter V the following series expansion was derived for the perturbed aperture field.

$$\sigma_n E_{on}(\eta') = \sqrt{\frac{2c}{\pi}}\, i^n R_{on}^{(1)}(c,1)\, e^{i\left(\frac{\pi}{4} - kb\right)} S_{on}(c,\eta') - 2ik\sqrt{\frac{2c}{\pi}}\, e^{i\left(\frac{\pi}{4} - kb\right)} \sum_m \frac{i^m R_{om}^{(1)}(c,1)}{N_{om}} \alpha_{mn} S_{om}(c,\eta') \tag{6.27}$$

As this solution is valid only for small perturbations, we would expect the correction represented here to be most discernable at a zero of the unperturbed field distribution. The first function to possess

a zero is $S_{o1}(c,\eta)$ which vanishes at $\eta = 0$. Let us now consider the filling-in of this zero due to the rough mirrors. For this case 6.27 becomes

$$- \frac{i\sigma_1}{R_{o1}^{(1)}(c,1)} \sqrt{\frac{\pi}{2c}}\, e^{-i(\frac{\pi}{4} - kb)} E_{o1}(\eta') = S_{o1}(c,\eta') \qquad (6.28)$$
$$- 2k \sum_m \frac{i^m}{N_{om}} \alpha_{m1} S_{om}(c,\eta') ,$$

where $c$ has been assumed large so that the radial spheroidal functions converge to the same value. Taking the first order corrections to the unperturbed mode, the right hand side of 6.28 becomes

$$S_{o1}(c,\eta') - 2k \left[ \frac{\alpha_{10}}{N_{oo}} S_{oo}(c,\eta') + \frac{i\alpha_{11}}{N_{o1}} S_{o1}(c,\eta') \right. \qquad (6.29)$$
$$\left. - \frac{\alpha_{12}}{N_{o2}} S_{o2}(c,\eta') \right] .$$

The relative energy at the null $(\eta' = 0)$ will be

$$4k^2 \left[ \frac{\alpha_{10}}{N_{oo}} S_{oo}(c,\eta') - \frac{\alpha_{12}}{N_{o2}} S_{o2}(c,\eta') \right]^2 . \qquad (6.30)$$

The normalization of the spheroidal functions is such that a mode's energy content is approximately proportional to its maximum value. The modes $m = 0,2$ have maxima at $\eta = 0$; therefore, the peak to valley energy ratio is approximately the ratio of normal to scattered energy. As an example if we consider $c = 100$, $\ell = 0.1$ and $g_o = \lambda/100$

and refer to Chapter V and Appendix III we find a peak to valley energy ratio of $1.5 \times 10^{-3}$.

In the foregoing discussion it was pointed out that the strongest contributions to the spatial scattering of a specific mode occurs in adjacent modes. Thus, if the unperturbed field is even, the scattering will be primarily of an odd character. Similarly, an odd field scatters into even modes. This suggests a possible experiment to investigate such scattering. Specifically, the relative phases at pairs of "zeros" will have the opposite phase relationship from that of the major portions of the mode so that performing a Young's experiment should show a shift in the fringes for interference from a pair of nodes in the field distribution.

## 6.5 Comparison of the Two Computations for the Scattered Field

In Chapter IV the radiation scattered from an imperfect confocal surface was computed neglecting any correlation between the incident field and the perturbation. From 4.21 the relative field intensity at a zero of the mode $n = 2$ will be

$$I(\eta_o) = \frac{8k^2\sigma^2}{c\ell^2} e^{-c\eta_o^2} \left[5 - 46c\eta_o^2 + 44c^2\eta^4 - 8c^3\eta^6\right], \quad (6.31)$$

where

$$\eta_o = \frac{1}{\sqrt{2c}} .$$

Taking the parameters of previous examples: $k^2\sigma^2 = (2\pi)^2 \times 10^{-4}$, $c = 100$ and $\ell = 0.1$, the relative intensity is

$$I_o(\eta_o) \cong 1.5 \times 10^{-1} .$$

Comparing this with the results of the preceding section we see that for identical resonator parameters approximately one hundred times as much scattered energy appears at a pattern node when spatial correlation between radiation and irregularities is neglected.

# CHAPTER VII

## SCATTERING FROM SMALL RANDOM IMPERFECTIONS

In this paper the emphasis has been placed on finding the distortion of the modes of a confocal resonator by small irregularities in the shapes of the mirrors. This deviation of the surface of the mirror must be small with respect to the radiation wavelength and in addition is allowed to change only by a negligible amount in a distance comparable to an optical wavelength along the mirror surface. However, Specht (32) has found that most of the scattering is from a distribution of small localized scattering centers. In this section we will treat a similar situation.

It is assumed that each mirror has a large number of very small, sharp irregularities. Each of these scattering centers is much smaller than the radiation wavelength. The reflection from such a surface will be characterized as coming from an undisturbed surface with a random distribution of multipoles with random strengths and phases. We presume the scattering centers are similar pinholes in the dielectric films and thus will be predominantly dipole scatterers with random phases and of strength proportional to the incident field intensity. To the approximation that $\cos\theta = 1$ as in Chapter II we may formulate the characteristic integral as follows;

$$\sigma_m E_m(\eta) = \sqrt{\frac{c}{2\pi}}\, e^{i(\frac{\pi}{4} - kb)} \left\{ \int_{-1}^{+1} e^{ic\eta\eta'}\, E_m(\eta')\, (1 - \Delta) d\eta' \right.$$

$$\left. + \int_{-1}^{+1} e^{ic\eta\eta'}\, \Delta E_m(\eta')\, e^{i\phi(\eta')} d\eta' \right\} , \tag{7.1}$$

where $\Delta$ is the fraction of the incident radiation scattered by the imperfections and $\phi(\eta')$ represents their distribution of phase shifts. As we are considering very fine scale imperfections we may take the field distribution $E_m(\eta')$ and the phase distribution $\phi(\eta')$ as being statistically independent and take their expectations independently. The expectation of 7.1 is then

$$\sigma_m \langle E_m(\eta) \rangle = \sqrt{\frac{c}{2\pi}}\, e^{i(\frac{\pi}{4} - kb)} \left\{ \int_{-1}^{+1} e^{ic\eta\eta'} \langle E_m(\eta') \rangle\, (1 - \Delta) d\eta' \right.$$

$$\left. + \int_{-1}^{+1} e^{ic\eta\eta'}\, \Delta \langle E_m(\eta') \rangle \langle e^{i\phi(\eta')} \rangle\, d\eta' \right\} . \tag{7.2}$$

Writing $F_m(\eta) \equiv \langle E_m(\eta) \rangle$ and evaluating $\langle e^{i\phi(\eta')} \rangle$ we have

$$\sigma_m F_m(\eta) = \sqrt{\frac{c}{2\pi}}\, e^{i(\frac{\pi}{4} - kb)} \left\{ \int_{-1}^{+1} e^{ic\eta\eta'}\, F_m(\eta')\, (1 - \Delta) d\eta' \right.$$

$$\left. + \int_{-1}^{+1} e^{ic\eta\eta'}\, \Delta\, F_m(\eta') \left\langle 1 - i\phi(\eta') + \frac{[i\phi(\eta')]^2}{2} \ldots \right\rangle d\eta' \right\} . \tag{7.3}$$

Taking $\phi(\eta) = 0$ and requiring that the variance $\phi^2(\eta) = \sigma^2$ be small we find

$$\sigma_m F_m(\eta) = \sqrt{\frac{c}{2\pi}}\, e^{i(\frac{\pi}{4} - kb)} \int_{-1}^{+1} e^{ic\eta\eta'} F_m(\eta') \left(1 - \frac{\Delta\sigma^2}{2}\right) d\eta' . \tag{7.4}$$

We see that $F_m(\eta')$ satisfies the same integral equation as the spheroidal wave functions $S_{om}(c,\eta')$. In this case the transfer ratio is

$$\sigma_m = \sqrt{\frac{2c}{\pi}}\, i^m\, e^{i(\frac{\pi}{4} - kb)} \left(1 - \frac{\Delta\sigma^2}{2}\right) R_{om}^{(1)}(c,1) . \tag{7.5}$$

It is clear that the phase shift of 7.5 is unaffected by the perturbation, and, therefore the resonance condition remains unchanged. On the other hand the magnitude of the transfer ratio is given by

$$|\sigma_m| = \sqrt{\frac{2c}{\pi}} \left(1 - \frac{\Delta\sigma^2}{2}\right) R_{om}^{(1)}(c,1) . \tag{7.6}$$

For $c > 1$ we have

$$\sqrt{\frac{2c}{\pi}}\, R_{om}^{(1)}(c,1) \cong 1 .$$

Therefore,

$$|\sigma_m| \cong 1 - \frac{\Delta\sigma^2}{2} , \tag{7.7}$$

and the diffraction loss is approximately

$$\alpha_D = 1 - |\sigma_m|^2 \cong \Delta\sigma^2 . \tag{7.8}$$

From 7.8 we see that the diffraction loss is proportional to the product of the relative area of the scattering centers and the variance of their

phase shifts.

An examination of 7.1 indicates that this same formula will apply to a three-dimensional resonator with rectangular mirrors as well. In this case $\Delta$ represents the relative cross-section of the scattering centers and again $\sigma^2$ is the variance of the phase shifts.

Specht (32) has determined that for typical dielectric film mirrors $\Delta = 0.04$. He finds that the corresponding power loss is about 1%. With this data and 7.8 we can obtain an approximate value for $\sigma^2$ (it must be borne in mind, however, that we have neglected any absorption losses in the scattering centers). Thus, we find

$$\sigma^2 = 0.25. \tag{7.9}$$

By setting the standard deviation $\sigma$ equal to twice an equivalent depth of pinholes in angular measure we find for the rms depth of the holes,

$$d = \frac{\lambda}{8\pi} .$$

If such a pinhole model conforms with the situation encountered in practice, this rough calculation would indicate that they are less than one film layer thick.

# CHAPTER VIII

## MEASUREMENT OF THE DIFFRACTION LOSS OF PERTURBED CONFOCAL RESONATORS

### 8.1 Quality Factor and Diffraction Loss of a Multimode Resonator

In the preceding analytical treatments of perturbed systems perhaps the most readily verifiable result is the predicted diffraction loss. Boyd and Gordon (8) show that the quality factor $Q_s$ is related to the parameters of a multimode resonator by the equation

$$Q_s = \frac{2\pi d}{\alpha_s \lambda} \tag{8.1}$$

where $d$ is the mirror separation, $\alpha_s$ is the fractional power loss of mode $s$ per bounce from a mirror and $\lambda$ is the optical wavelength. Thus, a measurement of the $Q_s$ for a particular confocal mode is a direct measure of its diffraction loss.

A gas laser with its exceedingly sharp output spectrum is well adapted as a diagnostic probe in $Q$ measurements on confocal resonators. Consider the scheme represented in Figure 8.1. Resonator 1 is a half confocal configuration containing an active region to provide stimulated emission. The spherical mirror is mounted so that the mirror separation may be varied electrically providing a frequency swept laser output. The passive resonator 2 is axially aligned to the laser beam and allows energy to reach the photodetector whenever the probe signal sweeps through one of its resonances. Consequently, a display of photodetector output versus laser sweep voltage will yield conventional resonance curves. Introducing a controlled perturbation

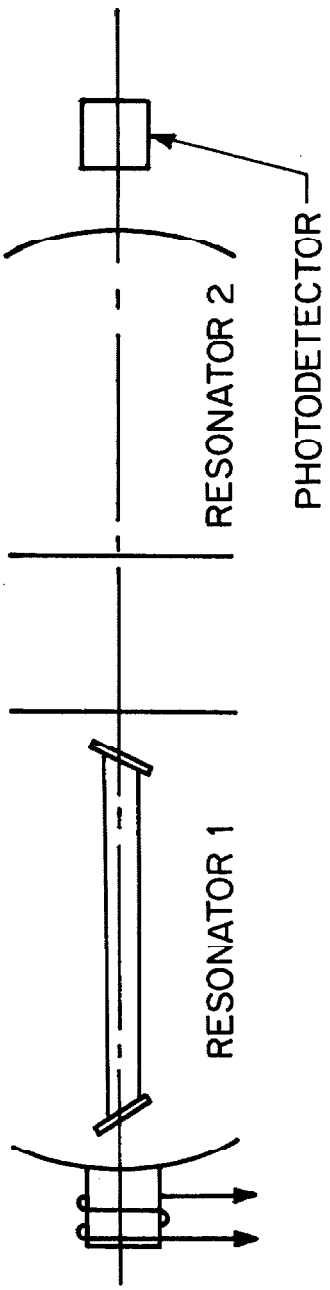


Fig. 8.1 Representation of Q measuring apparatus.

into the passive cavity should cause an enhanced diffraction loss and degraded $Q_s$ as predicted by the analysis of the preceding chapters.

In performing such measurements there are several complicating factors which must be considered and which will modify the experimental configuration as presented in Figure 8.1. These are listed below.

(1) In Appendix IV it is shown that a very slight mirror movement is sufficient to modulate a cavity resonance by many megacycles. Thus, acoustically induced mirror vibrations must be held to a very low level to insure negligible resonance broadening.

(2) Ambient turbulence will modify the optical length of the resonator and can broaden a line in much the same manner as mirror vibrations.

(3) With the laser operating simultaneously on several modes there is the possibility of certain resonance curves overlapping and leading to false line-broadening. Consequently, it is desirable to have as few laser modes as possible and proper resonator dimensions to insure evenly spaced resonances which do not overlap.

(4) If there is direct transmission between the active and passive resonators the laser output may be pulled and modulated by the test cavity. Therefore, it is desirable to provide isolation between them.

(5) Should there be imperfect alignment between the two resonators, a particular laser mode may couple into a different test cavity mode. With multimode laser operation this could lead to

overlapping resonances. In addition, without overlapping it still means that an observed resonance may be for an unwanted mode with a different $Q_s$ from that of interest. One must then be able to distinguish between wanted and unwanted resonances.

## 8.2 Experimental Details

Figure 8.1 of the preceding section illustrates a possible basic experimental configuration. However, it was found that a great deal of attention to detail was important in performing accurate measurements. The entire optical portion of the apparatus is mounted on a 3' x 6' Brown and Sharpe surface plate of approximately one thousand pounds total weight. This provides structural rigidity as well as inertial damping for the system. The surface plate is in turn supported six inches from floor level by a layered structure of felt, neoprene and metal sheets and low pressure rubber inner tubes. Finally, each mirror is isolated from its respective mount by felt cushioning. The resonators are hooded to absorb scattered light and minimize ambient turbulence. In addition an acoustically insulated hood surrounding the entire apparatus and capable of providing a helium atmosphere was available but not required for the measurements reported here. It was found that in the frequency range of 20-20,000 cps the peak table acceleration was approximately 1/28 that of the nearby floor.

The final form of the apparatus is shown schematically in Figure 8.2. Figure 8.3 is a photograph of the apparatus. In this arrangement it should be pointed out that the passive instead of the

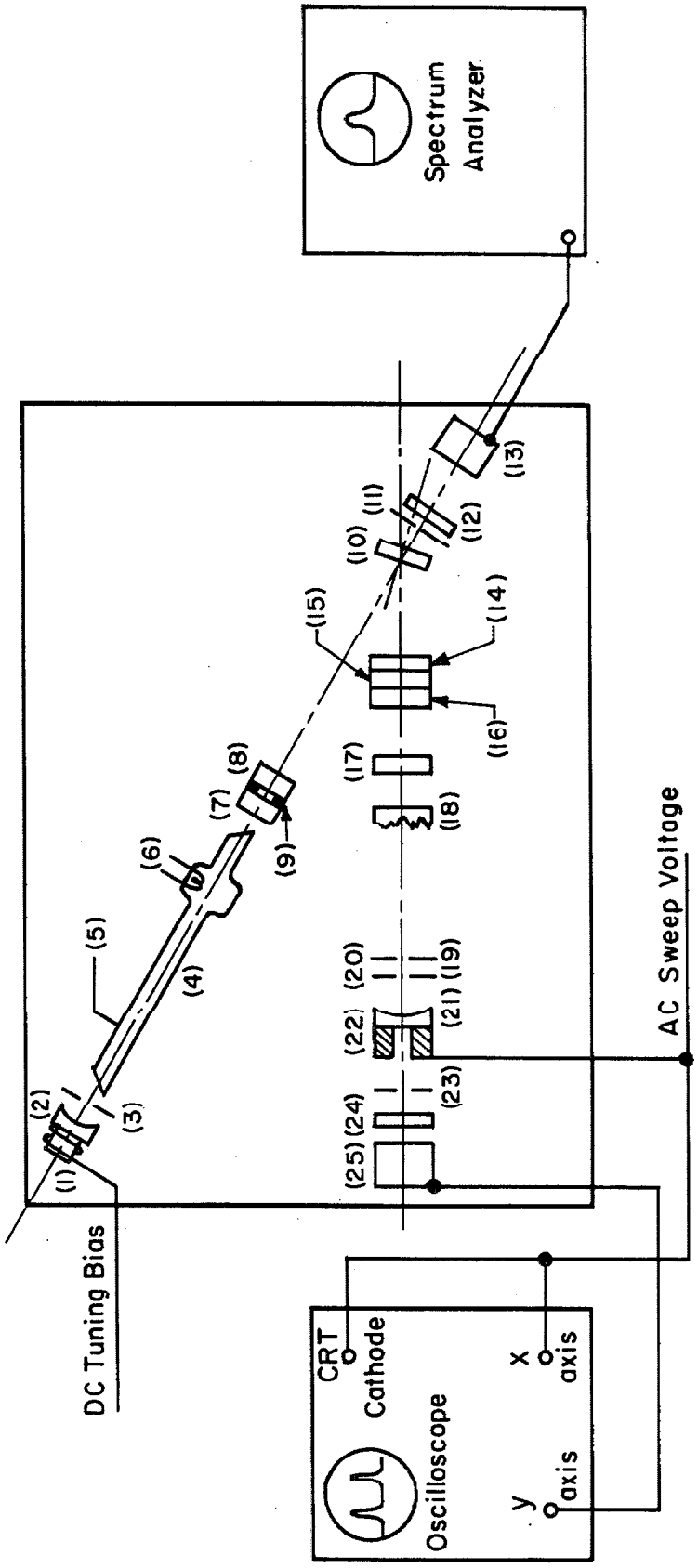


Fig. 8.2 Experimental apparatus.

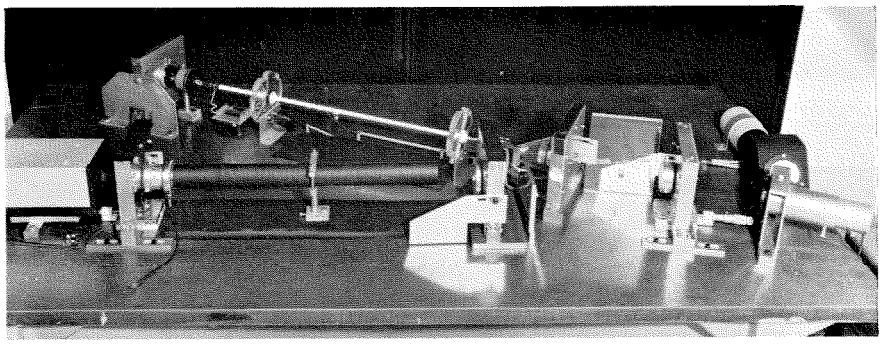

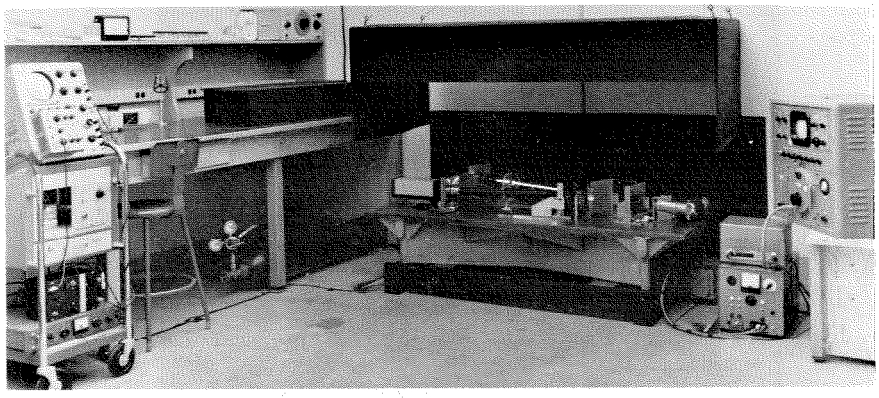

Fig. 8.3 Photographs of apparatus.

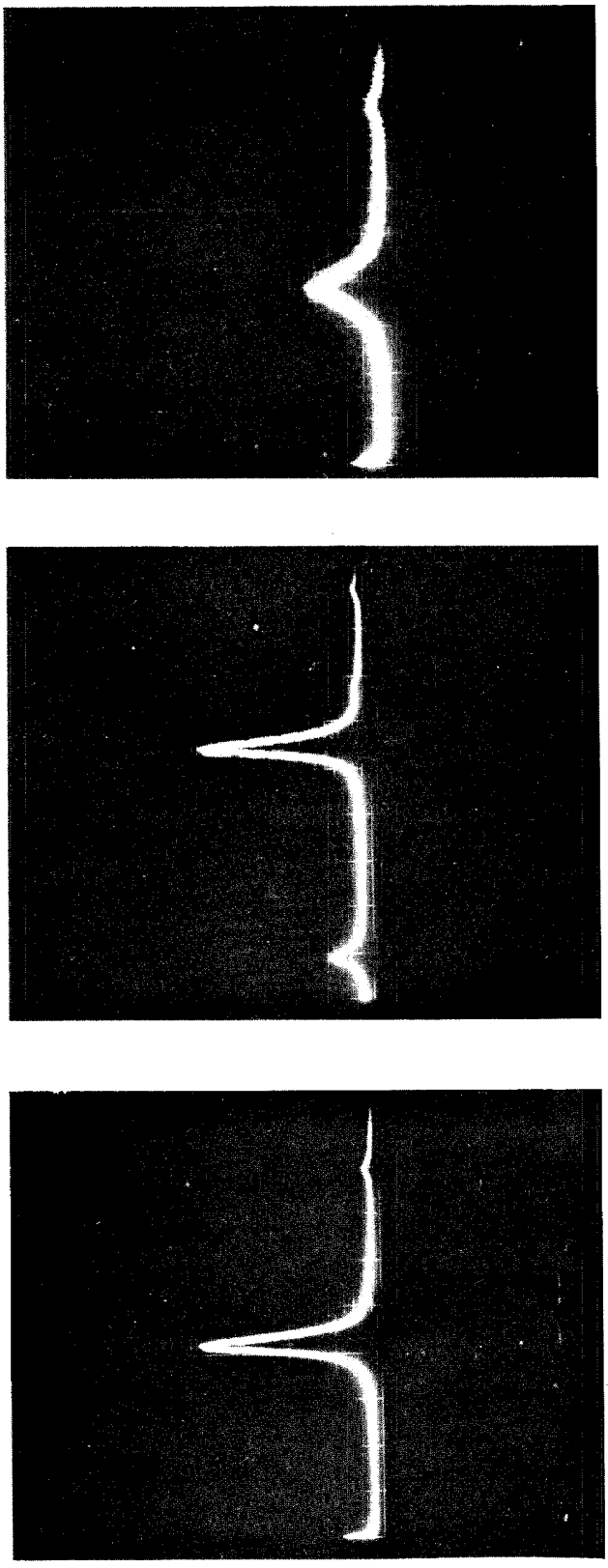

Fig. 3.4 Typical resonance photographs.

active resonator is swept. This is desirable as the laser can be operated then at constant power rather than inducing undesirable AM along with the FM laser sweep. Stable single mode operation is then not difficult to achieve.

The components are listed below.

(1) Electromagnetic driver which tunes the laser through the movement of curved mirror 2.

(2) Laser mirror of one inch diameter homosil and one-half inch thick. The front surface is 99.6% reflecting and has a 5 meter radius of curvature.

(3) Iris to cut out off-axis laser modes: 2-4 mm diameter.

(4) D.C. excited hot cathode Ne-He gas laser tube of 82 cm length.

(5) Arc anode

(6) Arc cathode

(7) First plane laser mirror of one inch diameter homosil with 10" wedge angle and one-half inch thick. Coating gives 98.6% reflection.

(8) Brass spacer between plane laser mirrors, 0.001" thick.

(9) Second plane laser mirror of same type as (7).

(10) Laser beam reflector. Same as (7).

(11) Iris to reduce background light reaching photomultiplier 13:2 mm diameter.

(12) Red Corning photomultiplier filter: Type CS2-60.

(13) Photomultiplier for monitoring laser output level and multimode beats: RCA Type 7102.

(14) Red Corning glass filter CS2-60 slightly misaligned to

reduce coupling between resonators and destroy resonances between mirrors 9 and 17.

(15) Neutral Density Filter: same function as (14), ND = 1.0

(16) Red Wratten Filter: same function as (14). A type 25.

(17) Passive resonator plane mirror; same as (7).

(18) Passive resonator perturbation sample.

(19) Shutter for zeroing photomultiplier 25.

(20) Iris to control diffraction losses of off-axis modes in passive resonator: 2-4 mm diameter.

(21) Passive resonator rear mirror; same as 2 but 1.2 meter radius of curvature.

(22) Barium Titanate slug to sweep passive resonator; 500 volts rms sweeps over approximately 280 mcs.

(23) Photomultiplier iris: 2-4 mm diameter.

(24) Red Glass Photomultiplier Filter: Corning CS2-60

(25) Photomultiplier EMI 9558/B.

Let us now go through a detailed functional discussion of this apparatus.

Mirror 1 is supported by two flexible metal diaphragms such that it may be moved axially without suffering misalignment. It is driven by an electromagnetic wobbulator adapted from an FM altimeter. A DC bias of a few millivolts is sufficient to center any particular laser mode on a line of the passive resonator. The basic laser resonator is formed by mirror 2 with a 5 meter radius of curvature and plane mirror 7 separated by 89 cm. Such a resonator is nearly plane parallel Fabry-Perot geometry and is relatively free of off axis modes. However,

iris 3 is useful in increasing still further the losses of such modes. Plane mirror 9 is useful in suppressing both off axis and multiple axial modes (31). In addition, mirror 9 provides sufficient decoupling to render negligible the effect of passive resonator feedback on the laser. Although the transmission through 9 is 1.5%, the laser output is only down to about one-fourth the intensity without 9. This results from the fact that the laser loss is greatly reduced giving rise to a greater radiation intensity in the laser resonator. It was found that the above features were sufficient to cause single mode laser operation when the discharge current was reduced from a normal value of 20 ma down to 5 ma.

Mirror 10 reflects 98.5% of the intensity of the laser beam into the passive resonator. Approximately 1.5% of the beam, therefore, is transmitted to iris 11, filter 12, and then to photomultiplier 13. The photomultiplier output is observed on a spectrum analyzer to determine the laser mode structure through optical beats. The photomultiplier also serves as a monitor of the laser output level.

Mirrors 17 and 21 define the passive confocal test resonator. However, the region between mirrors 9 and 17 will behave as a plane Fabry-Perot resonator. Consequently, the laser beam blooms in this parasitic resonator with the result that additional energy is coupled into higher order modes in the passive test resonator. This causes no real difficulty, as these unwanted resonances are easily recognized by their large width and low amplitude. Nevertheless, to achieve clearer resonance curves, additional decoupling between active and passive

resonators, and to improve the noise figure of the system, the filter elements 14, 15 and 16 were employed. In transmission they favor the red laser wavelength. By misaligning each filter by a few milliradians the surface reflections from each element are lost virtually eliminating any resonances in that region, while causing only a very minor distortion of the laser beam.

Mirrors 17 and 21 define the passive confocal resonator. The curver mirror 21 is mounted on a barium titanate slab. A sweep voltage applied to the barium titanate and the horizontal amplifier of an oscilloscope produces a swept interferometer display. The light transmitted by this resonator passes through a hole in the barium titanate to reach a photomultiplier driving the vertical amplifier of the oscilloscope. Thus, along the horizontal sweep a vertical displacement of the trace indicates that one of the passive system resonances coincides in wavelength to a laser line.

Element 18 represents an arbitrary transparent perturbation sample placed in the passive resonator. It is slightly misaligned to remove the effect of surface reflections on mode coupling. However, any surface irregularities will modify the optical length of the resonator across its aperture and give mirror 17 an effective roughness. A measurement of the resonance width of such an artificially perturbed interferometer can be compared then with the analysis of the previous chapters.

Finally, it should be pointed out that there is a non-integral ratio between the lengths of the two resonators. This causes a vernier

effect between the resonance lines of the laser and test interferometer. The reason for this is to eliminate any false broadening through the coincidence of multiples resonances.

## 8.3 Sweep Calibration

When sweeping the passive resonator of the experimental apparatus one observes resonance curves on the oscilloscope monitoring its transmission. The widths of the various resonances are proportional to the diffraction losses of the various modes. In order to determine the absolute diffraction loss of a particular mode, it is necessary to calibrate the sweep.

Referring to Appendix IV, it is evident that the passive resonator with a 58.3 cm mirror spacing will have a basic axial mode separation of 258 mc. For a sufficiently great sweep voltage one would expect a resonance separation of this value under conditions of single mode laser operation. Indeed such a resonance repetition was observed when the sweep voltage was increased to 510 volts rms. Subsidiary resonances were observed for energy coupling into off axis modes. These also exhibited the same periodicity. When the laser was caused to operate on several modes, resonances appeared which approximately trisected the basic spacing as would be expected from the basic 168 mc axial laser mode spacing. The relative amplitudes of such multiple resonances also indicate the spectral gain curve of the laser.

Photographs were taken of the multiple resonances with a sweep of 510 volts rms. On the photographs the basic axial mode separation was 5.54 cm or 46 mc/cm. With such a sweep voltage the resonance

width is extremely narrow. Thus for Q measurements a 290 volt rms sweep was employed. This corresponds to a sweep scale of 26 mc/cm on similar photographs.

## 8.4 Measurements

With a 290 volt sweep on the unperturbed passive resonator a line-width of 0.04 inches was measured on the photographs. This corresponds to a bandwidth of 2.7 mc and a Q of $1.75 \times 10^8$. From equation 8.1 we find an average power loss per bounce of 3.4%.

To perturb the resonator one-half inch thick discs of homosil were placed in front of the plane mirror. The first was polished and flat to 1/70 wavelength. Its function was to calibrate the surface reflection losses of the samples. It increased the line-width to 0.09 inches or 6.0 mc which corresponds to an average power loss per bounce of 7.6%. A second sample was secured upon which no effort had been taken during polishing to maintain surface flatness. Over the central one-half inch portion of this disc it was estimated to have a maximum surface deviation on each side of one-quarter fringe. It degraded the line-width to 0.15 inches or 10 mc and yielded an average power loss per bounce of 13%.

An additional disc was prepared by grinding with the finest grinding compound readily available which was 0.3 micron alumina. This produced a frosty surface when ground against a hard surface and could not be considered a small perturbation surface. When placed in the resonator the line-width was 0.72 inches or 48 mc. The measurements are summarized in Table 8.1.

| Perturbation | $\Delta f$(mc) | $Q_s$ | $\alpha_s$ |
|---|---|---|---|
| None | 2.7 | $17.5 \times 10^7$ | 3.4% |
| $\lambda/70$ Flat | 6.0 | 7.9 | 7.6 |
| Wavy Disc | 10.0 | 4.7 | 13.0 |
| Ground Disc | 48.0 | 0.9 | - |

Table 8.1 Summary of Measurements

## 8.5 Discussion and Conclusions

Let us now return to the measurements of the preceding section and consider their meaning and implications.

An average power loss per bounce of 3.4% was measured for the unperturbed resonator. With a measured 1.0% average transmission loss per bounce we compute a 2.4% scattering and absorption figure for each mirror. Specht (32) arrived at a figure of 1.0% for his mirrors. As the best mirrors available for these measurements were used in the laser resonator, it is not surprising that the passive resonator mirrors exhibited a greater loss than those studied by Specht.

Now considering the perturbed resonator it may be asked why the sample is not placed at the Brewster angle thereby improving the precision of the measurement. The primary reason for this is to prevent portions of the surface from being shadowed by higher peaks. This could happen for a finely ground surface. If such a situation did occur, it could no longer be considered a small perturbation. However, it would be quite reasonable to place the wavy polished surface at an angle. Let us now compare the implications of the alternate

orientations for the perturbation element. First we consider the effect of slight variations in the angle at which the perturbation plate is set. For an electric vector lying in the plane of incidence the power reflectivity from the dielectric boundary is given by

$$R = \frac{\tan^2(\theta_o - \theta_1)}{\tan^2(\theta_o - \theta_1)} \quad ,$$

where $\theta_o$ and $\theta_1$ are the angles of incidence and refraction, respectively. For slight deviations from near normal incidence the total derivative of $R$ is

$$\frac{dR}{d\theta_o} = - \frac{8n_{12}(1 - n_{12})}{3(1 + n_{12})} \, d\theta_o \quad , \quad \text{(normal incidence)}$$

where $n_{12}$ is the ratio of the velocities of light in the two media. Evaluating the constant we have approximately

$$\frac{dR}{d\theta_o} = - 0.33 \, d\theta_o \quad . \qquad \text{(normal incidence)}$$

Now at the Brewster angle

$$\frac{dR}{d\theta_o} = (1 + n_{12} \frac{\cos \theta_o}{\cos \theta_1})^2 \tan^2(\theta_o - \theta_1) \, d\theta_o$$

(Brewster angle)

Again we find the slope of the reflectivity is proportional to the angular error, and evaluating the constant,

$$\frac{dR}{d\theta_o} = 0.32\ d\theta_o \ . \qquad \text{(Brewster angle)}$$

Clearly, the two orientations are virtually equivalent regarding susceptibility to angular error. Next let us compare the perturbation to nonperturbation line width ratio in order to determine the relative signal sensitivities of the two orientations. With the perturbation plate normal to the resonator axis as described in Section 8.4, the ratio of perturbed to unperturbed line width is

$$r = \frac{10\ \text{mc}}{6\ \text{mc}} = 1.7$$

for the polished irregular disc. Consider placing the disc at the Brewster angle. The surface irregularities will have a projection along the axis of $\cos(53^\circ)$ times their normal height. Therefore the increase in perturbation line width will be $(\cos 53^\circ)^2$ times that observed at normal incidence. This yields a line width ratio of

$$r = \frac{4.1\ \text{mc}}{2.7\ \text{mc}} = 1.5 \ ,$$

where it is assumed that transmission at Brewster's angle is lossless. Again we see that the alternate configurations are virtually equivalent.

Now employing the results of Chapter V let us compute the expected diffraction loss for the resonator of the previous section perturbed by the irregular polished homosil disc. Monochromatic fringes were observed for the homosil surface against an optical flat.

It was estimated that in the central one-half inch portion the maximum deviation of both sides was one-quarter fringe. This corresponds to a maximum deviation of approximately 0.085 fringe over the diameter of the resonator aperture which is 0.17 inches. As the index of refraction of quartz is approximately 1.5, the irregular surfaces on each side will have the same net effect as a mirror with an identical deviation. Taking the correlation distance of the irregularity as equal to the aperture radius and the standard deviation equal to one-half the maximum deviation, or 0.042 fringe, and referring to Section 5.4, we have for the computed perturbation diffraction loss

$$\alpha \cong 8k^2(0.97)\, g_o^2$$

$$\cong 13.5\% \quad .$$

This is equivalent to an average loss per pass of 6.7%. This is to be compared with the difference between 13% and 7.6% or 5.4% of the preceding section. The agreement between 6.7% and 5.4% is entirely satisfactory as there is nc reason to suppose that the irregularities on the disc obey Gaussian statistics or can be described by an exponential correlation function. In addition, as the diffraction loss depends on the square of the deviation of the surface, a small error in the measured deviation is magnified in the computed loss. However, the above results are most dramatic when compared to the spectroscopic approximation presented in Section 1.2. According to this theory

$$Q \cong \frac{b}{\sigma} \quad .$$

For the perturbed test resonator discussed here we have by this approximation

$$Q \cong 4.5 \times 10^{7} \quad .$$

This is equivalent to an average diffraction loss per pass of 13% or approximately two and one-half times that observed experimentally. It thus seems clear that the perturbation analysis offers a significant improvement in accuracy over the earlier theory.

# CHAPTER IX

## SUMMARY AND CONCLUSIONS

A self consistent field analysis has been applied to perturbed confocal resonators and it has been demonstrated that such solutions may be applied to half confocal resonators. In addition both full and half resonators are readily amenable to a two-dimensional analysis and the three-dimensional solutions are products of solutions for infinite strip resonators. These solutions of Chapter V are given in general by an infinite series of the unperturbed mode solutions. The diffraction losses for several perturbation correlation distances are worked out and it is found that as this distance approaches the resonator aperture radius the loss becomes that predicted by the linear theory of Section 1.3, viz. equation 1.15. As the correlation length decreases, the corresponding loss becomes vanishingly small in agreement with a general conclusion of the theory of scattering from rough surfaces.

In Chapter IV an approximate technique is developed for obtaining closed form solutions of the perturbed integral equation. The method is then applied to a particular confocal mode and the null filling-in for a perturbed field distribution function is computed. Such solutions apply when correlation between the radiation field and the surface irregularities may be neglected as when the roughness has a very short correlation length. The corresponding eigenvalues and diffraction losses are worked out in Chapter VII.

Finally, in Chapter VIII an experiment is described for making diffraction loss measurements on multimode optical resonators. The technique involves measuring the resonance width of a particular mode of an open resonator by sweeping it through a sharp laser line (34). Two irregular quartz discs were prepared and introduced into the passive resonator. The sample conforming with the requirements of small roughness height and slope demanded by the perturbation analysis produced a change in resonance width exceedingly close to that predicted by the analysis.

## APPENDIX I

## EXPANSION OF THE MIRROR ROUGHNESS IN AN ORTHOGONAL SERIES (33)

In 3.3 we found it desirable to expand the mirror roughness in a series of spatial harmonics. For such an expansion to be useful it must be developed in a special manner in order that the coefficients will be uncorrelated random variables.

The required series will be of the form

$$g(\eta) = \sum_s c_s \phi_s(\eta) \quad , \tag{I.1}$$

where

$$c_s = 0 \quad ,$$

$$c_s c_t = \begin{cases} 0 \ , & s \neq t \\ 1 \ , & s = t \end{cases}$$

and

$$\phi_s(\eta) = d_s \theta_s(\eta)$$

such that

$$\int_{-1}^{+1} \theta_s(\eta)\, \theta_t(\eta)\, d\eta = \begin{cases} 0 \ , & s \neq t \\ 1 \ , & s = t \end{cases}$$

According to Karhunen's representation theorem the quantities $d_s$ and the orthogonal functions $\theta_s(\eta)$ satisfy the integral equation

$$\int_{-1}^{+1} R(\eta - \eta')\, \Theta_s(\eta)\, d\eta = d_s^2\, \Theta_s(\eta') \quad . \tag{I.2}$$

The kernel $R(\eta - \eta')$ is the correlation function of the random surface.

Consider now that the correlation function has an exponential form. Then

$$R(\eta - \eta') = g_o^2\, e^{-|\eta - \eta'|/\ell}$$

where $\ell$ is the correlation length and $g_o^2$ is the variance of the random process $g(\eta)$. Now the characteristic integral equation for the uncorrelated orthogonal functions becomes

$$\int_{-1}^{+1} e^{-|\eta - \eta'|/\ell}\, \Theta_s(\eta)\, d\eta = \frac{d_s^2}{g_o^2}\, \Theta_s(\eta') \quad . \tag{I.3}$$

Defining the new variables $x = \eta/\ell$, $y = \eta'/\ell$ and the constant $\omega = d_s^2/\ell g_o^2$, (I.3) takes on the form

$$\int_{-\ell}^{+\ell^{-1}} e^{-|x-y|}\, \Theta_s(x)\, dx = \omega\, \Theta_s(y) \quad . \tag{I.4}$$

This may be written

$$\omega\, \Theta_s(y) = \int_{-\ell^{-1}}^{y} e^{x-y}\, \Theta_s(x)\, dx + \int_{y}^{+\ell^{-1}} e^{y-x}\, \Theta_s(x)\, dx \quad . \tag{I.5}$$

Equation I.5 will be solved by finding a differential equation

satisfied by $\theta_s(x)$ and substituting the solution back into the integral to find $\omega$. Differentiating I.5 twice, we have

$$\omega\,\theta_s'(y) = \int_{-\ell^{-1}}^{y} e^{x-y}\,\theta_s(x)\,dx + \int_{y}^{+\ell^{-1}} e^{y-x}\,\theta_s(x)\,dx \,. \qquad (I.5)$$

$$\omega\,\theta_s''(y) = \int_{-\ell^{-1}}^{+\ell^{-1}} e^{-|x-y|}\,\theta_s(x)\,dx - 2\theta_s(y) \,.$$

Now using I.4 we find

$$\omega\,\theta_s''(y) + 2\theta_s(y) = \omega\,\theta_s(y) \,,$$

or

$$\theta_s''(y) + \frac{2-\omega}{\omega}\,\theta_s(y) = 0 \,. \qquad (I.6)$$

This second order differential has two solutions. The first is

$$\theta_s(y) = \left(\frac{1}{\ell} - \frac{\sin 2b_s/\ell}{2b_s}\right)^{-1/2} \sin b_s y \,,$$

where

$$\omega_s = \frac{2}{1+b_s^2} \,,$$

and $b_s$ satisfies

$$b_s \cot \frac{b_s}{\ell} = 1 \,.$$

The second is

$$\hat{\theta}_s(y) = \left(\frac{1}{2} + \frac{\sin 2\hat{b}_s/\ell}{2\hat{b}_s}\right)^{-1/2} \cos \hat{b}_s y$$

$$\hat{\omega}_s = \frac{2}{1 + \hat{b}_s^2} ,$$

$$\hat{b}_s \tan \hat{b}_s/\ell = 1 .$$

Finally we may write the expansion as

$$g(\eta) = \sum_s c_s d_s \theta_s(\eta) + \sum_s \hat{c}_s \hat{d}_s \hat{\theta}_s(\eta)$$

where the $c_s$ and $\hat{c}_s$ are mutually uncorrelated random variables with mean zero and variance one. In addition,

$$d_s = g_o \sqrt{\ell \omega_s}$$

$$= g_o \sqrt{\frac{2\ell}{1 + b_s^2}} ,$$

and

$$\hat{d}_s = g_o \sqrt{\ell \hat{\omega}_s}$$

$$= g_o \sqrt{\frac{2\ell}{1 + \tilde{b}_s^2}} .$$

For convenience we also introduce the alternate notation

$$g(\eta) = \sum_s c_s d_s n_s \sin p_s \eta + \sum_s \hat{c}_s \hat{d}_s \hat{n}_s \cos \hat{p}_s \eta ,$$

where

$$n_s = \left( \frac{1}{2} - \frac{\sin \frac{2b_s}{\ell}}{2b_s} \right)^{-1/2} ,$$

$$n_s = \left( \frac{1}{2} + \frac{\sin \frac{2b_s}{\ell}}{2b_s} \right)^{-1/2}$$

$$p_s = b_s/\ell \quad ,$$

$$p_c = b_c/\ell \quad .$$

## APPENDIX II

## NUMERICAL EXAMPLES OF ORTHOGONAL EXPANSIONS

In Appendix I the random irregularities on a mirror of finite extent were expanded formally in an orthogonal series with uncorrelated coefficients. Let us now consider a specific numerical example. The crucial parameter is the normalized correlation distance $\ell$. It will be taken as 1.0 or equal to the radius of the resonator aperture.

Having chosen $\ell$ we may proceed to calculate the quantities $b_s$ which are solutions of the equation

$$b_s \cot \frac{b_s}{\ell} = 1$$

which may be written

$$b_s = \tan \frac{b_s}{\ell} \quad .$$

The solutions of this equation are illustrated graphically in Figure I. The first few $b_s$'s are found to be

$$b_1 = 4.49$$
$$b_2 = 7.73$$
$$b_3 = 10.90$$
$$b_4 = 14.07$$
$$b_5 = 17.22$$

The complementary quantities $\hat{b}_s$ are solutions of the equation

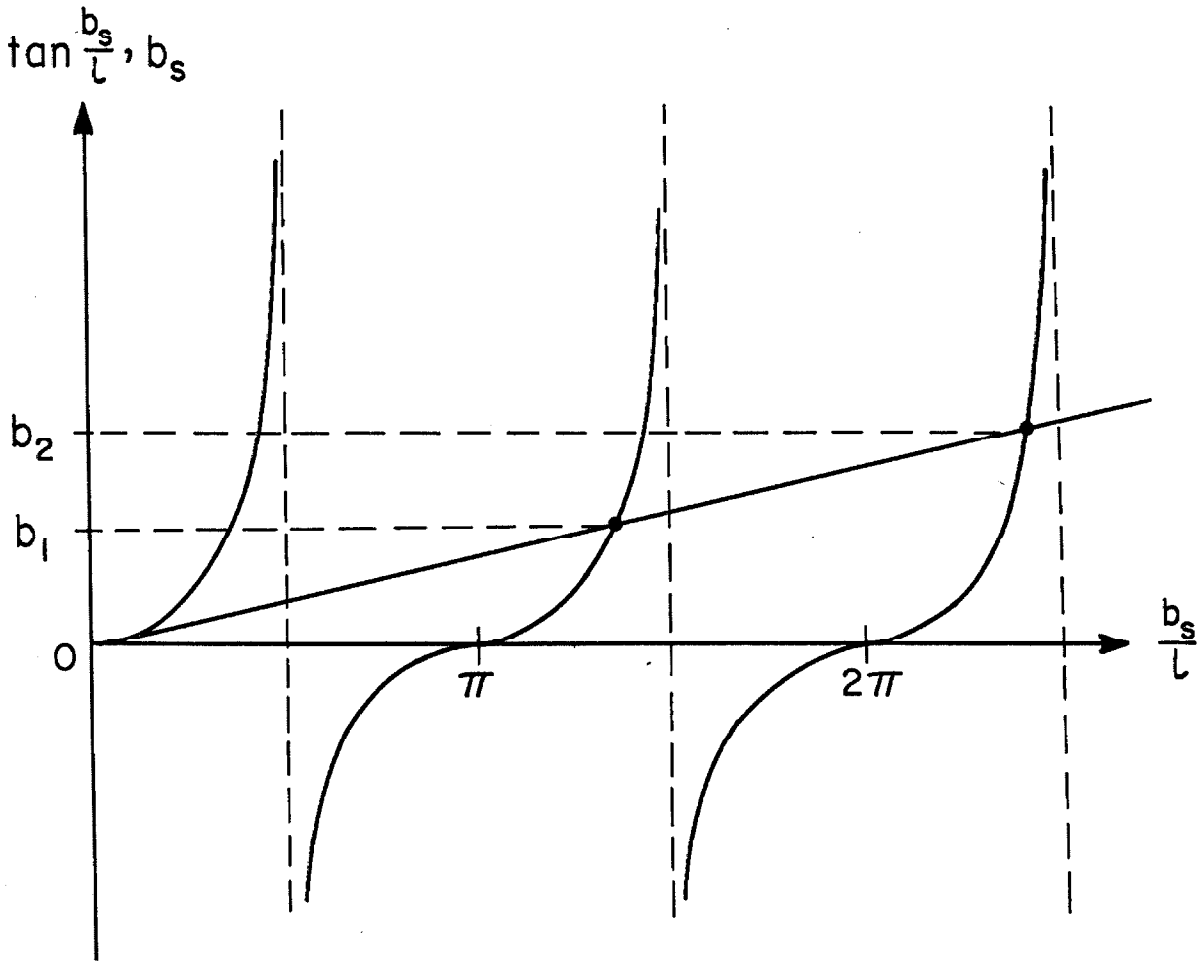


Fig. A.I Graphical solution of $b_s = \tan b_s/\ell$ for $\ell = 1.0$.

$$b_s \tan b_s/\ell = 1 \quad .$$

This may be rewritten as

$$\hat{b}_s = \cot \hat{b}_s/\ell \quad .$$

The solutions of this equation are illustrated graphically in Figure II.

Now, recapitulating, the orthogonal series has the form

$$g(\eta) = \sum_s c_s d_s n_s \sin p_s\eta + \sum_s \hat{c}_s \hat{d}_s \hat{n}_s \cos \hat{p}_s\eta \quad ,$$

where for a normalized correlation length $\ell = 1.0$ the coefficients are given in Tables I and II.

| s | $d_s^2/g_o^2$ | $n_s^2$ | $p_s$ |
|---|---|---|---|
| 1 | 0.095 | 1.12 | 4.49 |
| 2 | 0.033 | 1.02 | 7.73 |
| 3 | 0.017 | 1.01 | 10.90 |
| 4 | 0.010 | 1.00 | 14.07 |
| 5 | 0.007 | 1.00 | 17.22 |

Table I. Trigonometric expansion coefficients for $\ell = 1.0$

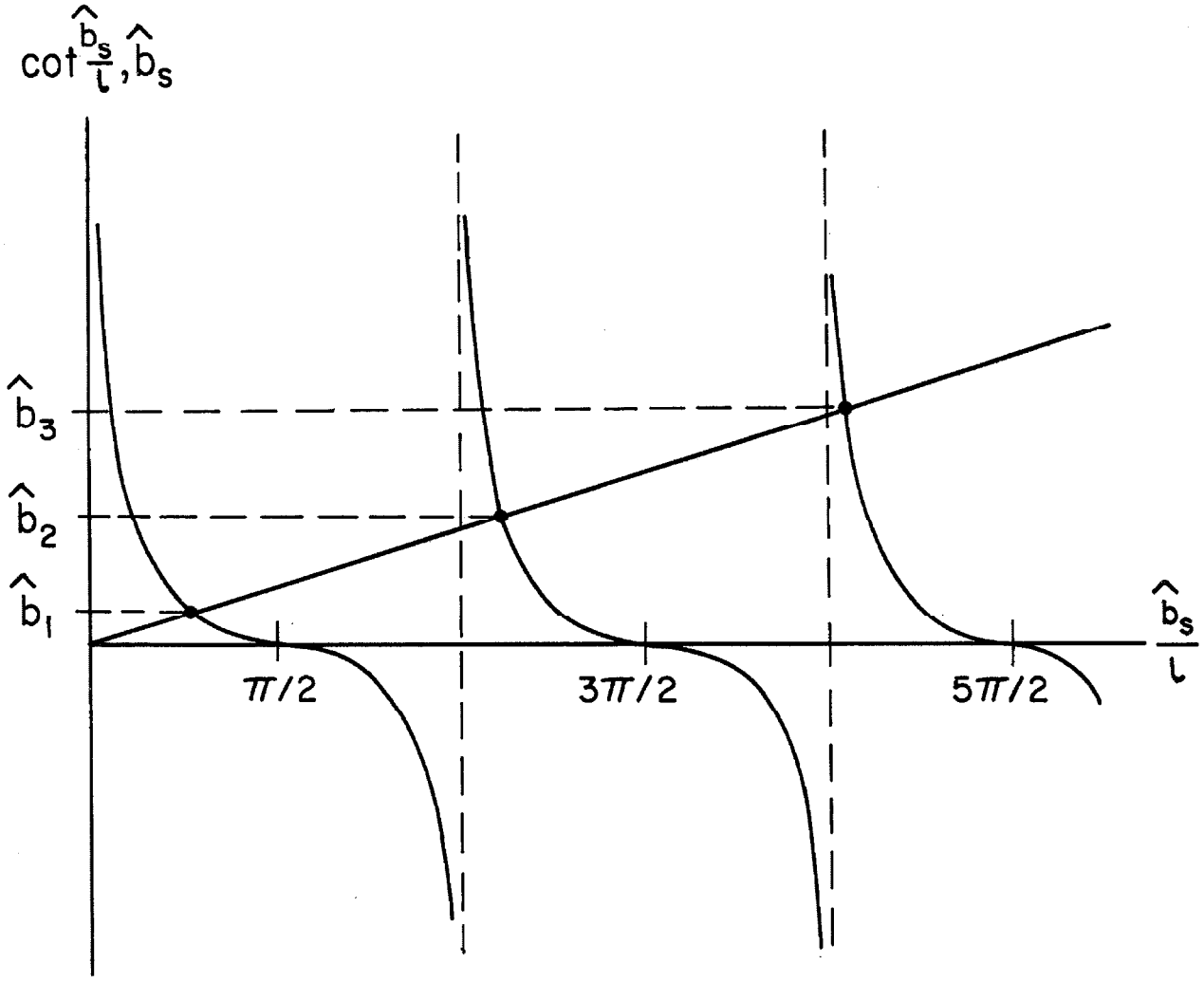


Fig. A.II Graphical solution of $\hat{b}_s = \cot \hat{b}_s/\ell$ for $\ell = 1.0$.

| s | $\hat{d}_s^2 / g_o^2$ | $\hat{n}_s^2$ | $\hat{p}_s$ |
|---|---|---|---|
| 1 | 1.150 | 0.635 | 0.86 |
| 2 | 0.157 | 0.93 | 3.42 |
| 3 | 0.047 | 0.98 | 6.44 |
| 4 | 0.022 | 0.99 | 9.53 |
| 5 | 0.012 | 1.00 | 12.65 |

Table II. Complementary expansion coefficients for $\ell = 1.0$

In exactly the same manner the coefficients may be computed for $\ell = 0.1$ . The first few $b_s$'s and $\hat{b}_s$'s are tabulated below.

$b_1 = 0.348$ $\quad$ $b_6 = 1.995$

$b_2 = 0.689$ $\quad$ $b_7 = 2.318$

$b_3 = 1.022$ $\quad$ $b_8 = 2.634$

$b_4 = 1.355$ $\quad$ $b_9 = 2.932$

$b_5 = 1.674$ $\quad$ $b_{10} = 3.269$

$\hat{b}_1 = 0.143$ $\quad$ $\hat{b}_6 = 1.626$

$\hat{b}_2 = 0.430$ $\quad$ $\hat{b}_7 = 1.933$

$\hat{b}_3 = 0.722$ $\quad$ $\hat{b}_8 = 2.241$

$\hat{b}_4 = 1.020$ $\quad$ $\hat{b}_9 = 2.551$

$\hat{b}_5 = 1.321$ $\quad$ $\hat{b}_{10} = 2.861$

The corresponding coefficients are given in Tables III and IV.

| s | $d_s^2 / g_o^2$ | $n_s^2$ | $p_s$ |
|---|---|---|---|
| 1 | 0.179 | 0.110 | 3.48 |
| 2 | 0.136 | 0.101 | 6.88 |
| 3 | 0.098 | 0.105 | 10.22 |
| 4 | 0.070 | 0.104 | 13.55 |
| 5 | 0.053 | 0.103 | 16.74 |
| 6 | 0.040 | 0.102 | 19.95 |
| 7 | 0.031 | 0.102 | 23.18 |
| 8 | 0.025 | 0.101 | 26.34 |
| 9 | 0.021 | 0.101 | 29.52 |
| 10 | 0.017 | 0.101 | 32.69 |

Table III. Trigonometric expansion coefficients for $\ell = 0.1$

| s | $\hat{d}_s^2 / g_o^2$ | $\hat{n}_s^2$ | $\hat{p}_s$ |
|---|---|---|---|
| 1 | 0.196 | 0.091 | 1.430 |
| 2 | 0.169 | 0.092 | 4.300 |
| 3 | 0.131 | 0.094 | 7.220 |
| 4 | 0.098 | 0.095 | 10.200 |
| 5 | 0.073 | 0.096 | 13.21 |
| 6 | 0.055 | 0.097 | 16.26 |
| 7 | 0.042 | 0.098 | 19.33 |
| 8 | 0.033 | 0.098 | 22.41 |
| 9 | 0.027 | 0.099 | 25.51 |
| 10 | 0.022 | 0.099 | 28.61 |

Table IV. Complementary expansion coefficients for $\ell = 0.1$

Similarly, for $\ell = 0.01$ the first few $b_s$'s and $\hat{b}_s$'s are tabulated below.

$b_1 = 3.17 \times 10^{-2}$ $\quad$ $b_6 = 19.03 \times 10^{-2}$

$b_2 = 6.35$ $\quad$ $b_7 = 22.21$

$b_3 = 9.52$ $\quad$ $b_8 = 25.38$

$b_4 = 12.69$ $\quad$ $b_9 = 28.55$

$b_5 = 15.86$ $\quad$ $b_{10} = 31.45$

$\hat{b}_1 = 1.55 \times 10^{-2}$ $\quad$ $\hat{b}_6 = 17.11 \times 10^{-2}$

$\hat{b}_2 = 4.67$ $\quad$ $\hat{b}_7 = 20.22$

$\hat{b}_3 = 7.78$ $\quad$ $\hat{b}_8 = 23.33$

$\hat{b}_4 = 10.89$ $\quad$ $\hat{b}_9 = 26.44$

$\hat{b}_5 = 14.00$ $\quad$ $\hat{b}_{10} = 29.56$

The corresponding coefficients are given in Tables V and VI.

| s | $d_s^2 / g_o^2$ | $n_s^2$ | $p_s$ |
|---|---|---|---|
| 1 | 0.020 | 0.01 | 3.17 |
| 2 | 0.020 | 0.01 | 6.32 |
| 3 | 0.020 | 0.01 | 9.52 |
| 4 | 0.020 | 0.01 | 12.69 |
| 5 | 0.019 | 0.01 | 15.86 |
| 6 | 0.019 | 0.01 | 19.03 |
| 7 | 0.019 | 0.01 | 22.21 |
| 8 | 0.019 | 0.01 | 25.38 |
| 9 | 0.019 | 0.01 | 28.55 |
| 10 | 0.018 | 0.01 | 31.72 |

Table V. Trigonometric expansion coefficients for $\ell = 0.01$

| s | $\hat{d}_s^2 / g_o^2$ | $\hat{n}_s^2$ | $\hat{p}_s$ |
|---|---|---|---|
| 1 | 0.020 | 0.01 | 1.55 |
| 2 | 0.020 | 0.01 | 4.67 |
| 3 | 0.020 | 0.01 | 7.78 |
| 4 | 0.020 | 0.01 | 10.89 |
| 5 | 0.020 | 0.01 | 14.00 |
| 6 | 0.019 | 0.01 | 17.11 |
| 7 | 0.019 | 0.01 | 20.22 |
| 8 | 0.019 | 0.01 | 23.33 |
| 9 | 0.019 | 0.01 | 26.44 |
| 10 | 0.018 | 0.01 | 29.56 |

Table VI. Complementary coefficients for $\ell = 0.01$

# APPENDIX III

## COMPUTATION OF THE PERTURBATION TERMS

With the aid of the numerical examples of Appendix II we may proceed to evaluate the perturbation elements as derived in 5.2. The results are given in the following tables.

| s | $B_{00}$ | $B_{01}$ | $B_{11}$ | $B_{02}$ | $B_{12}$ | $B_{22}$ | $B_{03}$ | $B_{13}$ | $B_{23}$ | $B_{33}$ |
|---|---|---|---|---|---|---|---|---|---|---|
| 1 | 0.176 | 0.034 | 0.103 | 0.001 | 0.033 | 0.086 | 0.001 | 0.0011 | 0.032 | 0.072 |
| 2 | 0.169 | 0.061 | 0.077 | 0.008 | 0.054 | 0.070 | 0.005 | 0.0097 | 0.047 | 0.053 |
| 3 | 0.156 | 0.079 | 0.042 | 0.020 | 0.058 | 0.040 | 0.014 | 0.0235 | 0.041 | 0.021 |
| 4 | 0.136 | 0.086 | 0.006 | 0.035 | 0.046 | 0.006 | 0.026 | 0.0485 | 0.019 | -0.010 |
| 5 | 0.115 | 0.083 | -0.023 | 0.049 | 0.025 | -0.021 | 0.039 | 0.0453 | -0.006 | -0.028 |
| 6 | 0.091 | 0.074 | -0.042 | 0.061 | 0.000 | -0.032 | 0.049 | 0.0430 | -0.026 | -0.028 |
| 7 | 0.070 | 0.061 | -0.050 | 0.065 | -0.021 | -0.036 | 0.054 | 0.0313 | -0.029 | -0.013 |
| 8 | 0.050 | 0.047 | -0.049 | 0.063 | -0.034 | -0.021 | 0.054 | 0.0131 | -0.021 | 0.007 |
| 9 | 0.035 | 0.034 | -0.043 | 0.057 | -0.039 | -0.004 | 0.049 | -0.0060 | -0.007 | 0.020 |
| 10 | 0.023 | 0.023 | -0.034 | 0.046 | -0.038 | +0.014 | 0.041 | -0.0217 | +0.009 | 0.024 |

Table V. Perturbation elements for $\ell = 0.1$, $c = 100$

| s | $B_{00}$ | $B_{01}$ | $B_{11}$ | $B_{02}$ | $B_{12}$ | $B_{22}$ | $B_{03}$ | $B_{13}$ | $B_{23}$ | $B_{33}$ |
|---|---|---|---|---|---|---|---|---|---|---|
| 1 | 0.176 | 0.031 | 0.111 | 0.001 | 0.030 | 0.086 | 0.001 | 0.001 | 0.029 | 0.072 |
| 2 | 0.168 | 0.057 | 0.095 | 0.010 | 0.051 | 0.066 | 0.004 | 0.013 | 0.046 | 0.049 |
| 3 | 0.153 | 0.076 | 0.068 | 0.023 | 0.059 | 0.034 | 0.012 | 0.026 | 0.044 | 0.015 |
| 4 | 0.133 | 0.085 | 0.035 | 0.039 | 0.051 | -0.001 | 0.023 | 0.040 | 0.026 | -0.016 |
| 5 | 0.109 | 0.084 | 0.001 | 0.053 | 0.031 | -0.026 | 0.035 | 0.046 | 0.001 | -0.030 |
| 6 | 0.085 | 0.076 | 0.025 | 0.063 | 0.007 | -0.036 | 0.046 | 0.041 | -0.018 | -0.025 |
| 7 | 0.064 | 0.065 | -0.043 | 0.065 | -0.015 | -0.032 | 0.054 | 0.026 | -0.030 | -0.008 |
| 8 | 0.045 | 0.052 | -0.049 | 0.062 | -0.031 | -0.017 | 0.055 | 0.007 | -0.026 | +0.011 |
| 9 | 0.031 | 0.037 | -0.049 | 0.054 | -0.038 | -0.002 | 0.050 | -0.014 | -0.011 | 0.023 |
| 10 | 0.020 | 0.026 | -0.043 | 0.044 | -0.039 | +0.018 | 0.043 | -0.025 | +0.004 | 0.022 |

Table VI. Perturbation elements for $\ell = 0.01$, $c = 100$

The quantities which determine the magnitude of the perturbation on the eigenfunctions and eigenvalues are the $\alpha_{mn}$. These may be obtained by multiplying the $B_{mn}$ by the coefficients of the orthogonal expansion. These coefficients and their products are given in Table VII and Table VIII for two correlation distances.

| s | $d_s/g_o$ | $n_s$ | $d_s n_s/g_o$ | $\hat{d}_s/g_o$ | $\hat{n}_s$ | $\hat{d}_s \hat{n}_s/g_o$ |
|---|---|---|---|---|---|---|
| 1 | 0.423 | 0.332 | 0.141 | 0.443 | 0.302 | 0.134 |
| 2 | 0.369 | 0.318 | 0.117 | 0.411 | 0.303 | 0.125 |
| 3 | 0.313 | 0.324 | 0.102 | 0.362 | 0.307 | 0.111 |
| 4 | 0.264 | 0.323 | 0.085 | 0.313 | 0.308 | 0.097 |
| 5 | 0.230 | 0.321 | 0.074 | 0.270 | 0.310 | 0.084 |
| 6 | 0.200 | 0.319 | 0.064 | 0.234 | 0.312 | 0.073 |
| 7 | 0.176 | 0.319 | 0.056 | 0.205 | 0.313 | 0.064 |
| 8 | 0.158 | 0.318 | 0.050 | 0.182 | 0.313 | 0.057 |
| 9 | 0.145 | 0.318 | 0.046 | 0.164 | 0.315 | 0.052 |
| 10 | 0.130 | 0.318 | 0.041 | 0.148 | 0.315 | 0.047 |

Table VII. Orthogonal expansion coefficients for $\ell = 0.1$

| s | $d_s/g_o$ | $n_s$ | $d_s n_s/g_o$ | $\hat{d}_s/g_o$ | $\hat{n}_s$ | $\hat{d}_s \hat{n}_s/g_o$ |
|---|---|---|---|---|---|---|
| 1 | 0.141 | 0.100 | 0.0141 | 0.141 | 0.100 | 0.0141 |
| 2 | 0.141 | 0.100 | 0.0141 | 0.141 | 0.100 | 0.0141 |
| 3 | 0.141 | 0.100 | 0.0141 | 0.141 | 0.100 | 0.0141 |
| 4 | 0.141 | 0.100 | 0.0141 | 0.141 | 0.100 | 0.0141 |
| 5 | 0.141 | 0.100 | 0.0141 | 0.141 | 0.100 | 0.0141 |
| 6 | 0.138 | 0.100 | 0.0138 | 0.138 | 0.100 | 0.0138 |
| 7 | 0.138 | 0.100 | 0.0138 | 0.138 | 0.100 | 0.0138 |
| 8 | 0.138 | 0.100 | 0.0138 | 0.138 | 0.100 | 0.0138 |
| 9 | 0.138 | 0.100 | 0.0138 | 0.138 | 0.100 | 0.0138 |
| 10 | 0.134 | 0.100 | 0.0134 | 0.134 | 0.100 | 0.0134 |

Table VIII. Orthogonal expansion coefficients for $\ell = 0.01$

Forming the pertinent products between the coefficients and the perturbation elements of the preceding tables yields values for the

perturbation terms $\alpha^s_{mn}$ defined in the solution of the perturbed characteristic integral equation.

| s | $\alpha^s_{00}/c_s g_o$ | $\alpha^s_{01}/c_s g_o$ | $\alpha^s_{11}/c_s g_o$ | $\alpha^s_{02}/c_s g_o$ | $\alpha^s_{12}/c_s g_o$ |
|---|---|---|---|---|---|
| 1 | 0.0236 | 0.00473 | 0.01380 | -0.00012 | 0.00460 |
| 2 | 0.0210 | 0.00720 | 0.00955 | -0.00097 | 0.00634 |
| 3 | 0.0173 | 0.00798 | 0.00461 | -0.00225 | 0.00590 |
| 4 | 0.0132 | 0.00730 | 0.00055 | -0.00343 | 0.00388 |
| 5 | 0.00965 | 0.00615 | -0.00188 | -0.00415 | 0.00185 |
| 6 | 0.00670 | 0.00473 | -0.00304 | -0.00442 | 0.000024 |
| 7 | 0.00447 | 0.00340 | -0.00267 | -0.00388 | -0.00116 |
| 8 | 0.00287 | 0.00234 | -0.00280 | -0.00362 | -0.00171 |
| 9 | 0.00181 | 0.00155 | -0.00223 | -0.00294 | -0.00182 |
| 10 | 0.00106 | 0.00095 | -0.00159 | -0.00207 | -0.00157 |

| s | $\alpha^s_{22}/c_s g_o$ | $\alpha^s_{03}/c_s g_o$ | $\alpha^s_{13}/c_s g_o$ | $\alpha^s_{23}/c_s g_o$ | $\alpha^s_{33}/c_s g_o$ |
|---|---|---|---|---|---|
| 1 | 0.01160 | -0.000095 | -0.000154 | 0.00445 | 0.0097 |
| 2 | 0.00863 | -0.000564 | -0.00120 | 0.00554 | 0.0066 |
| 3 | 0.00445 | -0.00141 | -0.00261 | 0.00420 | 0.00234 |
| 4 | 0.00059 | -0.00221 | -0.00468 | 0.00161 | -0.00095 |
| 5 | -0.00173 | -0.00286 | -0.00379 | -0.00042 | -0.00238 |
| 6 | -0.00234 | -0.00313 | -0.00314 | -0.00169 | -0.00204 |
| 7 | -0.00206 | -0.00304 | -0.00276 | -0.00163 | -0.0018 |
| 8 | -0.00119 | -0.00270 | -0.000238 | -0.00108 | +0.00039 |
| 9 | -0.00018 | -0.00226 | +0.00031 | -0.000336 | 0.00105 |
| 10 | +0.00065 | -0.00170 | +0.00101 | +0.00039 | 0.00114 |

Table IX. Perturbation terms for $\ell = 0.1$ and $c = 100$

| s | $\alpha^s_{00}/c_s g_o$ | $\alpha^s_{01}/c_s g_o$ | $\alpha^s_{11}/c_s g_o$ | $\alpha^s_{02}/c_s g_o$ | $\alpha^s_{12}/c_s g_o$ |
|---|---|---|---|---|---|
| 1 | 0.00248 | 0.00044 | 0.00156 | -0.00001 | 0.00042 |
| 2 | 0.00237 | 0.00081 | 0.00135 | -0.00013 | 0.00073 |
| 3 | 0.00216 | 0.00107 | 0.00095 | -0.00032 | 0.00083 |
| 4 | 0.00188 | 0.00120 | 0.00049 | -0.00054 | 0.00072 |
| 5 | 0.00154 | 0.00119 | 0.00002 | -0.00075 | 0.00044 |
| 6 | 0.00118 | 0.00105 | 0.00035 | -0.00086 | 0.00010 |
| 7 | 0.00088 | 0.00089 | -0.00059 | -0.00090 | -0.00021 |
| 8 | 0.00063 | 0.00072 | -0.00068 | -0.00085 | -0.00043 |
| 9 | 0.00043 | 0.00051 | -0.00075 | -0.00074 | -0.00053 |
| 10 | 0.00027 | 0.00034 | -0.00058 | -0.00058 | -0.00052 |

| s | $\alpha^s_{22}/c_s g_o$ | $\alpha^s_{03}/c_s g_o$ | $\alpha^s_{13}/c_s g_o$ | $\alpha^s_{23}/c_s g_o$ | $\alpha^s_{33}/c_s g_o$ |
|---|---|---|---|---|---|
| 1 | 0.00121 | -0.00001 | -0.00002 | 0.00041 | 0.00102 |
| 2 | 0.00094 | -0.00005 | -0.00018 | 0.00065 | 0.00069 |
| 3 | 0.00047 | -0.00016 | -0.00037 | 0.00062 | 0.00021 |
| 4 | -0.00001 | -0.00032 | -0.00056 | 0.00036 | -0.00022 |
| 5 | -0.00037 | -0.00050 | -0.00064 | 0.00002 | -0.00043 |
| 6 | -0.00049 | -0.00064 | -0.00056 | -0.00025 | -0.00035 |
| 7 | -0.00044 | -0.00074 | -0.00036 | -0.00040 | -0.00011 |
| 8 | -0.00023 | -0.00077 | -0.00011 | -0.00036 | +0.00016 |
| 9 | -0.00002 | -0.00070 | +0.00020 | -0.00016 | 0.00031 |
| 10 | +0.00024 | -0.00057 | 0.00034 | +0.00006 | 0.00030 |

Table X. Perturbation terms for $\ell = 0.01$ and $c = 100$

# APPENDIX IV

## RESONANCE PROPERTIES OF CONFOCAL RESONATORS

In performing Q measurements on Spherical Fabry-Perot Resonators there are some crucial calculations which must be carried out before designing the experimental apparatus. Among the numbers required are mode separation as a function of mirror separation and the mirror movement necessary to sweep the resonance over a given frequency range.

The resonance condition for a three-dimensional cavity is

$$\frac{4b}{\lambda} = 2q + m + n + 1 . \qquad \text{(IV.1)}$$

With b fixed the frequency separation between adjacent axial modes is given by

$$\Delta f_a = \frac{c}{2b} . \qquad \text{(IV.2)}$$

The separation between adjacent transverse modes is

$$\Delta f_t = \frac{c}{4b} . \qquad \text{(IV.3)}$$

The mode separations for various values of the length b are given in Table XI. The quantity c in the above equations is the free-space velocity of light not to be confused with the dimensionless quantity introduced earlier.

| b | $\Delta f_a$ | $\Delta f_t$ |
|---|---|---|
| 0.1m | $1.50 \times 10^9$cps | $7.50 \times 10^8$cps |
| 0.2 | $7.50 \times 10^8$ | 3.75 |
| 0.3 | 5.00 | 2.50 |
| 0.4 | 3.75 | 1.88 |
| 0.5 | 3.00 | 1.50 |
| 0.6 | 2.50 | 1.25 |
| 0.7 | 2.14 | 1.07 |
| 0.8 | 1.88 | $9.38 \times 10^7$ |
| 0.9 | 1.67 | 8.33 |
| 1.0 | 1.50 | 7.50 |
| 1.1 | 1.36 | 6.82 |
| 1.2 | 1.25 | 6.25 |
| 1.3 | 1.15 | 5.77 |
| 1.4 | 1.07 | 5.36 |
| 1.5 | 1.00 | 5.00 |

Table XI. Mode Separation vs. Resonator Length.

For a given axial and transverse resonance condition we may compute the frequency shift for a slight variation in mirror separation. The center frequency of a particular mode is given by

$$f_{m,n,q} = \frac{c}{4b}(2q + m + n + 1) . \qquad \text{(IV.4)}$$

A shift $\Delta b$ in the spacing represents a frequency shift,

$$\Delta f = \frac{c}{4b} (2q + m + n + 1) \left(\frac{\Delta b}{b}\right) , \qquad \text{(IV.5)}$$

or

$$\frac{\Delta f}{f} = \frac{\Delta b}{b} . \qquad \text{(IV.6)}$$

As an example let us say $\Delta f$ equals the axial mode separation, then

$$\Delta f = \frac{c}{2b} ,$$

and

$$\Delta b = \frac{\lambda}{2} . \qquad \text{(IV.7)}$$

The above equations show that in a resonator sweeping scheme there is no point in moving the mirror more than $\frac{\lambda}{2}$. In addition it is clear that microphonic jitter must be kept well below this level. The shift in frequency is inversely proportional to $b$. Thus, it takes less mirror movement to achieve a given frequency sweep in a shorter resonator; however, microphonic problems will be correspondingly worse in such a resonator. Table XII gives the mirror movement necessary to produce a 100 mc shift in frequency for various resonator lengths.

Next we look at the half resonator in the same manner as the full resonator. We note that the resonance condition becomes

$$\frac{4b}{\lambda} = 4q + m + n + 1 . \qquad \text{(IV.8)}$$

To compare full and half resonators of the same physical length we define a new parameter

$$d \equiv \frac{b}{2}$$

| b | $\Delta b(\lambda = 1.15\mu)$ | $\Delta b(\lambda = 6328\text{Å})$ |
|---|---|---|
| 0.1m | 0.038μ | 0.021μ |
| 0.2 | 0.077 | 0.042 |
| 0.3 | 0.115 | 0.063 |
| 0.4 | 0.153 | 0.084 |
| 0.5 | 0.192 | 0.105 |
| 0.6 | 0.230 | 0.127 |
| 0.7 | 0.268 | 0.148 |
| 0.8 | 0.306 | 0.169 |
| 0.9 | 0.345 | 0.190 |
| 1.0 | 0.383 | 0.211 |
| 1.1 | 0.421 | 0.232 |
| 1.2 | 0.460 | 0.253 |
| 1.3 | 0.498 | 0.274 |
| 1.4 | 0.536 | 0.295 |
| 1.5 | 0.575 | 0.316 |

Table XII. Mirror Movement to Produce 100 mc Frequency Shift vs. Resonator Length.

which is the length of the half resonator. With this substitution IV.8 becomes

$$\frac{4d}{\lambda} = 2q + \frac{m + n + 1}{2} . \qquad \text{(IV.9)}$$

From IV.9 we see that the axial mode separation is

$$f_a = \frac{c}{2d} \cdot \qquad \text{(IV.10)}$$

The transverse mode separation is

$$f_t = \frac{c}{8d} \cdot \qquad \text{(IV.11)}$$

Equations IV.10 and IV.11 show that full and half resonators of the same physical length $(d = b)$ have the same axial mode separation, but the half resonator has half the transverse separation.

Inspection of IV.9 indicates the same modulation characteristics for full and half systems with mirror movement.

REFERENCES


1. A. L. Schawlow and C. H. Townes, "Infrared and Optical Masers", Phys. Rev. 112, pp. 1940-1949 (1958).

2. A. M. Prokhorov, "Molecular Amplifier and Generator for Submillimeter Waves", Soviet Physics JETP 7, pp. 1140-1141 (1958).

3. R. H. Dicke, U. S. Patent No. 2, 851, 652, (1958).

4. A. G Fox and T. Li, "Resonant Modes in a Maser Interferometer", B.S.T.J. 40, pp. 453-488 (1961).

5. G. D Boyd and J. P. Gordon, "Confocal Multimode Resonator for Millimeter Through Optical Wavelength Masers", B.S.T.J. 40, pp. 489-508 (1961).

6. G. D. Boyd and H. Kogelnik, "Generalized Confocal Resonator Theory", B.S.T.J. 41, pp. 1347-1369 (1962).

7. R. F. Soohoo, "Nonconfocal Multimode Resonators for Masers", Proc. IRE 51, pp. 70-75 (1963).

8. P. Connes, "L'Etalon de Fabry-Perot Spherique", J. Phys. Rad. 19, pp. 261-269 (1958).

9. A. G. Fox and T. Li, "Modes in a Maser Interferometer with Curved and Tilted Mirrors", Proc. IRE 51, pp. 80-89 (1963).

10. C. L. Tang, "On Diffraction Losses in Laser Interferometers", Appl. Optics 1, pp. 768-770 (1962).

11. W. Culshaw, "Further Considerations on Fabry-Perot Type Resonators", IRE Trans. on Microwave Theory and Techniques MTT-10, pp. 331-339 (1962).

12. A. G. Fox et al, "On Diffraction Losses in Laser Interferometers", Appl. Optics 2, pp. 544-545 (1963).

13. J. Kotik and M. C. Newstein, "Theory of Laser Oscillations in Fabry-Perot Resonators", J. Appl. Phys. 32, pp. 178-186 (1961).

14. S. R. Barone, "Resonances of the Fabry-Perot Resonator", J. Appl. Phys. 34, pp. 831-843 (1963).

15. L. A. Vainshtein, "Open Resonators for Lasers", Soviet Physics JETP 17, pp. 709-719 (1963).

16. R. W. Zimmerer, "Spherical Mirror Fabry-Perot Resonators", IEEE Trans. on Microwave Theory and Techniques MTT-11, pp. 371-379 (1963).

17. V. Evtuhov, "Mode Structure of Laser Resonators and Problems of Mode Control", Invited paper presented at the 1963 Winter Meeting of the American Physical Society, Pasadena, California.

18. P. O. Clark, "Multireflector Optical Resonators", Proc. IEEE (Correspondence) 51, pp. 949-950 (1963).

19. G. Toraldo di Francia, "On the Theory of Optical Resonators", Paper presented at the April 1963 Microwave Research Institute Symposia on Optical Masers, New York, N. Y.

20. R. Courant and D. Hilbert, Methods of Mathematical Physics, Vol. II, Interscience (1962), pp. 677-681.

21. J. Stratton, Electromagnetic Theory, McGraw-Hill (1941).

22. M. Born and E. Wolf, Principles of Optics, Pergamon Press (1959), pp. 558-559.

23. F. Borgnis and C. Papas, "Electromagnetic Waveguides and Resonators", Handbuch der Physik, Springer-Verlag (1958).

24. C. Flammer, Spheroidal Wave Functions, Stanford Univ. Press (1957).

25. F. Bass and V. Bocharov, Radio Engineering and Electronics (translation of Radiotekhnika: Elektronika), 3 (1958), pp. 251-258.

26. S. Rice, Communs. Pure and Appl. Math., 4 (1951), pp. 351-378.

27. H. Davies, Inst. of Elect. Engrs. IV, 7 (1954) p. 101.

28. H. Bennett and J. Porteus, Jour. Opt. Soc. Am. 51 (1961) p. 123.

29. K. Mitzner, "Theory of the Scattering of Electromagnetic Waves by Irregular Interfaces", Thesis, Calif. Inst. of Tech. (1964).

30. A. Erdelyi et al., Tables of Integral Transforms, Vol. 2, Bateman manuscript project McGraw-Hill (1954).

31. D. A. Kleinman and P. P. Kisliuk, "Discrimination Against Unwanted Orders in the Fabry-Perot Resonator", B.S.T.J. 41, pp. 453-462 (1962).

32. W. Specht Jr., "Light Scattering from Dielectric Film Laser Mirrors", S.R. 1, Quantum Electronics Laboratory, Calif. Inst. of Tech., (1963).

33. W. Davenport and W. Root, Random Signals and Noise, McGraw-Hill (1958).

34. R. A. Paananen, "Direct Measurement of Optical Cavity Q", Proc. IRE (Correspondence) 50, p. 2115 (1962).